NASA
Technical
Paper
2721

July 1987

Static Internal Performance of a Two-Dimensional Convergent-Divergent Nozzle With Thrust Vectoring

E. Ann Bare and
David E. Reubush

NASA

NASA Technical Paper 2721

1987

Static Internal Performance of a Two-Dimensional Convergent-Divergent Nozzle With Thrust Vectoring

E. Ann Bare and
David E. Reubush

Langley Research Center
Hampton, Virginia

National Aeronautics
and Space Administration

**Scientific and Technical
Information Office**

CONTENTS

SUMMARY

A parametric investigation of the static internal performance of multifunction two-dimensional convergent-divergent nozzles has been made in the static test facility of the Langley 16-Foot Transonic Tunnel. All nozzles had a constant throat area and aspect ratio. The effects of upper and lower flap angles, divergent flap length, throat approach angle, sidewall containment, and throat geometry were determined. All nozzles were tested at a thrust vector angle that varied from 5.60° to 23.00°. The nozzle pressure ratio was varied up to 10 for all configurations.

The results show that the nozzle discharge coefficient was insensitive to changes in geometry downstream of the throat for a constant geometric vector angle. The effect on internal performance of cutting back the sidewalls was in effect the same as decreasing the nozzle expansion ratio. Radiusing the lower flap throat improved the nozzle performance.

INTRODUCTION

The next generation of fighter airplanes will be both versatile and highly maneuverable. One approach for providing these characteristics consists of using the propulsion system to enhance maneuverability and attitude control. Several studies have been conducted using nonaxisymmetric nozzles to vector thrust in order to generate other forces and moments (refs. 1 to 7). One type of nonaxisymmetric nozzle that has been successfully adapted for pitch thrust vectoring is the two-dimensional convergent-divergent (2D-CD) nozzle (refs. 8 to 12). Most of these investigations addressed specific 2D-CD nozzle designs with only limited nozzle component variations. There are limited static-performance data available on the effects of parametrically varying the nozzle internal geometry, for example, data on the expansion ratio, flap length, sidewall length, and flap divergence angle (ref. 13). Another investigation (ref. 14) studied the effects of throat contouring. Other investigations included thrust-vectoring effects (refs. 14, 15, and 16).

The present paper presents static internal performance data for 2D-CD nozzles of constant throat area and aspect ratio having geometric variations of upper flap angle, lower flap angle, divergent flap length, and throat approach angle in combinations to achieve pitch thrust vectoring. Upper flap divergence angle varied from -20.4° to 1.4°, lower flap divergence angle varied from 11.6° to 25.0°, divergent flap length varied from 1.0 to 2.7 in., and throat approach angle varied from 5.0° to 30.0°. The effects of sidewall containment and throat radius were also studied for selected configurations. All nozzles were tested at nozzle pressure ratios of 1.7 to 10.0. Nozzle internal performance data were obtained from force balance and flow measurements. All upper and lower nozzle flaps were instrumented with internal surface static pressure orifices. This investigation was conducted in the static test facility adjacent to the Langley 16-Foot Transonic Tunnel.

SYMBOLS AND ABBREVIATIONS

A_e geometric nozzle exit area computed at trailing edge of nozzle flaps, in^2

A_t geometric nozzle throat area at $x = 3.0$ in., in^2

A_e/A_t geometric nozzle expansion ratio

F measured thrust along body axis, lbf

F_i ideal isentropic gross thrust, $w_p\left\{RT_{t,j}\frac{2\gamma}{\gamma - 1}\left[1 - \left(\frac{p_a}{p_{t,j}}\right)^{\frac{\gamma-1}{\gamma}}\right]\right\}^{1/2}$, lbf

F_r resultant gross thrust, $(F^2 + N^2)^{1/2}$, lbf

$h_{t,n}$ nominal nozzle throat height of 1.0 in. (see fig. 2)

l length of divergent flap (see fig. 2), in.

M_Y measured pitching moment about point on model centerline at station 29.39, in-lb

N measured normal force, lbf

NPR nozzle pressure ratio, $p_{t,j}/p_a$

p local static pressure, psi

p_a ambient pressure, psi

$p_{t,j}$ jet total pressure, psi

R gas constant, 53.364 ft-lb/lb-°R for air

$T_{t,j}$ jet total temperature

w_i ideal mass-flow rate

w_p measured mass-flow rate, slugs/sec

x axial coordinate measured from nozzle connect station (Sta. 41.13), positive downstream, in.

y vertical coordinate measured from horizontal model centerline, positive upward, in.

α_l lower flap angle measured from horizontal reference line (see fig. 2), deg

α_u upper flap angle measured from horizontal reference line (see fig. 2), deg

β throat approach angle measured from horizontal reference line (see fig. 2), deg

γ ratio of specific heats, 1.3997 for air

δ resultant thrust vector angle, $\tan^{-1}(N/F)$, deg

δ_v geometric thrust vector angle, $(\alpha_\ell - \alpha_u)/2.0$, deg

Abbreviations:

Sta. model station

2D-CD two-dimensional convergent-divergent

First character in nozzle configuration designation (see fig. 3):

A sidewall pair 301, 302

B sidewall pair 303, 304

C sidewall pair 305, 306

D sidewall pair 307, 308

E sidewall pair 309, 310

Number in nozzle configuration designation (see table AII):

01 to 27 upper flap

Last character(s) in nozzle configuration designation (see table AI):

F to AA lower flap

APPARATUS AND METHODS

Static Test Facility

This investigation was conducted in the static test facility (ref. 17) of the Langley 16-Foot Transonic Tunnel. All tests were conducted with the jet exhausting to the atmosphere. This facility utilizes the same clean, dry air supply and a similar air-control system as that used in the 16-Foot Transonic Tunnel, including valving, filters, and a heat exchanger (to operate the jet flow at constant stagnation temperature).

Single-Engine Propulsion-Simulation System

A sketch of the single-engine air-powered nacelle model (described in ref. 17) on which the various nozzles were mounted is presented in figure 1 with a typical vectored 2D-CD nozzle configuration attached. An external high-pressure air system provided a continuous flow of clean, dry air at a controlled temperature of about 530°R (measured at the instrumentation section). This high-pressure air was brought through a dolly-mounted support strut by six tubes that connect to a high-pressure plenum chamber. In order to minimize any forces imposed by the transfer of axial

momentum as the air is passed from the nonmetric high-pressure plenum to the metric low-pressure plenum (attached to the force balance), the air was discharged radially into the model low-pressure plenum through eight multiholed sonic nozzles equally spaced around the high-pressure plenum, as shown in figure 1. Two flexible metal bellows were used as seals and served to eliminate the transfer of forces caused by pressurization.

The air was then passed from the model low-pressure plenum through a transition section that provided a smooth flow path for the airflow from the round low-pressure plenum to the rectangular choke plate and instrumentation section. The transition section, choke plate, and instrumentation section were common for all 2D-CD nozzles tested. The instrumentation section had a flow path width-to-height ratio of 1.437. All nozzle configurations were attached to the instrumentation section at model station 41.13.

Nozzle Design and Models

Nozzle concept.- The basic nozzle components of the two-dimensional convergent-divergent (2D-CD) nozzle are upper and lower flaps that regulate the internal contraction and expansion process which takes place in the vertical plane, and flat sidewalls that contain the flow laterally. The two-dimensional nature of the flaps and sidewalls of this nozzle makes it readily adaptable to the incorporation of thrust-vectoring capabilities. This is achieved by varying the geometry of both the upper and lower flaps aft of the throat in order to direct the flow from the axial direction.

Nozzle models.- The nozzle models of the present investigation were attached to the propulsion simulation system at station 41.13 (see fig. 1) and had a nominally constant throat height of 1.0 in. and width of 4.0 in. Interchangeable upper and lower nozzle flaps and sidewalls were combined to vary the nozzle geometry. Figure 2(a) presents a sketch showing typical nozzle upper and lower flaps having sharp throats (a radius equal to 0.0). Figure 2(b) presents a sketch of a radiused lower flap (a radius equal to 1.0 in.). Six configurations utilizing a radiused lower flap were tested to determine the effect of throat geometry on static performance. Table I shows the geometry of each configuration along with the geometric thrust vector angle and nozzle expansion ratio. The effect of sidewall cutback was examined for selected configurations. Sidewall geometry is shown in figure 3.

The flaps and sidewalls used to assemble each nozzle may be determined from the configuration notation described in the "Symbols and Abbreviations" section. The internal geometry of all upper and lower flaps is presented in appendix A.

Instrumentation

A six-component strain-gauge balance was used to measure the forces and moments on the model downstream of station 20.50 in. (See fig. 1.) Jet total pressure was measured by means of a four-probe rake through the upper surface, a three-probe rake through the side, and a three-probe rake through the corner of the rectangular instrumentation section (fig. 1). Jet total temperature was measured by a shielded thermocouple probe also located in the instrumentation section. Mass-flow rate of the high-pressure air was measured by a calibrated choked venturi. All upper and lower flaps were instrumented with internal static pressure orifices located on the

planview centerline. The internal static pressures for all the configurations tested are presented in appendix B. Axial location of the static pressure orifices for each configuration are given in tables BI and BII.

Data Reduction

All data were recorded on magnetic tape with 50 frames of data averaged over 5 sec at each data point for use in the computations. With the exception of resultant thrust F_r, data for the force and resultant thrust vector angle are referenced to the model centerline. Nominal throat height $h_{t,n}$ was selected arbitrarily as a nondimensionalizing length.

Data are presented in basic performance parameters of internal thrust ratio, resultant thrust ratio, resultant thrust vector angle, nondimensionalized pitching moment, and nozzle discharge coefficient (ratio of measured mass-flow rate to ideal mass-flow rate). The balance measurements are corrected for model weight tares and balance interactions. Although the bellows arrangement previously described was designed to eliminate pressure and momentum interactions with the balance, small bellows tares still exist on all balance components. When the bellows are pressurized there are small differences in the forward and aft spring constants; there are also small differences in the pressure between the ends of the bellows at high internal velocities. These differences result in the bellows tares. In order to determine the bellows tares, calibration nozzles were run over a range of expected normal force and pitching moments, and the balance data were corrected in a manner similar to that discussed in reference 15. Although six balance components were computed, none of the nozzle configurations produced any significant levels of lateral forces or moments, and as a result none are presented. External pressure measurements on previous models (see ref. 13) showed no base pressure effects. Therefore, no external pressure measurements were made on this model.

To ensure the integrity of the system, one of the nozzle configurations was tested several times throughout the investigation and repeat data were found to be within balance accuracy. The corrected balance data are then used to determine the basic performance parameters. The ideal gross thrust is computed based on measured mass-flow rate, jet total pressure, and jet total temperature. The pitching moment that results from vectored thrust is presented as a ratio to ideal thrust multiplied by throat height to give a nondimensionalized quantity. The computed ideal mass-flow rate is based on jet total pressure, jet total temperature, and measured nozzle throat area. Nozzle throat area was measured for each nozzle tested. Nozzle discharge coefficient is the ratio of the measured mass-flow rate to the ideal mass-flow rate and is the measure of the ability of a nozzle to pass mass flow. The internal nozzle static pressures are presented as a ratio to jet total pressure.

PRESENTATION OF RESULTS

The basic internal nozzle performance data and pitching-moment-ratio data for all configurations and the pressure data for selected configurations are presented graphically in figures 4 to 18. The pitching-moment data are presented for information purposes and will not be discussed in that the results noted for the resultant thrust vector angle are the same as would be noted for the pitching-moment-ratio data. The local static pressure data for all the configurations are presented in ratio form as a function of NPR and the x-location in appendix B. All data were

machine plotted and the curves were faired with a spline curve fit. The results of this investigation are plotted in the following figures:

RESULTS AND DISCUSSION

There are a number of different ways to vector the thrust from a 2D-CD nozzle. One example would be to gimbal the entire nozzle. Although this method would not affect the internal nozzle performance in that the flow path would be unchanged, the necessary actuators and gimbal hardware would add extra weight to the configuration. Also, as the thrust vector angle of this concept varies, the change in the nozzle external geometry has the potential for significantly increasing drag as was reported in reference 6. The method of vectoring thrust studied in the current investigation is the independent deflection of the upper and lower divergent flaps which could be accomplished by using the existing actuators and hardware necessary for changing nozzle power setting and expansion ratio. This method eliminates the need for the extra actuators necessary for gimballing the entire nozzle, but it leaves the throat orientation essentially unchanged as compared with that of the forward thrust mode. This in effect means that the supersonic flow downstream of the nozzle throat must be turned by the nozzle divergent flaps. There is a potential for thrust losses when this is done, as previous studies have indicated (refs. 6 and 15).

Flap Angle

The geometric thrust vector angle can be increased by decreasing the upper flap angle α_u while the lower flap angle α_l is held constant, or by increasing α_l while α_u is held constant; however, this would also change the nozzle expansion ratio. In order to maintain the same expansion ratio, the upper and lower divergent flap angles are varied simultaneously. Figure 4 shows the effect of increasing the thrust vector angle. There were no discernible changes in the shape of the internal performance curves, but there was only an incremental decrease in gross thrust ratio and discharge coefficient attributable to the increase in geometric thrust vector

angle. The increase of 7.5° in geometric thrust vector angle produced an approximate 8.0° incremental increase in resultant thrust vector angle.

Previous studies (ref. 13) have shown that nozzle expansion ratio is the predominant parameter affecting nozzle internal performance. Because of this, it is difficult to separate effects due to changes in upper flap divergence angle from effects due to expansion ratio change. Figure 5 shows the effect of changing the upper flap angle and, consequently, the geometric thrust vector angle and expansion ratio while holding other parameters constant. The resultant thrust ratio shows effects due to expansion ratio variation that are similar to those observed in reference 13. That is, the peak performance occurs at an NPR near the design NPR and then drops with increasing NPR, with the lowest expansion ratio configuration showing the largest performance loss as a result of nozzle underexpansion losses. Discharge coefficient shows a decrease with increasing geometric vector angle similar to that previously discussed for figure 4. The thrust vector angle is influenced by both expansion ratio and geometric vector angle; it is difficult to separate the two effects. Figure 6 shows the static pressure data for configurations C19P and C20P. The pressure on the last two-thirds of the lower flap of C19P is much higher than that on the upper flap. This difference tends to reduce significantly the normal force and thus the resultant thrust vector angle. The pressures also indicate a highly inclined throat, thus making the nozzle effectively an inverted single-expansion-ramp nozzle. This tends to produce large resultant thrust vector angles at low NPR and low values of resultant thrust vector angle at high NPR (see ref. 18), as can be seen for configuration C19P in figure 5. The pressures for configuration C20P indicate a fairly vertical nozzle throat with the upper flap having a higher pressure than the lower flap over most of the flap length. This condition tends to produce the lower values of resultant thrust vector angles at low NPR as indicated in figure 5 for configuration C20P. It is apparent that increasing the geometric vector angle by decreasing only the upper flap divergent angle does not provide efficient thrust vectoring.

Flap Length

Figures 7 to 9 show data at different divergent flap lengths (and consequently different nozzle expansion ratios) with all other parameters held constant. Figures 7(b) and 9(b) show comparisons between data at values of $l/h_{t,n}$ of 1.00 and 2.50 with only small differences in expansion ratio. There are only small effects of flap length on the performance data of configurations having almost the same expansion ratio. This result was also indicated by the data in reference 13. Figures 7(a) and 9(a) show the same comparison in flap length but with the increase in expansion ratio being four times larger. The changes in the thrust ratios are also much larger. These differences are similar to those shown in figure 5 and are believed to be primarily due to differences in expansion ratio. It is apparent that any effect of flap length on internal performance is far less than the effect of changing the expansion ratio.

Differences in expansion ratio also influence the ability of the configuration to vector the thrust. The higher expansion ratio nozzles (longer flaps) produced resultant thrust vector angles that peaked at a value nearly double that of the lower expansion ratio nozzles, and then these angles rapidly dropped with increasing NPR to a value approximately one-half that of the lower expansion ratio nozzles (figs. 7(a) and 9(a)). That is, thrust vectoring is most effective and least erratic for nozzles having a low expansion ratio. This result might be expected since the

high expansion ratio nozzles are operating overexpanded at the low NPR's and the internal flow separation characteristics would be expected to vary greatly with varying NPR.

Figure 8 presents data for the configurations with minimum to maximum flap lengths tested (low to high expansion ratio). Except for the magnitude of peak resultant thrust vector angle, these data indicate results similar to those discussed for figures 7 and 9. Figure 10 presents the internal static pressure distributions for the configurations shown in figure 8. There is no effect of changing flap length on the pressure data. The data indicate an inclined throat and higher pressure on the lower flap over the last two-thirds of the longer flaps. This pressure distribution has the same effect on the resultant thrust vector angles shown in figure 9 as was previously discussed. (See the section entitled "Flap Angle.") The shorter nozzle flaps do not provide a long expansion surface, and thereby the reduction in normal force and the consequent reduction in resultant thrust vector angle do not occur.

Sidewall Containment

Figure 11 shows the effect of cutting back the nozzle sidewalls on the internal performance of configurations at three different vector angles and expansion ratios. Tests were made with the sidewalls cut back 30 and 60 percent from full containment. In general, the effect of cutting back the sidewall on thrust ratio and resultant thrust vector angle was small, as previously documented in references 16 and 19. Cutting back the sidewall appears to cause a decrease in the effective nozzle expansion ratio. Figure 11(b) shows the configuration that has the highest expansion ratio. This configuration, which shows the largest result of the effective decrease in expansion ratio with the 60-percent-cutback sidewall, displays a larger gross thrust ratio at low NPR and a lower gross thrust ratio at high NPR. These same results were also found in references 16 and 19.

Sidewall cutback was referenced to the nozzle throat; that is, a 100-percent cutback would mean that the sidewalls would end at the nozzle throat. Since all nozzle sidewalls tested extended downstream of the nozzle throat, the discharge coefficient showed essentially no change with sidewall containment. Figure 12 shows the internal static pressure distribution for the configurations shown in figure 11(a). Lower flap pressure distributions show no influence of sidewall cutback. There are some slight differences in the upper flap pressure distribution with varying sidewall cutback. A small change in the magnitude of the shock, which is positioned very near the end of the 30-percent-cutback sidewall ($x/h_{t,n} = 4.50$), can be seen at NPR $\approx$ 4.0 and also, though to a lesser degree, at NPR $\approx$ 10.0.

Throat Approach Angle

The effect of changing throat approach angle on nozzle internal performance and resultant thrust vector angle is shown in figures 13 to 15. There are only slight changes in the thrust ratios and the resultant thrust vector angle with increasing throat approach angle. The magnitude of the increment due to a change in throat approach angle was dependent on the values of geometric thrust vector angle and nozzle expansion ratio, thus making it difficult to quantify the effect. However, it can be generally stated that an increase in the throat approach angle decreased the resultant thrust ratio while increasing the resultant thrust vector angle. The discharge coefficient is most sensitive to varying the throat approach angle, with more

than a 6-percent decrease with increasing β in the worst case (fig. 13(b)). Similar effects were noted for conical nozzles as was reported in reference 20.

Figure 16 shows the internal static pressure distributions for two of the configurations presented in figure 14(a). The primary change in the lower flap flow is an increase in the magnitude of the shock with increasing throat approach angle. Throat approach angle had little effect on the upper flap static pressure distributions.

Throat Geometry

Three lower flaps (U, V, and W) were constructed with a throat of 1.0-in. radius (see table AI), and these radiused flaps had the same throat approach angle as three sharp-corner-throat flaps (H, M, and P). That is, a configuration in which the sharp-corner-throat lower flap was replaced by a radiused lower flap would still have the same throat approach angle and geometric expansion ratio. Six configurations with a radiused lower flap were tested (two different upper flaps with each radiused lower flap). The lower flap angle and, consequently, the geometric vector angle differed slightly between the configurations with the sharp-corner throat and the configuration with the radiused throat. (See table I.) Figure 17 shows the basic internal performance data for these configurations. In general, changing the lower flap throat geometry from a sharp corner to a radiused throat increased the resultant thrust ratios. The differences in performance are greater at the higher throat approach angles and/or the low nozzle expansion ratios. This result would be expected since the radiused throat provided a much smoother flow path than the sharp corner throat, particularly at the large throat approach angles. The influence of expansion ratio on the effect of throat geometry is also obvious by comparing parts (a) and (b), (c) and (d), and (e) and (f) of figure 17. The largest effect of throat geometry was on the discharge coefficient, which has been shown to be basically insensitive to changes in geometry downstream of the nozzle throat for a constant geometric vector angle and is affected only by changes that occur upstream of the throat and, in this case, in the throat. Figure 17(f) shows the largest increase in the discharge coefficient. Similar results of the effect of throat radiusing on the discharge coefficient are reported in reference 14. It is obvious that the radiused throat is a more efficient configuration not only because of its internal performance but even more so because of its ability to pass mass flow.

Figure 18 shows the internal static pressure distributions for the configurations shown in figure 17(f). The radiused flap caused the throat (where $p/p_{t,j} = 0.528$) to move downstream not only on the lower flap but also on the upper flap which was the same hardware for both configurations. There was also a decrease in the severity of the shock on both the upper and lower flaps when a radius was added to the throat on the lower flap.

CONCLUSIONS

A parametric investigation of two-dimensional convergent-divergent nozzles with thrust vectoring has given the following conclusions:

1. The effect of expansion ratio on nozzle internal performance is predominant over any effect caused by changes in divergent flap angle.

2. Because of reduced internal flow separation at low nozzle pressure ratios, thrust vectoring is most effective for nozzles having a low expansion ratio.

3. Reduced sidewall containment (cutting back the nozzle sidewalls) results in a decrease in effective nozzle expansion ratio, but the effect on nozzle performance is small.

4. Discharge coefficient is insensitive to changes in geometry downstream of the throat for a constant geometric vector angle. Increasing throat approach angle, however, results in reduced values of discharge coefficient.

5. Changing throat geometry from a sharp corner to a radius on the lower flap produces configurations more efficient in internal performance and with a better ability to pass mass flow, particularly for the configurations with low expansion ratios and/or large throat approach angles.

NASA Langley Research Center
Hampton, VA 23665-5225
June 1, 1987

REFERENCES

1. Sedgwick, T. A.: Investigation of Non-Symmetric Two-Dimensional Nozzles Installed in Twin-Engine Tactical Aircraft. AIAA Paper No. 75-1319, Sept.-Oct. 1975.

2. Stevens, H. L.: F-15/Nonaxisymmetric Nozzle System Integration Study Support Program. NASA CR-135252, 1978.

3. F-15 2-D Nozzle System Integration Study. Volume I - Technical Report. NASA CR-145295, 1978.

4. Bergman, D.; Mace, J. L.; and Thayer, E. B.: Non-Axisymmetric Nozzle Concepts for an F-111 Test Bed. AIAA Paper No. 77-841, July 1977.

5. Hiley, P. E.; Wallace, H. W.; and Booz, D. E.: Nonaxisymmetric Nozzles Installed in Advanced Fighter Aircraft. J. Aircr., vol. 13, no. 12, Dec. 1976, pp. 1000-1006.

6. Berrier, B. L.; and Re, R. J.: A Review of Thrust-Vectoring Schemes for Fighter Aircraft. AIAA Paper No. 78-1023, July 1978.

7. Goetz, G. F.; Petit, J. E.; and Sussman, M. B.: Non-Axisymmetric Nozzle Design and Evaluation for F-111 Flight Demonstration. AIAA Paper 78-1025, July 1978.

8. Stevens, H. L.; Thayer, E. B.; and Fullerton, J. F.: Development of the Multi-Function 2-D/C-D Nozzle. AIAA-81-1491, July 1981.

9. Capone, Francis J.; and Berrier, Bobby L.: Investigation of Axisymmetric and Nonaxisymmetric Nozzles Installed on a 0.10-Scale F-18 Prototype Airplane Model. NASA TP-1638, 1980.

10. Capone, Francis J.; and Reubush, David E.: Effects of Varying Podded Nacelle-Nozzle Installations on Transonic Aeropropulsive Characteristics of a Supersonic Fighter Aircraft. NASA TP-2120, 1983.

11. Hiley, P. E.; and Bowers, D. L.: Advanced Nozzle Integration for Supersonic Strike Fighter Application. AIAA-81-1441, July 1981.

12. Berrier, Bobby L.; Palcza, J. Lawrence; and Richey, G. Keith: Nonaxisymmetric Nozzle Technology Program - An Overview. AIAA Paper 77-1225, Aug. 1977.

13. Berrier, Bobby L.; and Re, Richard J.: Effect of Several Geometric Parameters on the Static Internal Performance of Three Nonaxisymmetric Nozzle Concepts. NASA TP-1468, 1979.

14. Mason, Mary L.; Putnam, Lawrence E.; and Re, Richard J.: The Effect of Throat Contouring on Two-Dimensional Converging-Diverging Nozzles at Static Conditions. NASA TP-1704, 1980.

15. Capone, Francis J.: Static Performance of Five Twin-Engine Nonaxisymmetric Nozzles With Vectoring and Reversing Capability. NASA TP-1224, 1978.

16. Re, Richard J.; and Leavitt, Laurence D.: Static Internal Performance Including Thrust Vectoring and Reversing of Two-Dimensional Convergent-Divergent Nozzles. NASA TP-2253, 1984.

17. Peddrew, Kathryn H., compiler: A User's Guide to the Langley 16-Foot Transonic Tunnel. NASA TM-83186, 1981.

18. Re, Richard J.; and Leavitt, Laurence D.: Static Internal Performance of Single-Expansion-Ramp Nozzles With Various Combinations of Internal Geometric Parameters. NASA TM-86270, 1984.

19. Yetter, Jeffery A.; and Leavitt, Laurence D.: Effects of Sidewall Geometry on the Installed Performance of Nonaxisymmetric Convergent-Divergent Exhaust Nozzles. NASA TP-1771, 1980.

20. Grey, Ralph E., Jr.; and Wilsted, H. Dean: Performance of Conical Jet Nozzles in Terms of Flow and Velocity Coefficients. NACA TN 1757, 1948.

TABLE I.- NOZZLE PARAMETERS

Configuration	α_l, deg	α_u, deg	$l/h_{t,n}$	β, deg	δ_v, deg	A_e/A_t	Design NPR
A01F	11.60	-8.60	1.00	7.60	10.10	1.05	2.6
A02G	23.40	-20.40	↓	↓	21.90	1.05	2.6
A03F	11.60	1.40	↓	↓	5.10	1.23	4.1
A04G	23.40	-10.40	↓	↓	16.90	1.22	4.0
B05H	11.60	-8.60	2.50	↓	10.10	1.13	3.3
B06I	23.40	-20.40	↓	↓	21.90	1.12	3.2
B07H	11.60	1.40	↓	↓	5.10	1.56	6.7
B08I	23.40	-10.40	↓	↓	16.90	1.55	6.7
A09J	11.60	-8.60	1.00	27.40	10.10	1.05	2.6
A10K	23.40	-20.40	↓	↓	21.90	1.05	2.6
A11J	11.60	1.40	↓	↓	5.10	1.23	4.1
A12K	23.40	-10.40	↓	↓	16.90	1.22	4.0
B13L	11.60	-8.60	2.50	↓	10.10	1.13	3.3
B14M	23.40	-20.40	↓	↓	21.90	1.12	3.2
B15L	11.60	1.40	↓	↓	5.10	1.56	6.7
B16M	23.40	-10.40	↓	↓	16.90	1.55	6.7
C17N	10.00	-2.00	1.75	17.50	6.00	1.24	4.1
C18O	25.00	-17.00	↓	↓	21.00	1.23	4.1
C19P	17.50	-15.80	↓	↓	16.65	1.05	2.6
C20P	↓	-3.20	↓	↓	10.35	1.43	5.6
D21Q	↓	-9.50	.80	↓	13.50	1.11	3.1
E22R	↓	↓	2.70	↓	↓	1.37	5.2
C23S	↓	↓	1.75	5.00	↓	1.24	4.1
C24T	↓	↓	1.75	30.00	↓	1.24	4.1

TABLE I.- Concluded

Configuration	α_l, deg	α_u, deg	$l/h_{t,n}$	β, deg	δ_v, deg	A_e/A_t	Design NPR
C25P	17.50	-9.50	1.75	17.50	13.50	1.24	4.1
A05H	11.60	-8.60	2.50	7.60	10.10	1.13	3.3
C05H	11.60	-8.60	↓	↓	10.10	1.13	3.3
A06I	23.40	-20.40	↓	↓	21.90	1.12	3.2
C06I	↓	-20.40	↓	↓	21.90	1.12	3.2
A08I	↓	-10.40	↓	↓	16.90	1.55	6.7
C08I	↓	-10.40	↓	↓	16.90	1.55	6.7
B05U	12.10	-8.60	↓	↓	10.35	1.13	3.3
B07U	12.10	1.40	↓	↓	5.35	1.56	6.7
B14V	25.60	-20.40	↓	27.40	23.00	1.10	3.1
B16V	25.60	-10.40	↓	27.40	18.00	1.53	6.4
C19W	19.30	-15.80	1.75	17.50	17.55	1.04	2.5
C20W	19.30	-3.20	↓	17.50	11.25	1.42	5.6
C26X	20.00	-10.00	↓	45.00	15.00	1.30	4.7
C27Y	20.00	-10.00	↓	55.00	15.00	1.30	4.7
C26Z	15.00	-10.00	↓	45.00	12.50	1.15	3.5
C27AA	15.00	-10.00	↓	55.00	12.50	1.15	3.5

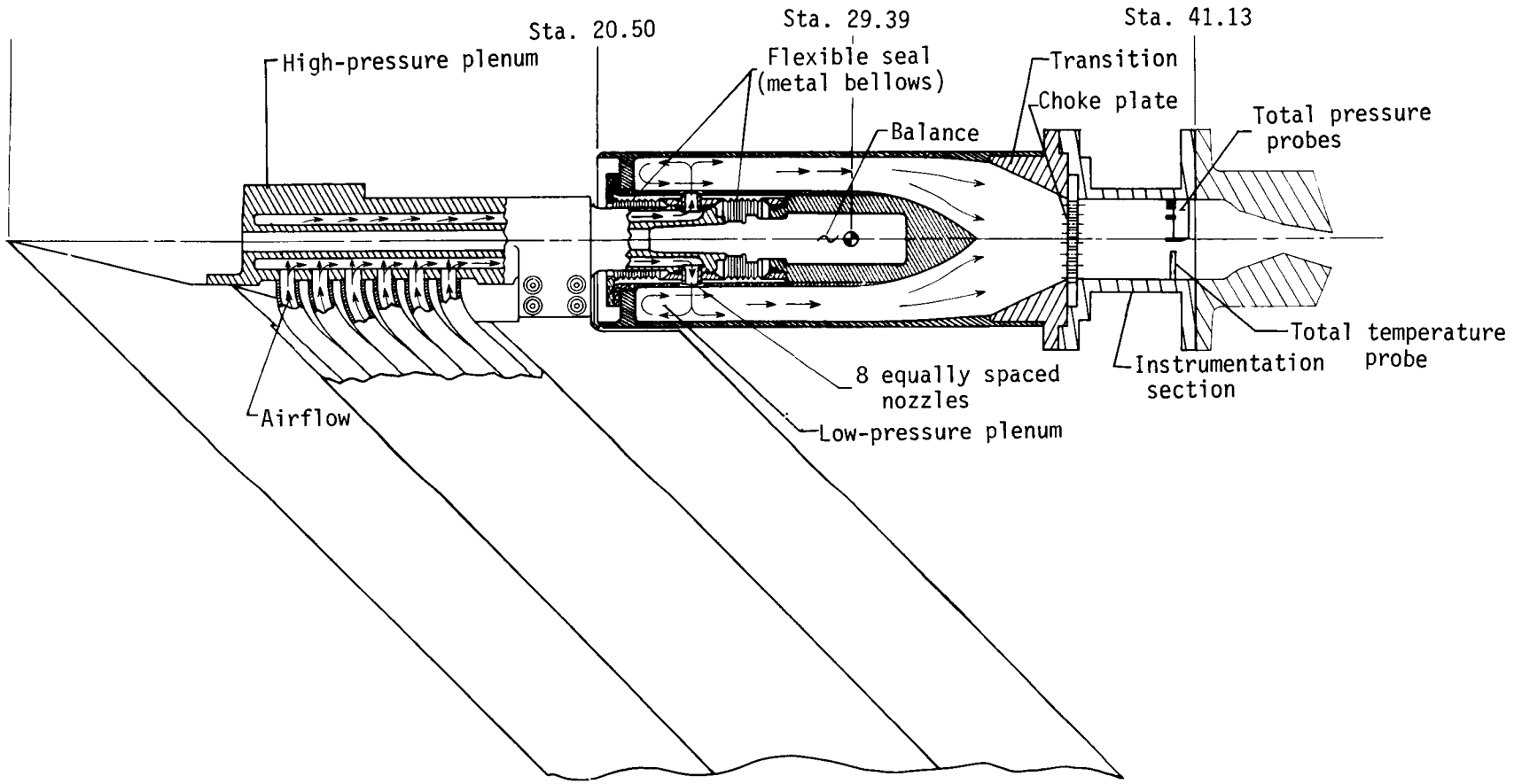

Figure 1.- Sketch of air-powered nacelle model with typical nozzle configuration installed. Linear dimensions are in inches.

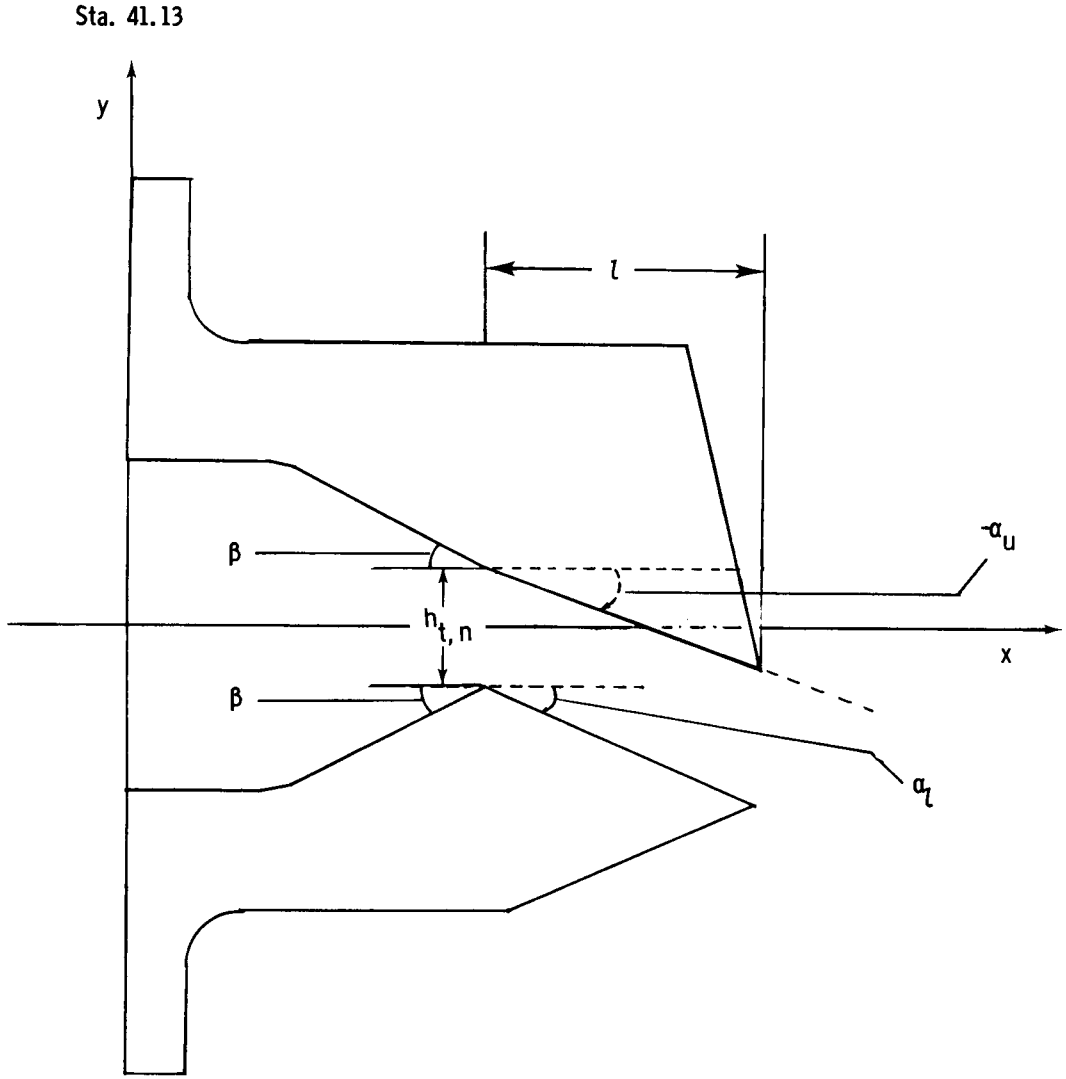

(a) Upper and lower flaps.

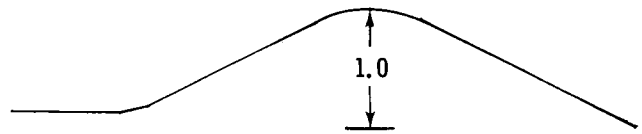

(b) Radiused lower flap.

Figure 2.- Sketch of typical nozzle flaps defining flap parameters. All dimensions are in inches unless otherwise noted.

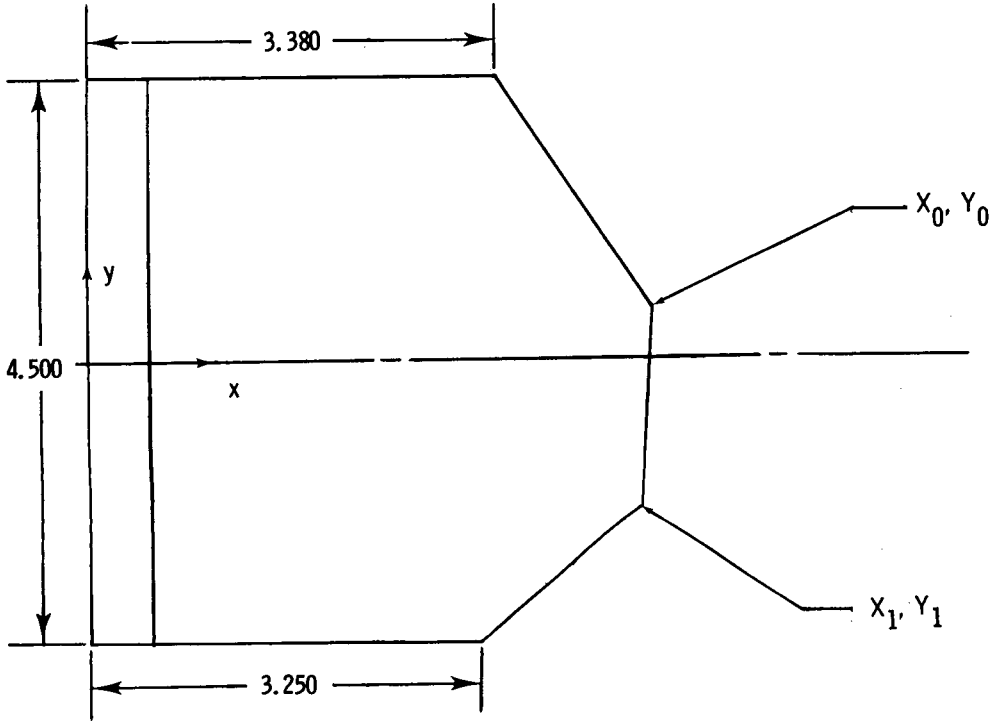

Sidewall pair	X_0, Y_0	X_1, Y_1
301, 302	3.9442, 0.5230	3.9178, -0.8971
303, 304	5.3837, 0.5598	5.2546, -1.4714
305, 306	4.7056, 0.4395	4.5860, -1.2396
307, 308	3.7890, 0.3680	3.7630, -0.7406
309, 310	5.6630, 0.0544	5.5750, -1.3119

Figure 3.- Sketch of typical sidewall showing sidewall geometry. All dimensions are in inches.

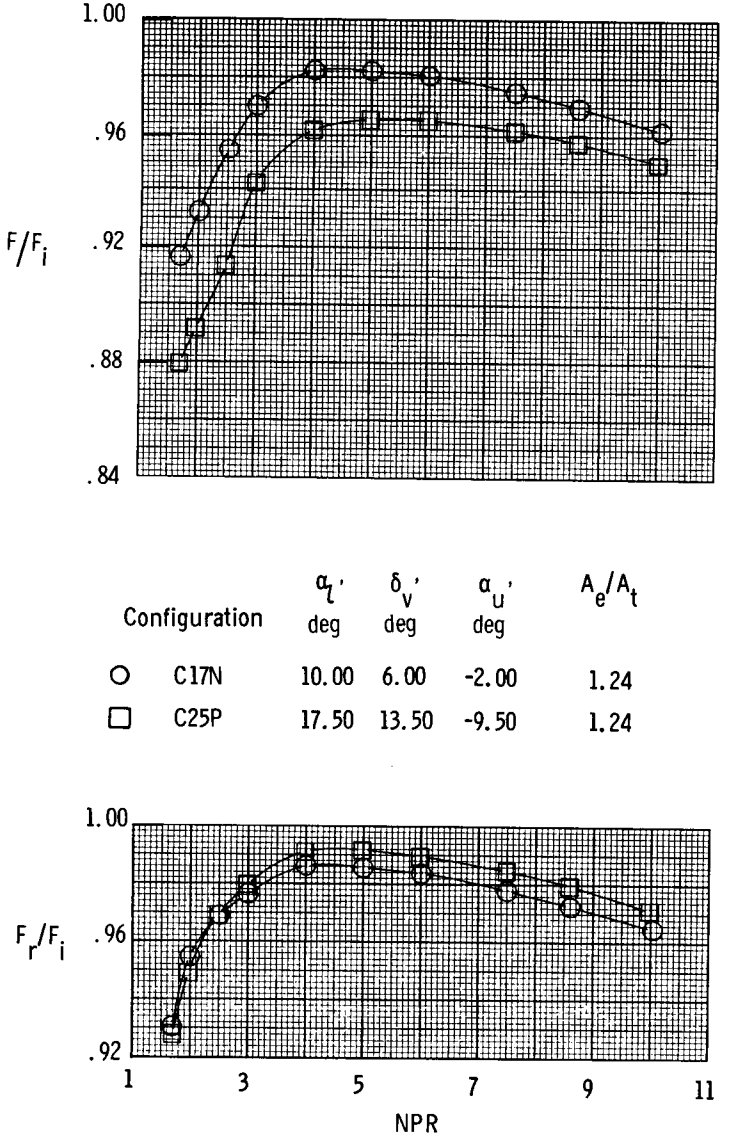

Configuration		α_l, deg	δ_v, deg	α_u, deg	A_e/A_t
○	C17N	10.00	6.00	-2.00	1.24
□	C25P	17.50	13.50	-9.50	1.24

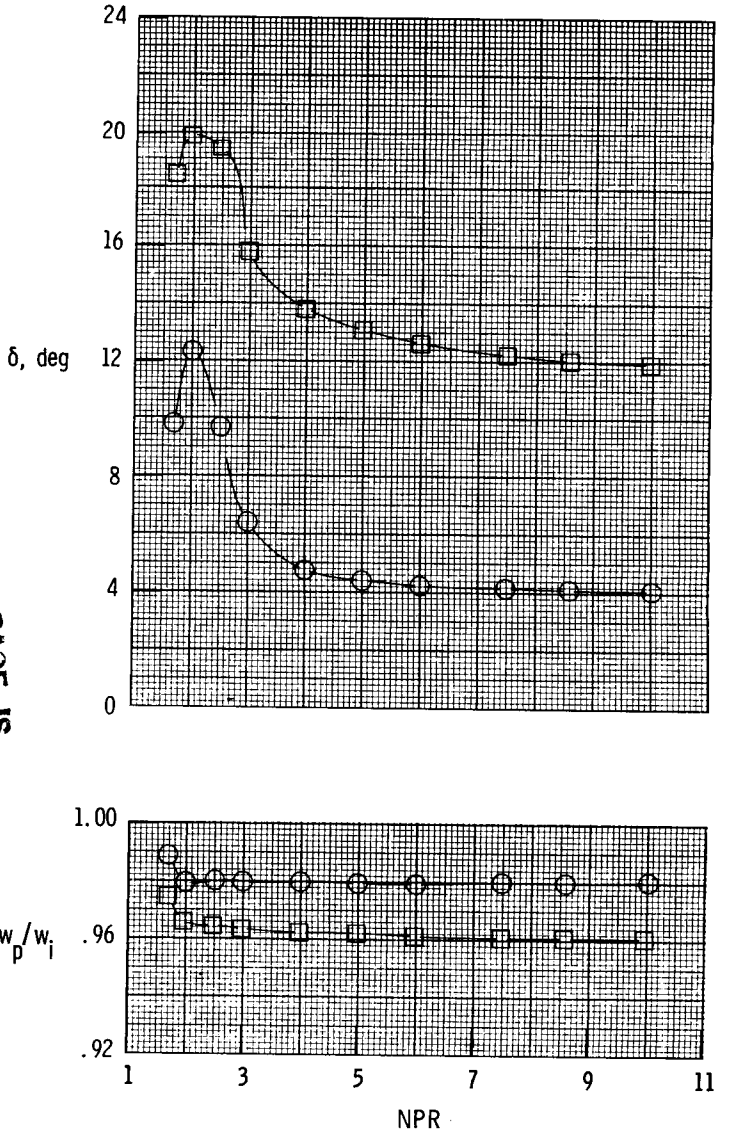

(a) Nozzle performance.

Figure 4.- Effect of geometric thrust vector angle on nozzle performance parameters and pitching moment.

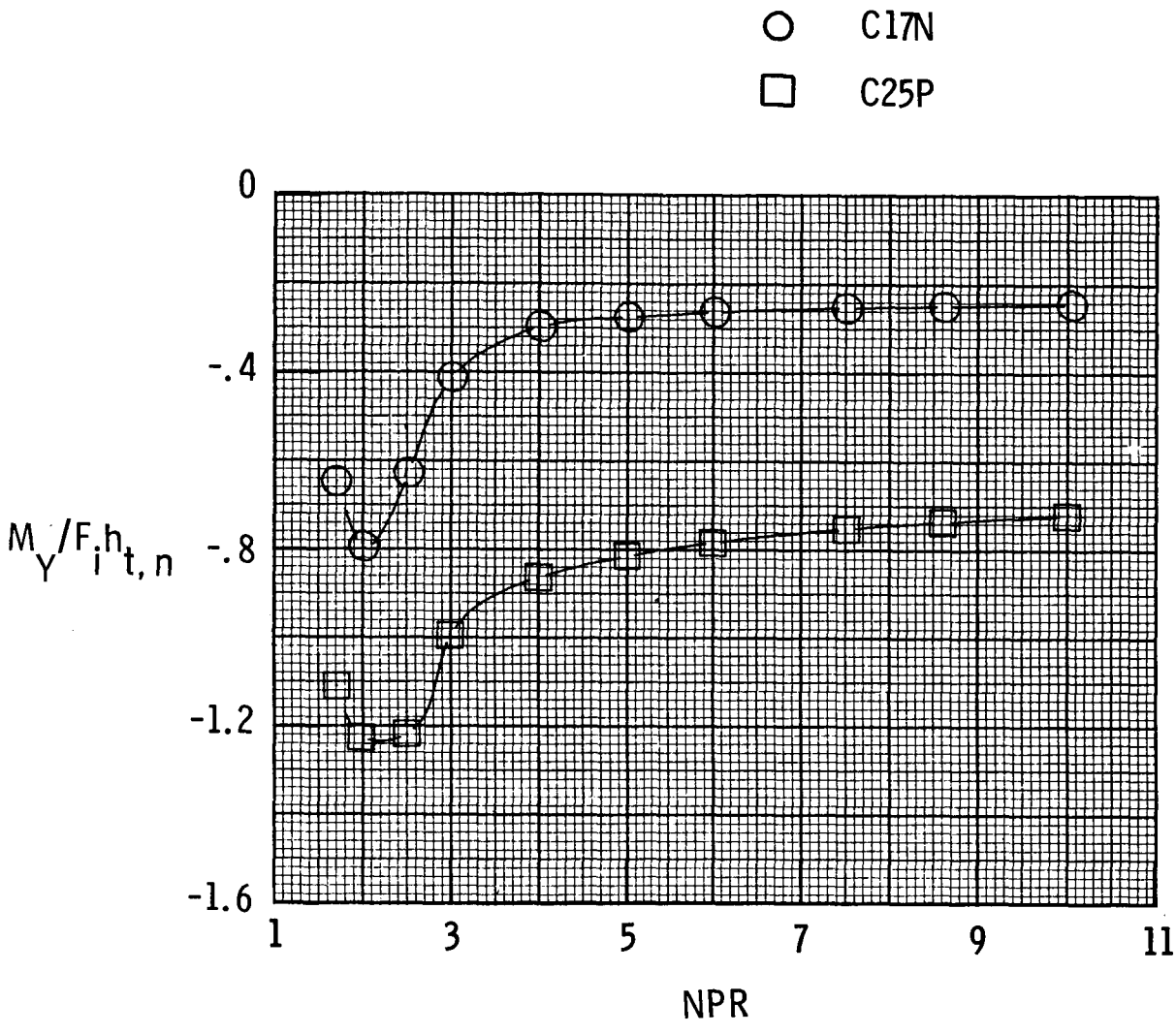

(b) Pitching moment.

Figure 4.- Concluded.

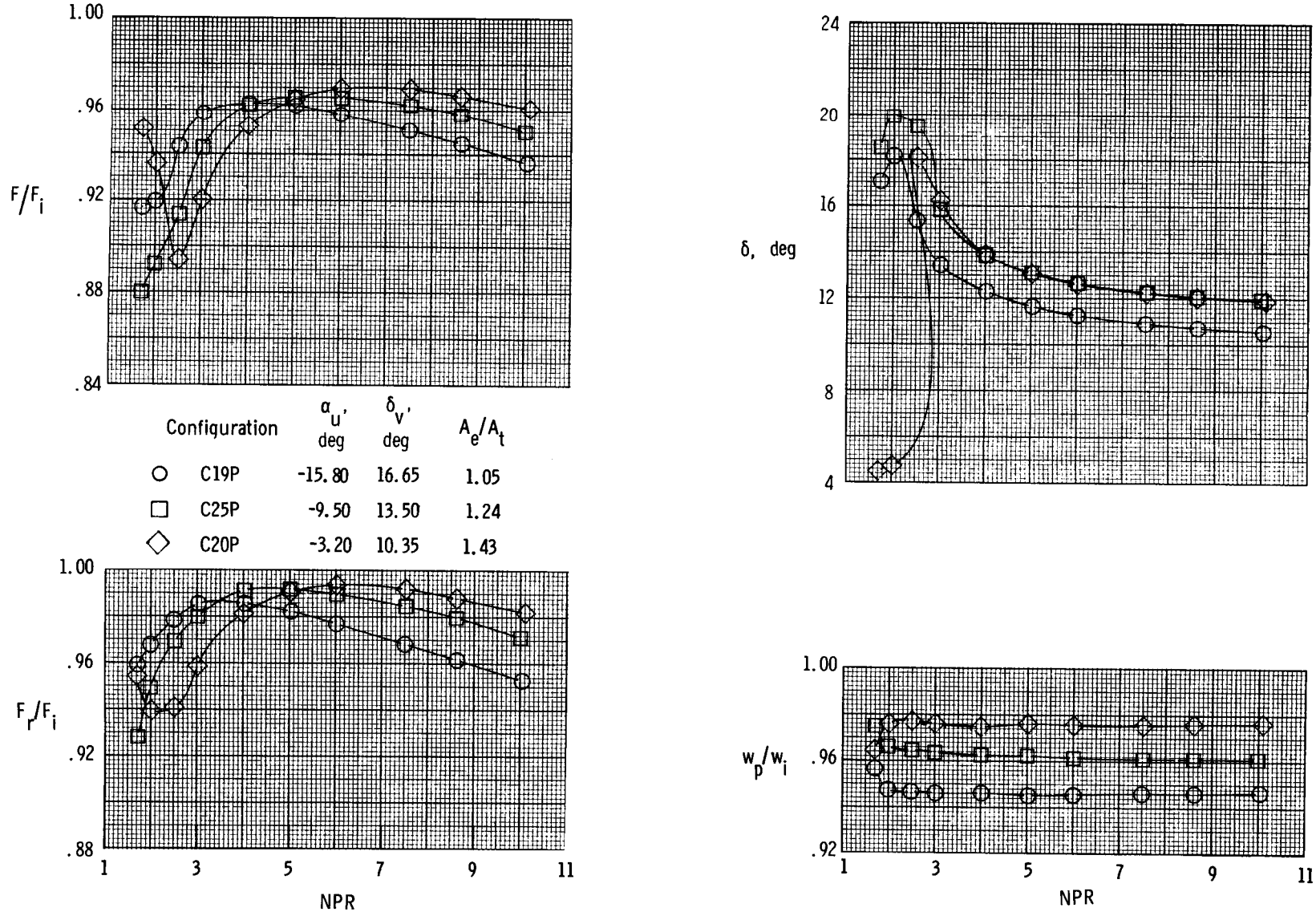

(a) Nozzle performance.

Figure 5.- Effect of upper flap angle on nozzle performance parameters and pitching moment.

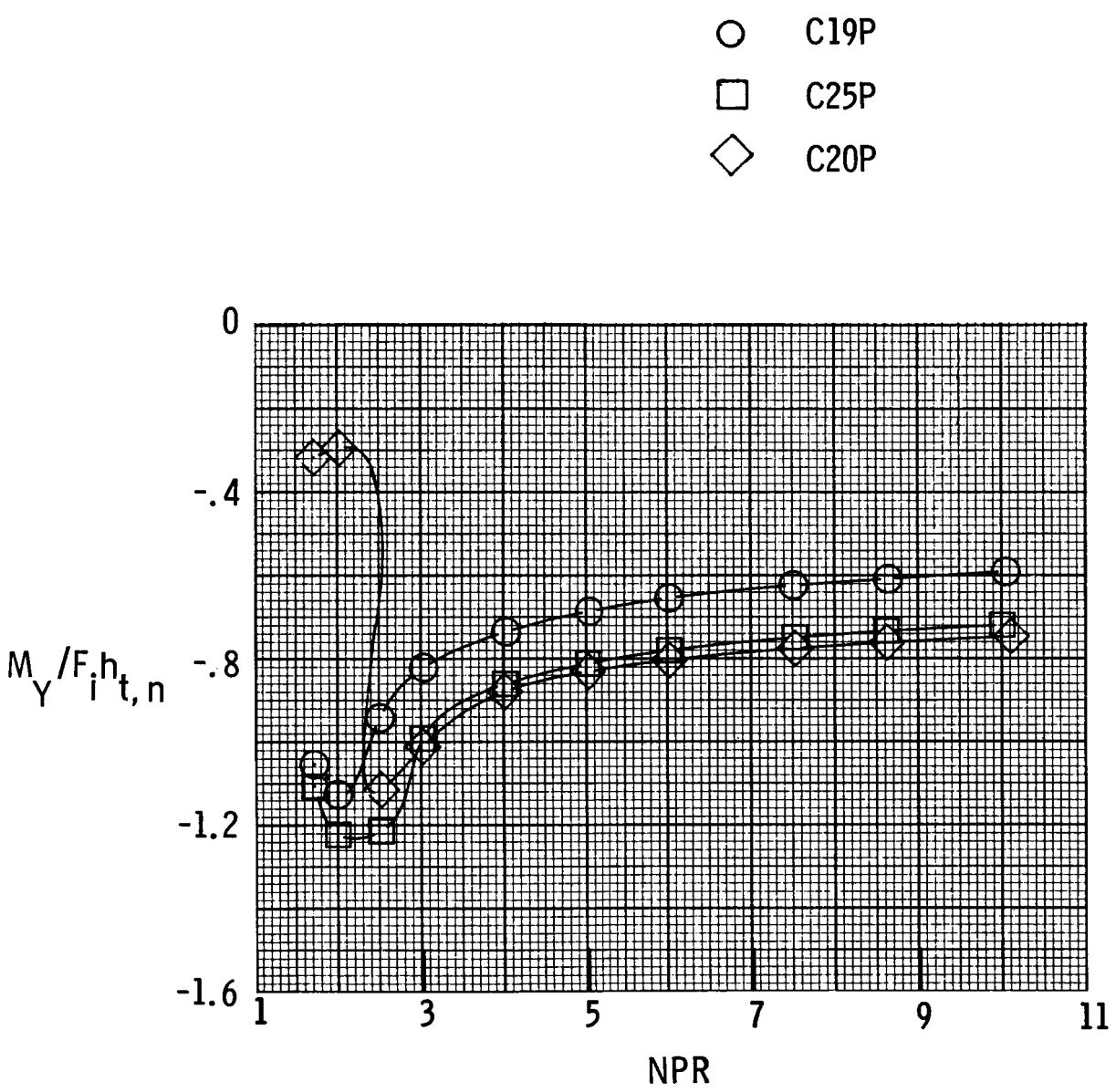

(b) Pitching moment.

Figure 5.- Concluded.

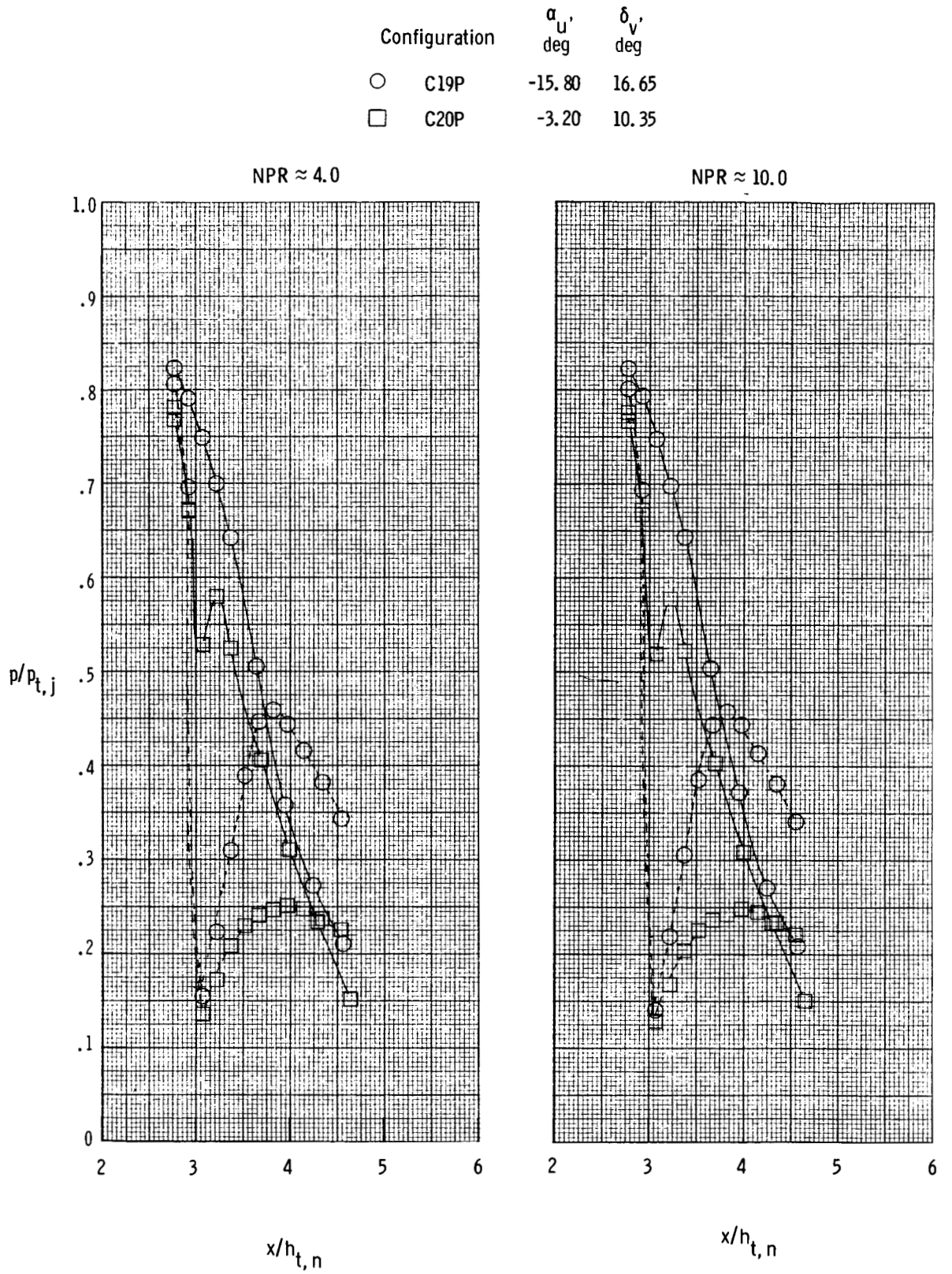

Figure 6.- Effect of upper flap angle on internal static pressure distributions for configurations C19P and C20P. Dashed lines indicate lower flap.

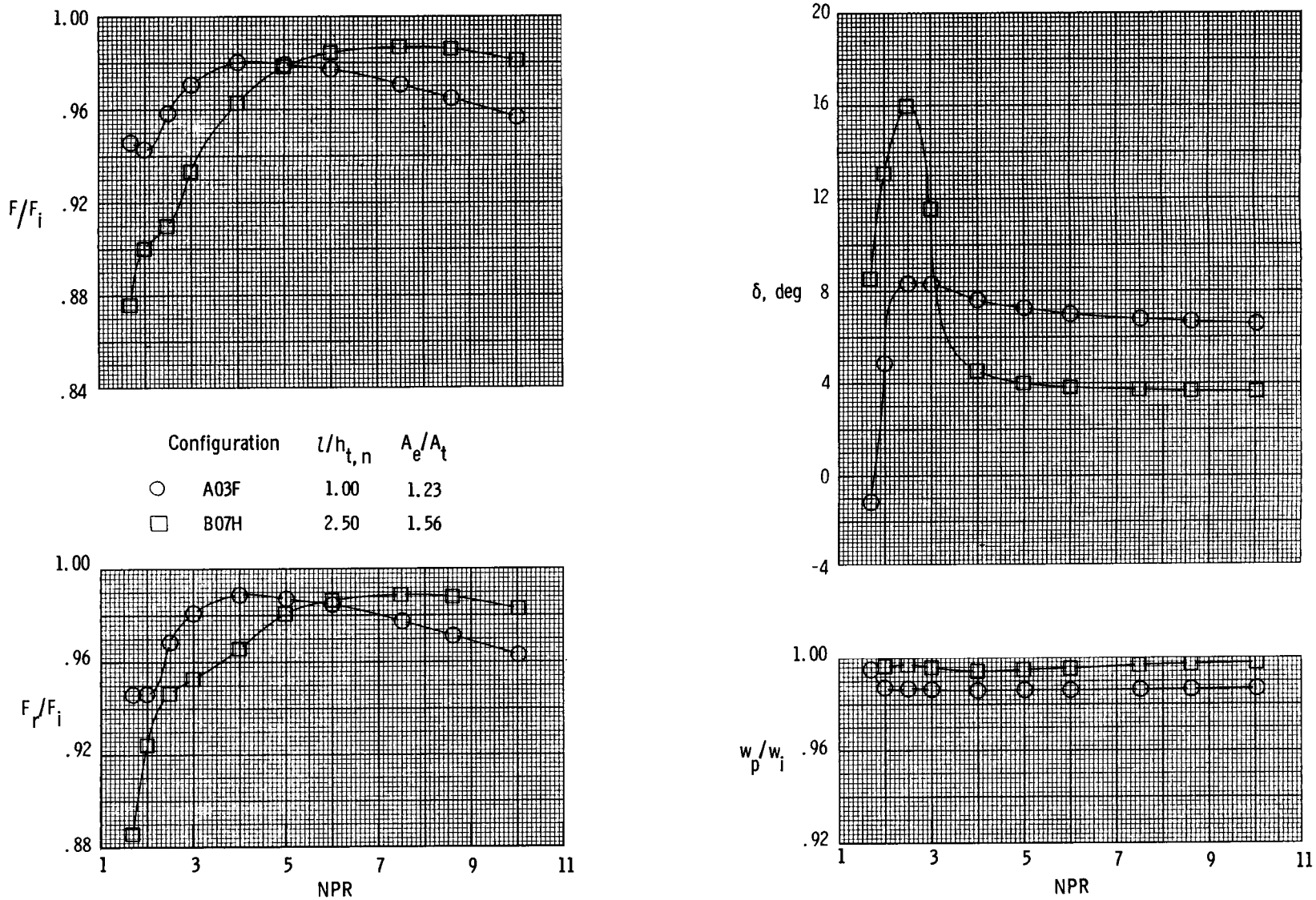

(a) Nozzle performance with $\delta_v = 5.10°$.

Figure 7.- Effect of divergent flap length on nozzle performance parameters and pitching moment with $\beta = 7.60°$.

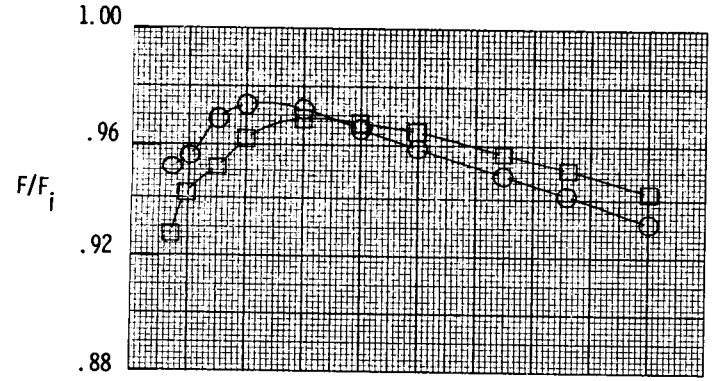

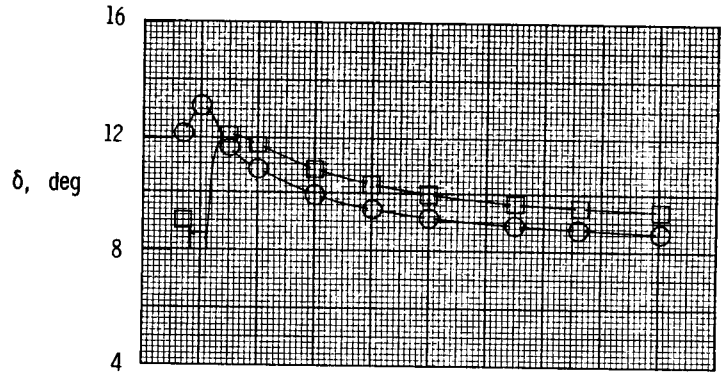

Configuration		$l/h_{t,n}$	A_e/A_t
○	A01F	1.00	1.05
□	B05H	2.50	1.13

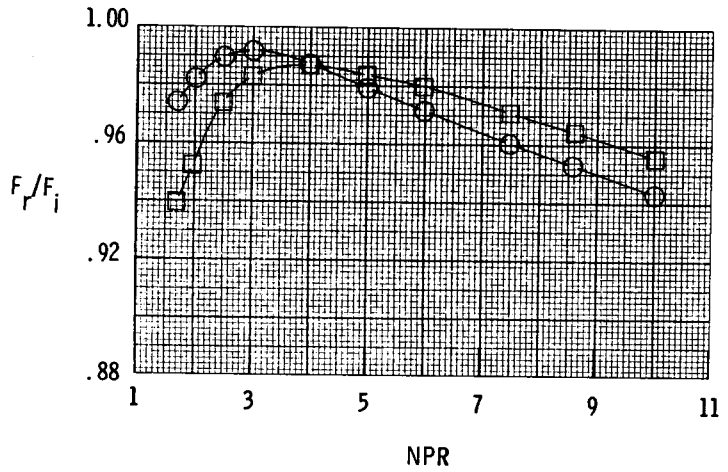

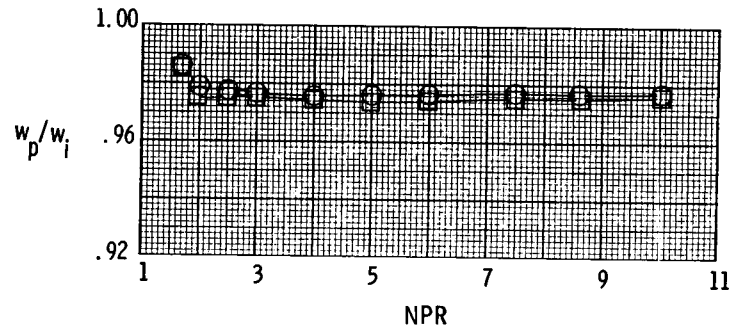

(b) Nozzle performance with $\delta_v = 10.10°$.

Figure 7.- Continued.

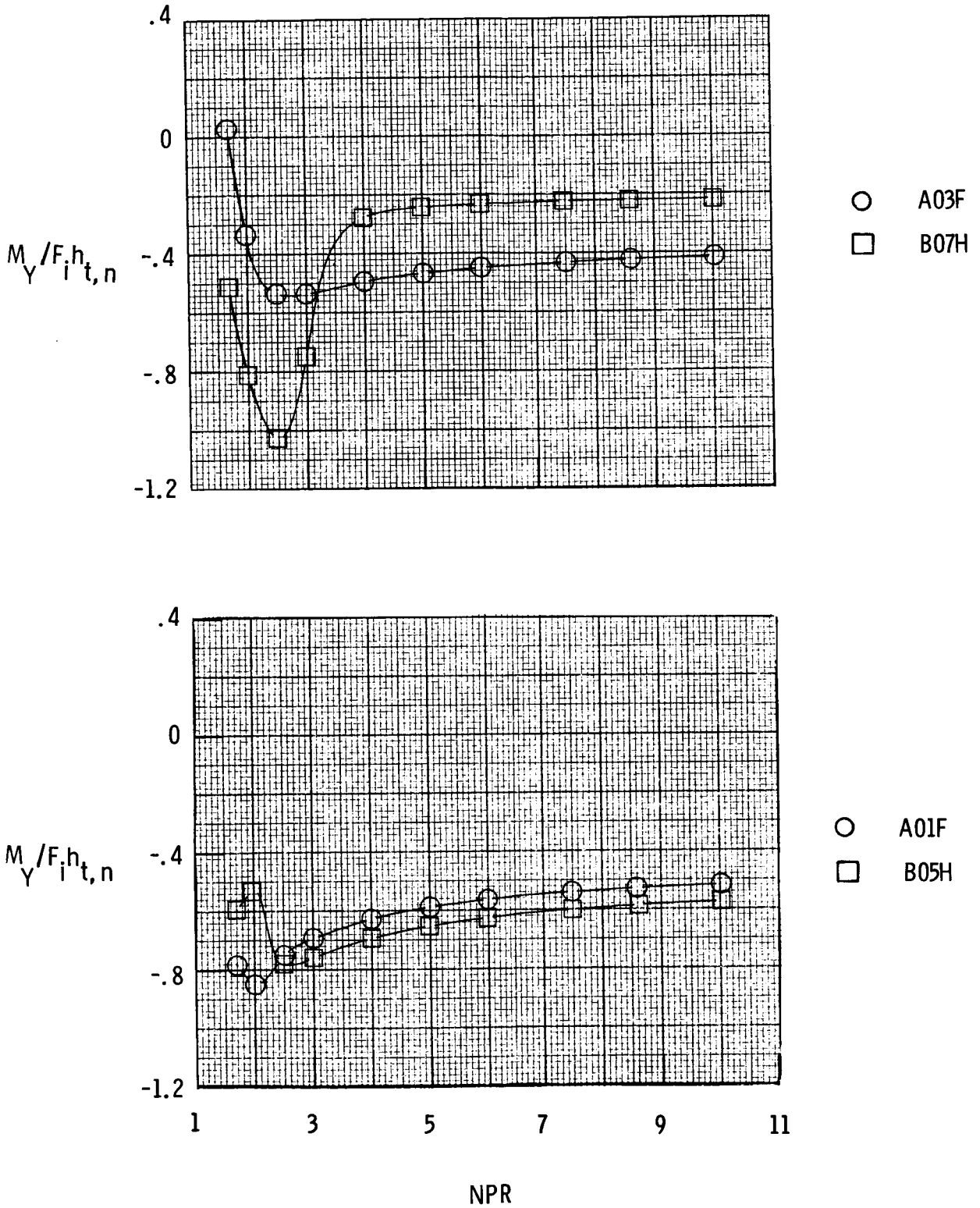

(c) Pitching moment.

Figure 7.- Concluded.

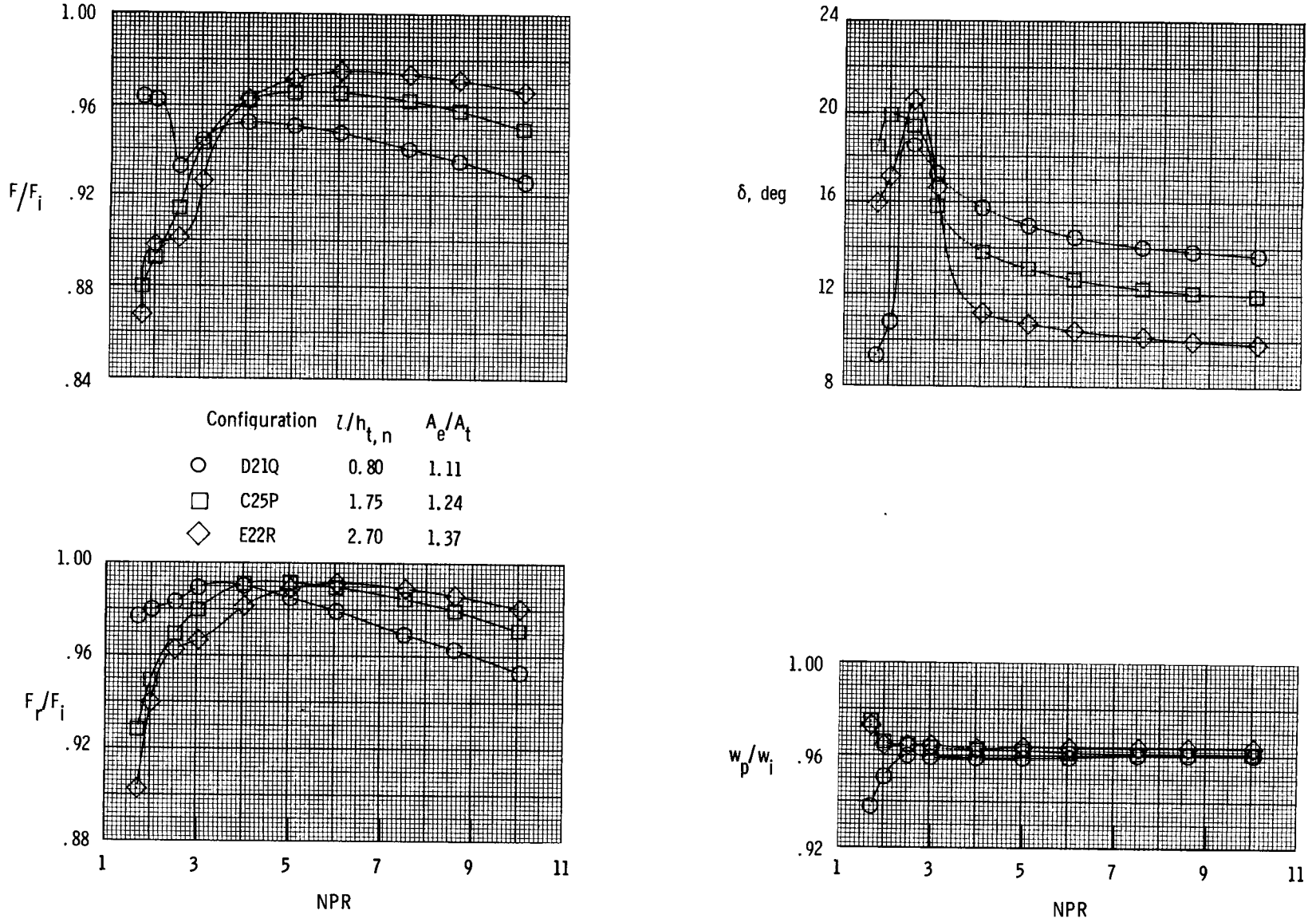

(a) Nozzle performance with $\delta_v = 13.50°$.

Figure 8.- Effect of divergent flap length on nozzle performance parameters and pitching moment with $\beta = 17.50°$.

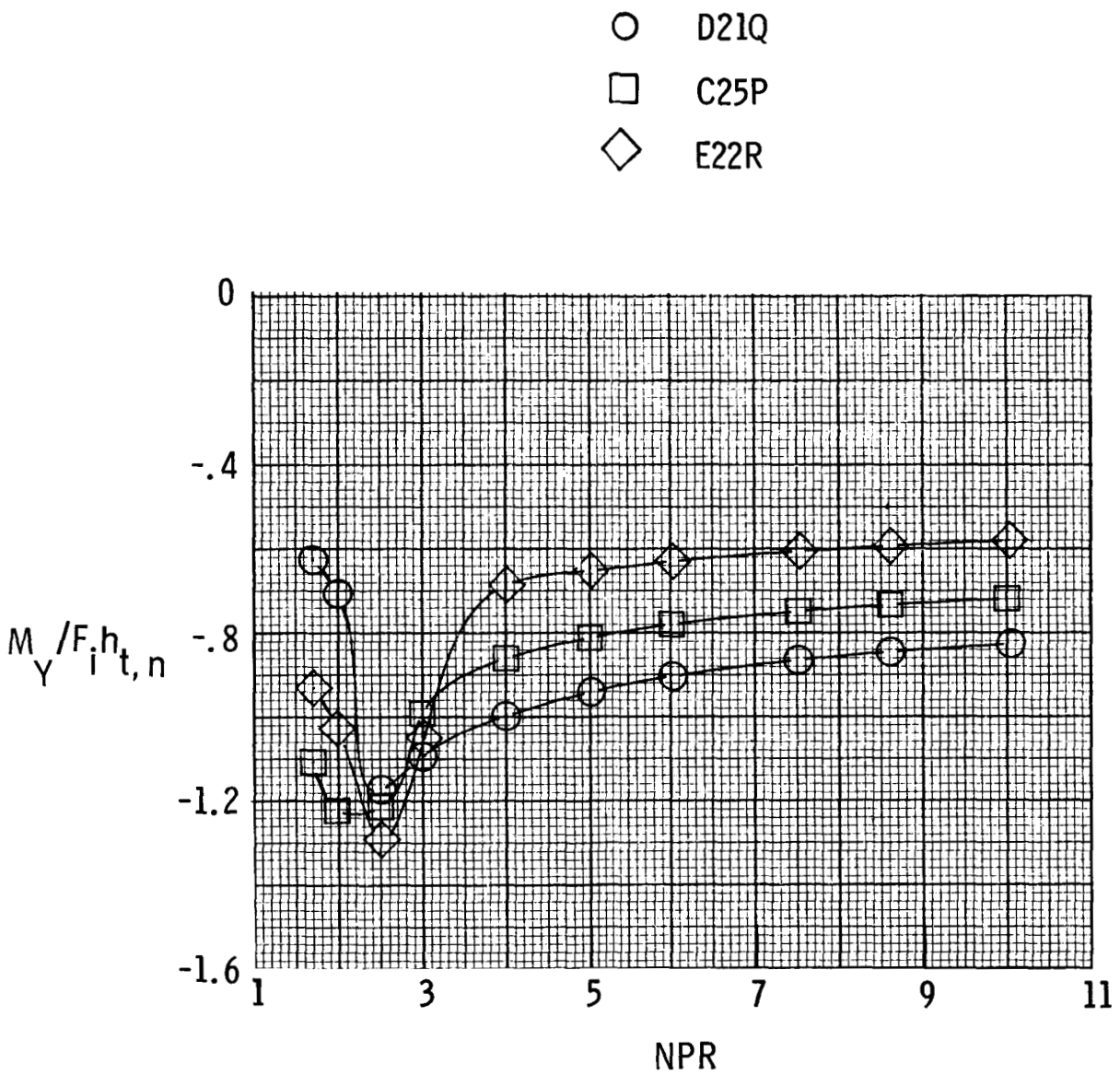

(b) Pitching moment.

Figure 8.- Concluded.

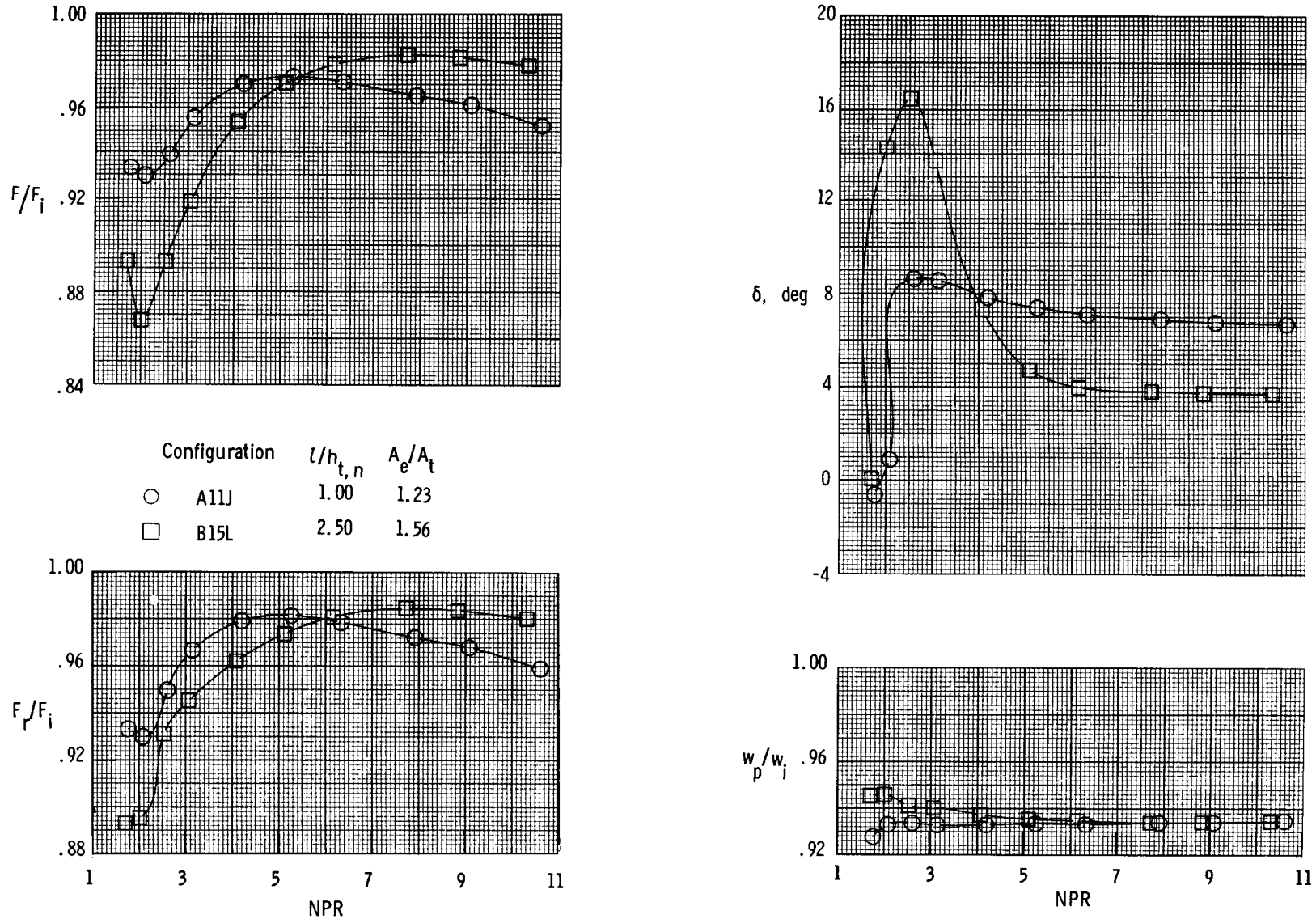

(a) Nozzle performance with $\delta_v = 5.10°$.

Figure 9.- Effect of divergent flap length on nozzle performance parameters and pitching moment with $\beta = 27.40°$.

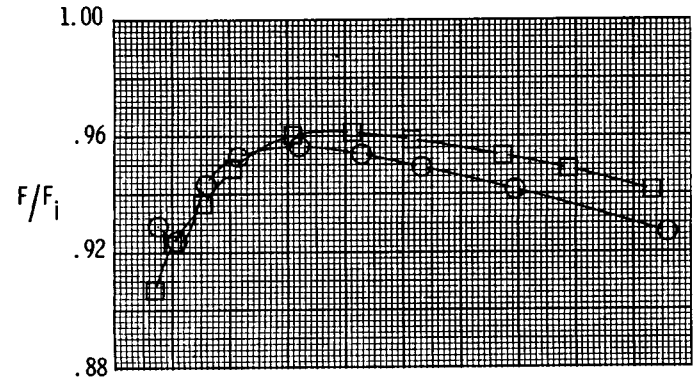

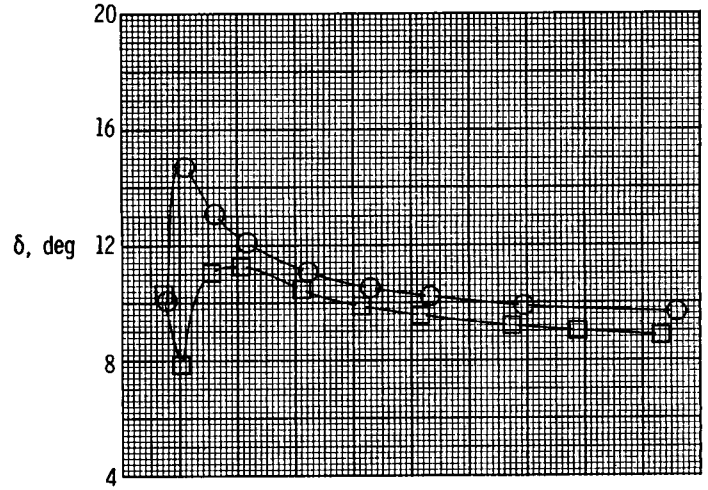

Configuration		$l/h_{t,n}$	A_e/A_t
○	A09J	1.00	1.05
□	B13L	2.50	1.13

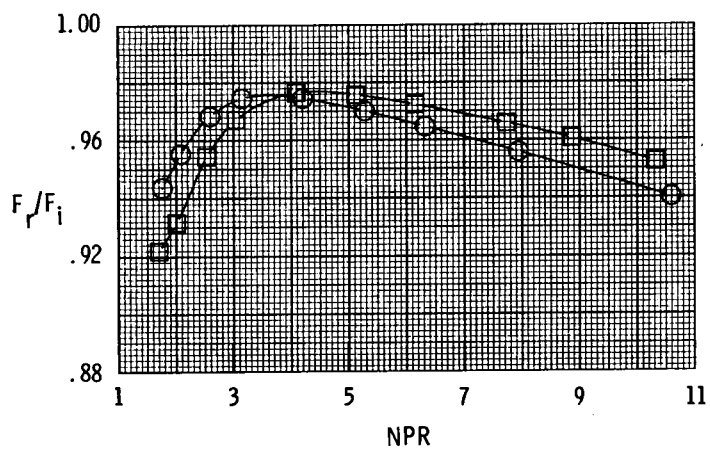

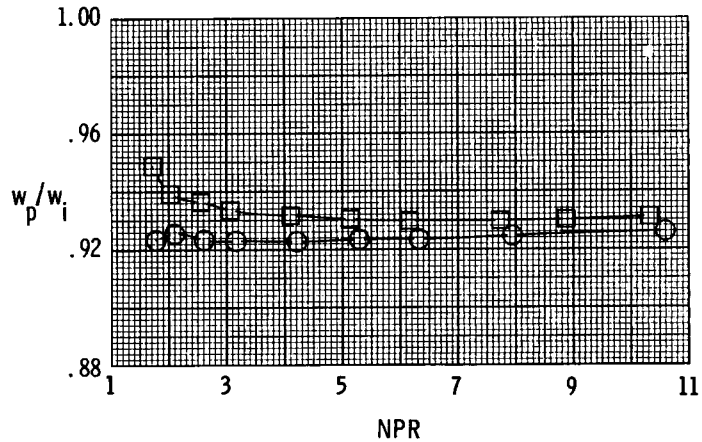

(b) Nozzle performance with $\delta_v = 10.10°$.

Figure 9.- Continued.

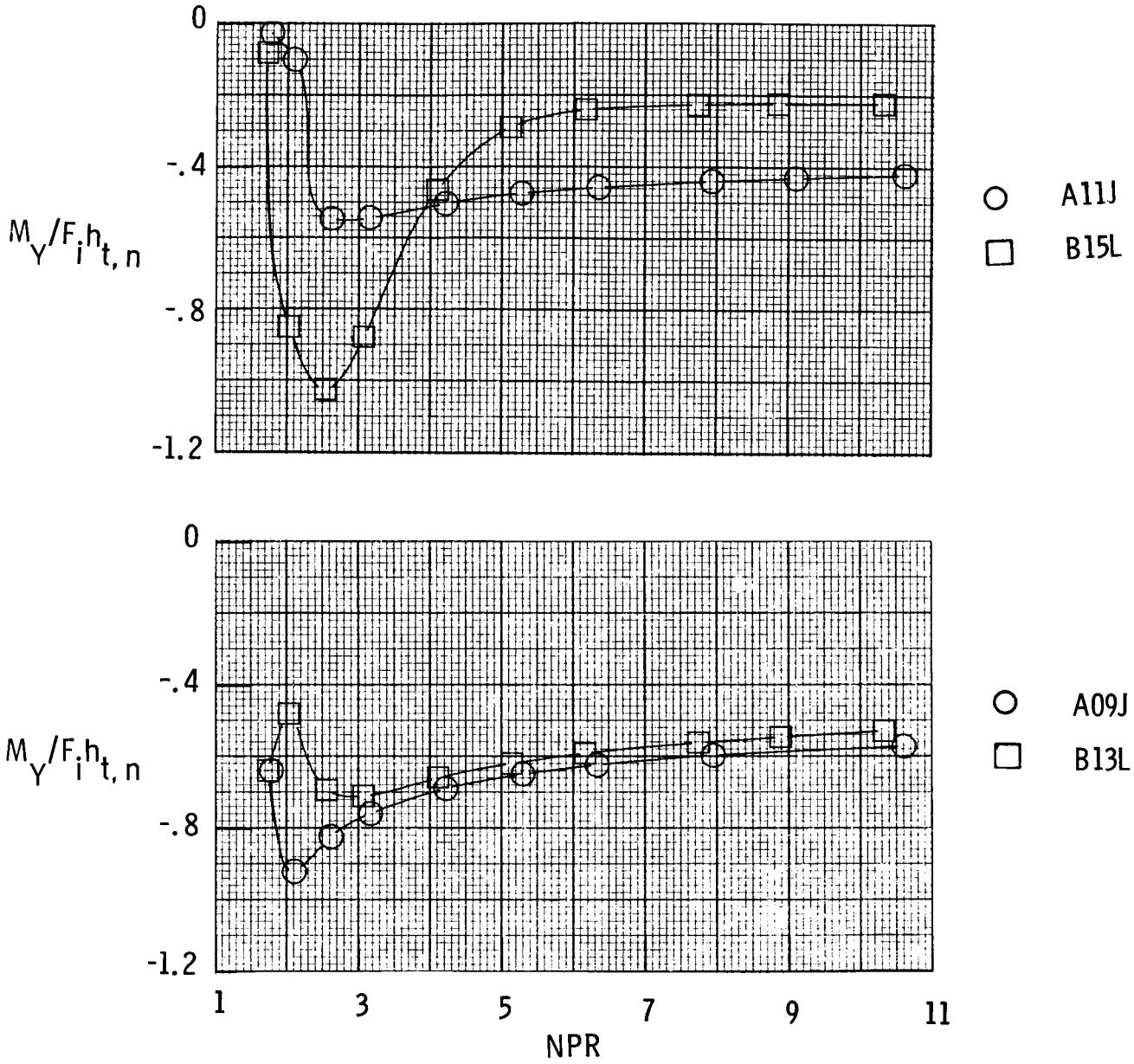

(c) Pitching moment.

Figure 9.- Concluded.

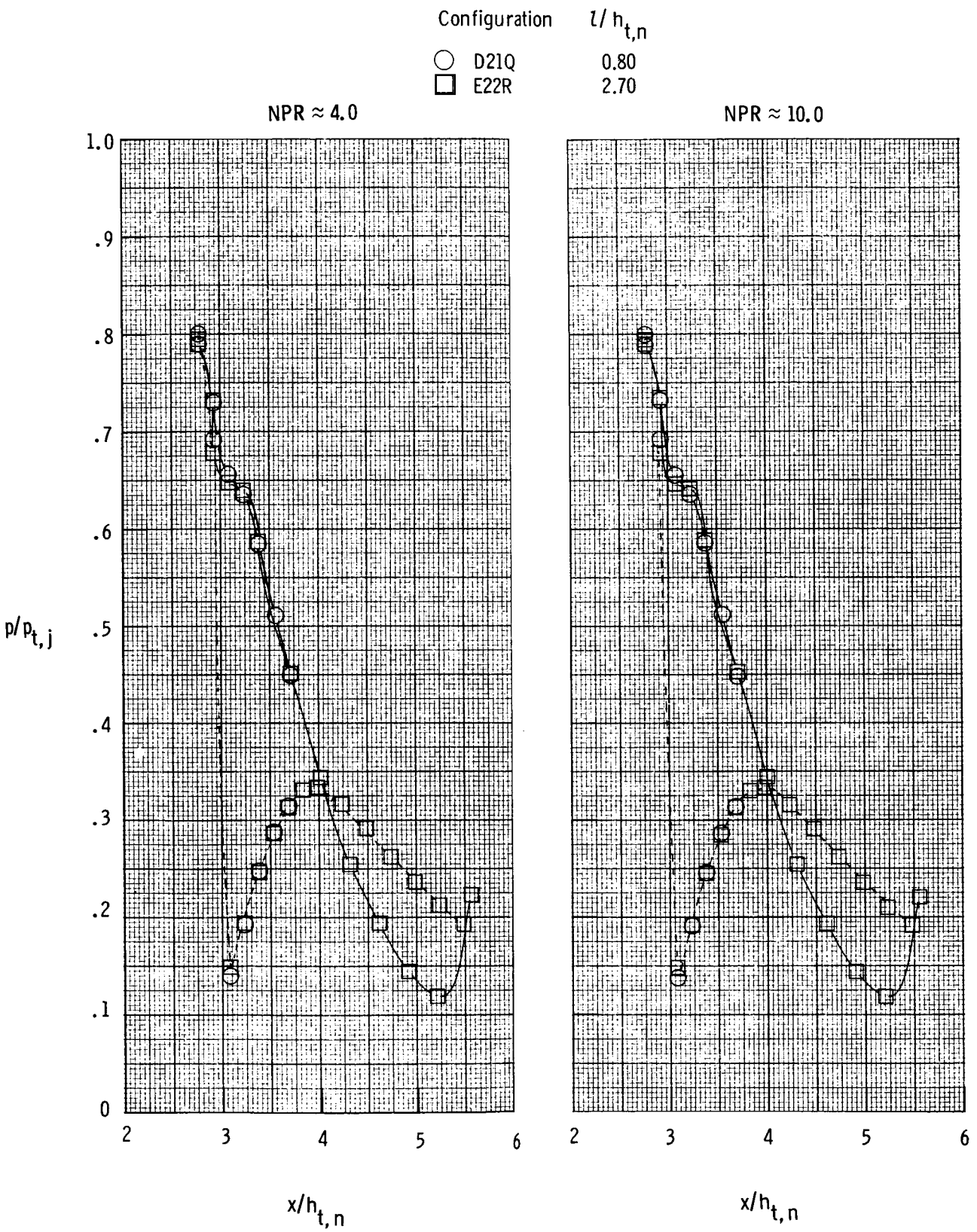

Figure 10.- Effect of divergent flap length on internal static pressure distributions for configurations D21Q and E22R. Dashed lines indicate lower flap.

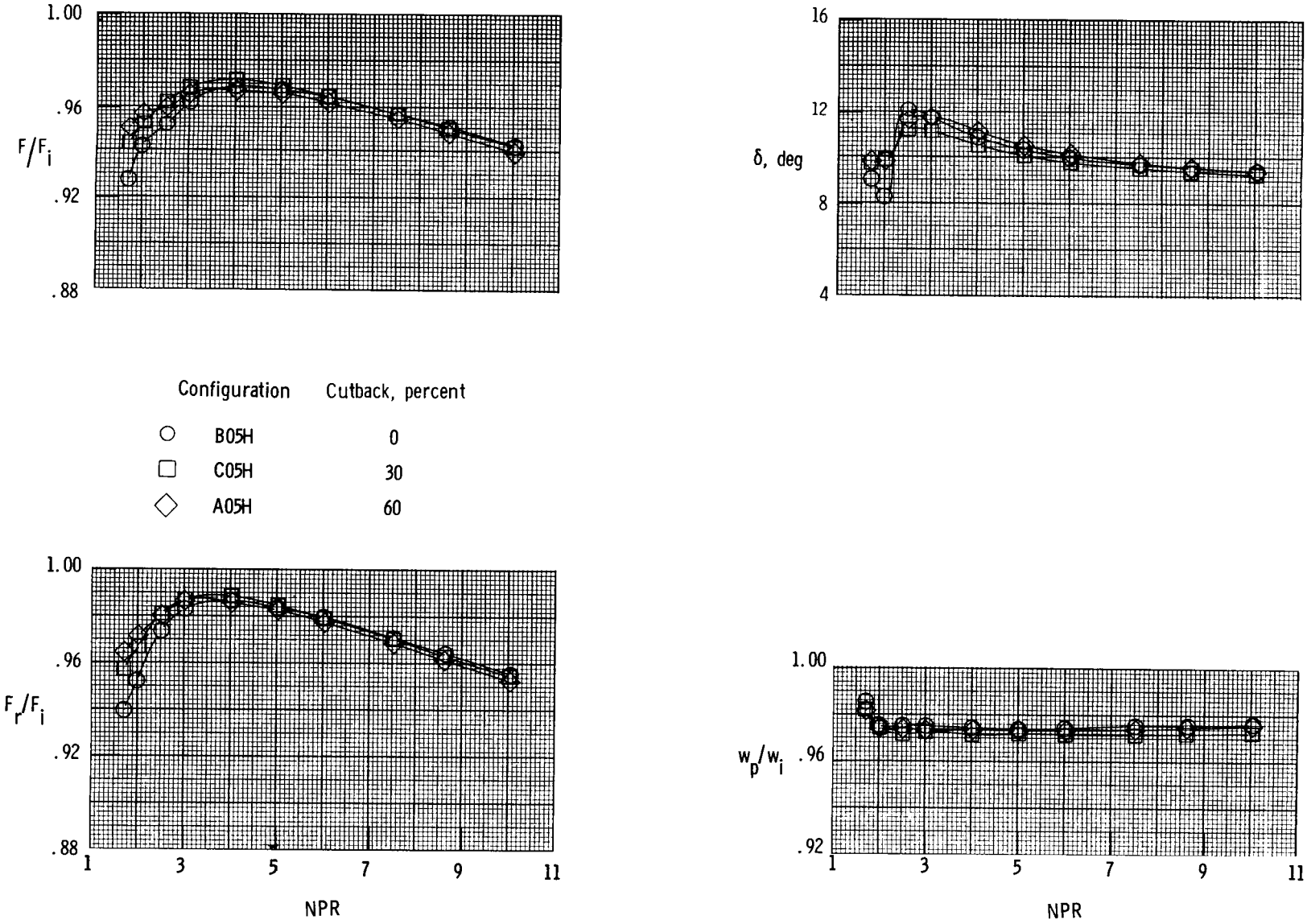

(a) Nozzle performance with $\delta_v = 10.10°$.

Figure 11.- Effect of sidewall containment on nozzle performance parameters and pitching moment.

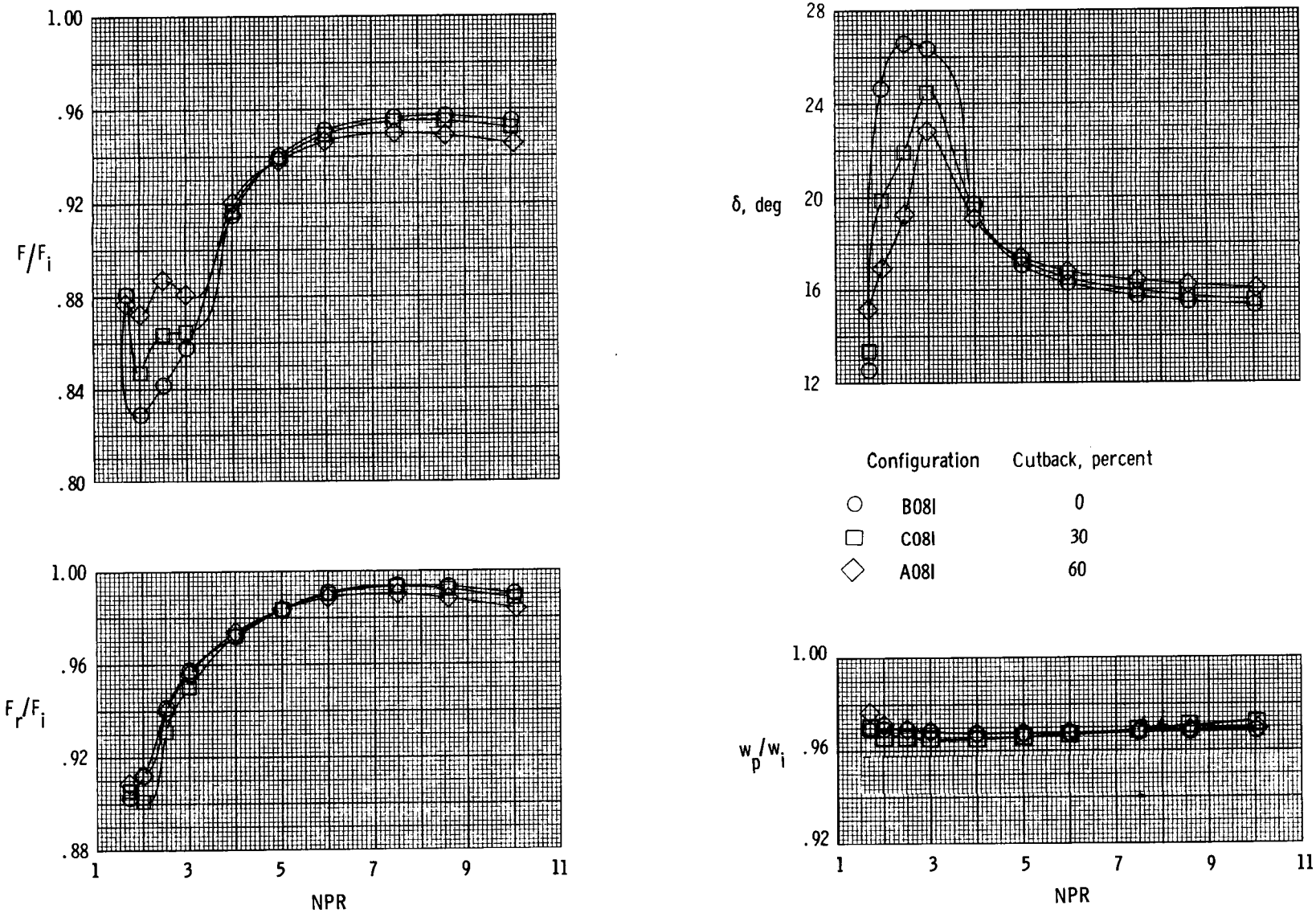

(b) Nozzle performance with δ_v = 16.90°.

Figure 11.- Continued.

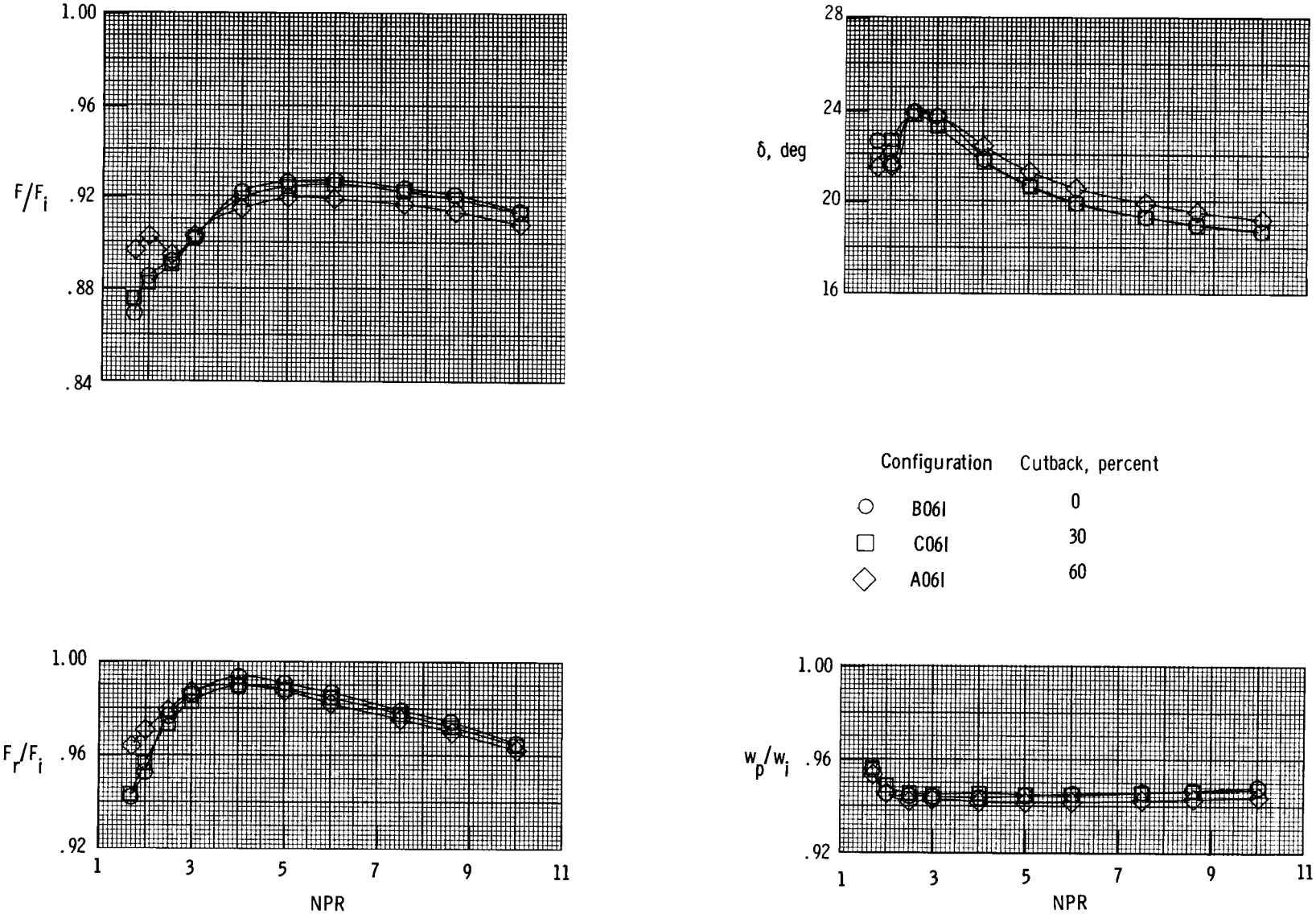

(c) Nozzle performance with $\delta_v = 21.90°$.

Figure 11.- Continued.

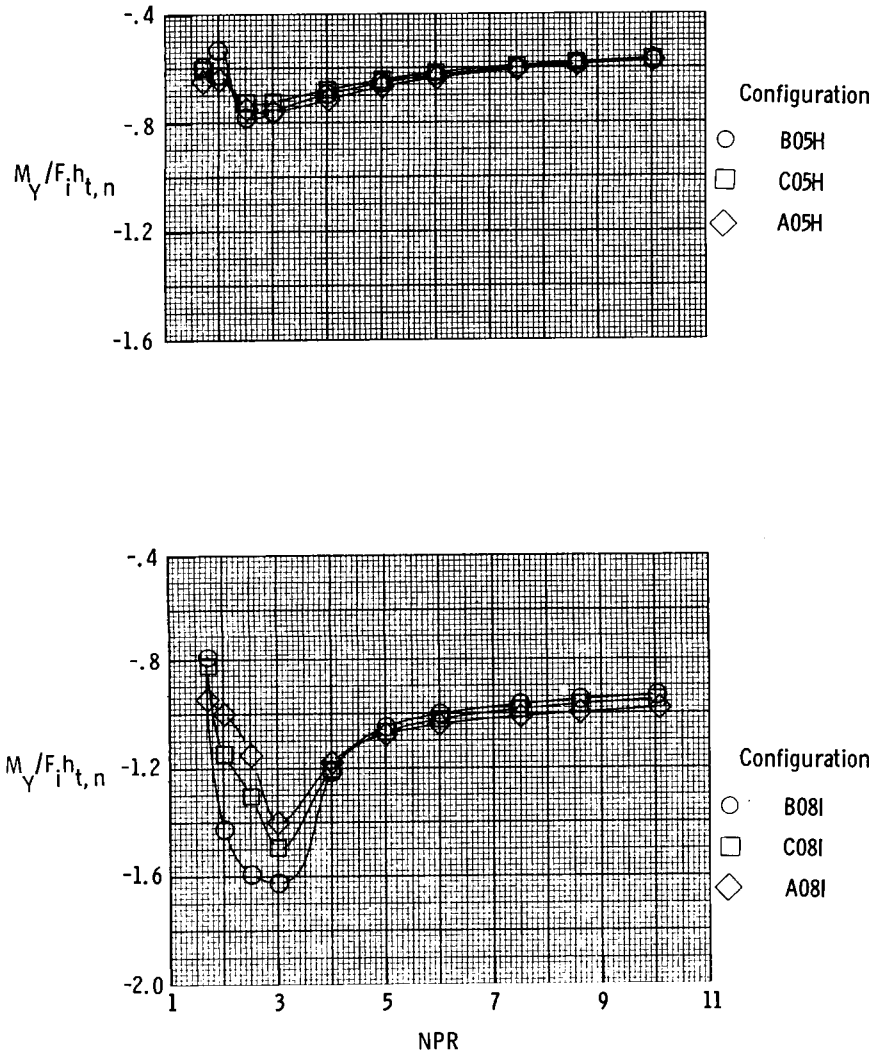

(d) Pitching moment.

Figure 11.- Concluded.

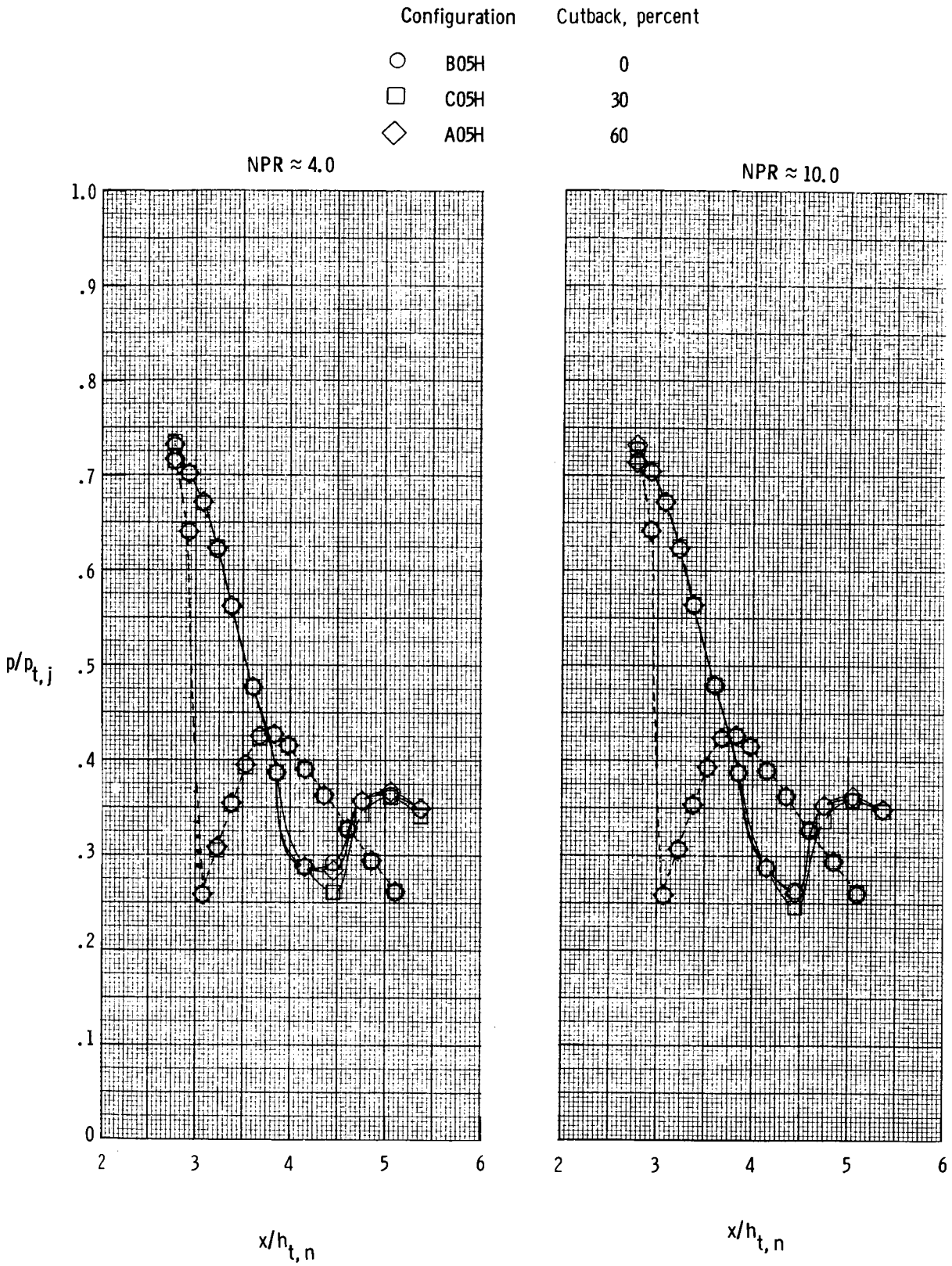

Figure 12.- Effect of sidewall containment on internal static pressure distributions for configurations B05H, C05H, and A05H. Dashed lines indicate lower flap.

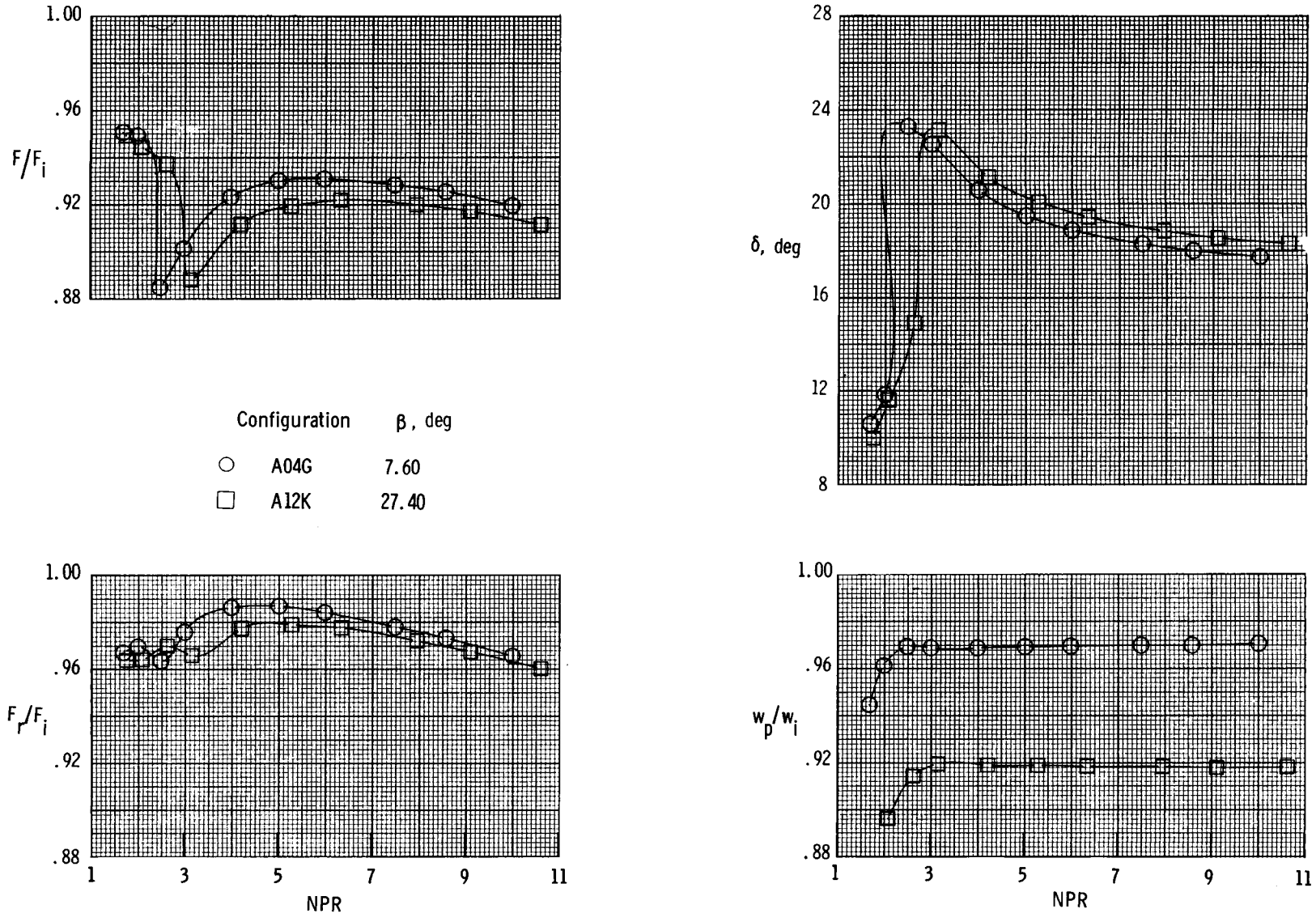

(a) Nozzle performance with $\delta_v = 16.90°$.

Figure 13.- Effect of throat approach angle on nozzle performance parameters and pitching moment with $\ell/h_{t,n} = 1.0$.

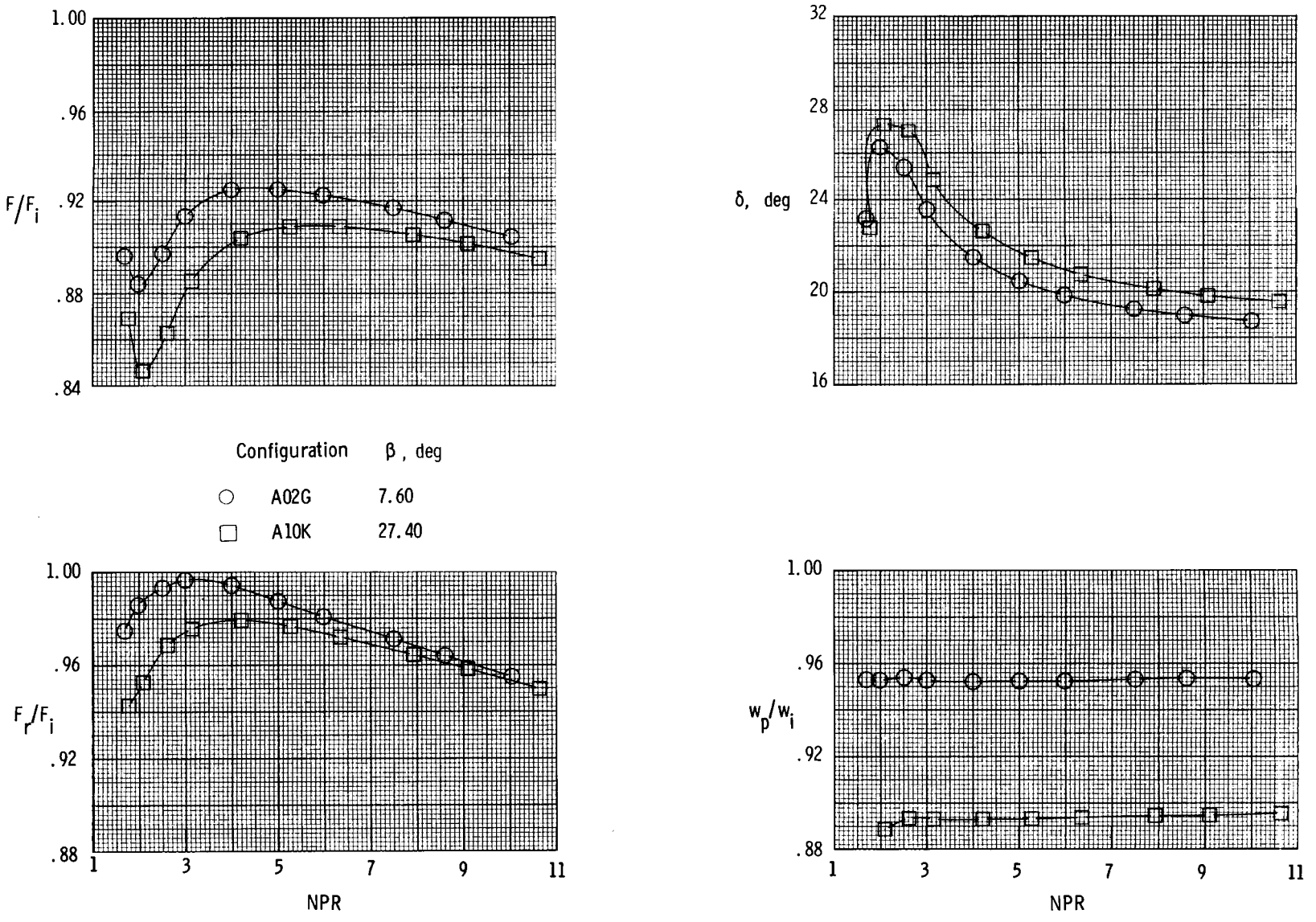

(b) Nozzle performance with δ_v = 21.90°.

Figure 13.- Continued.

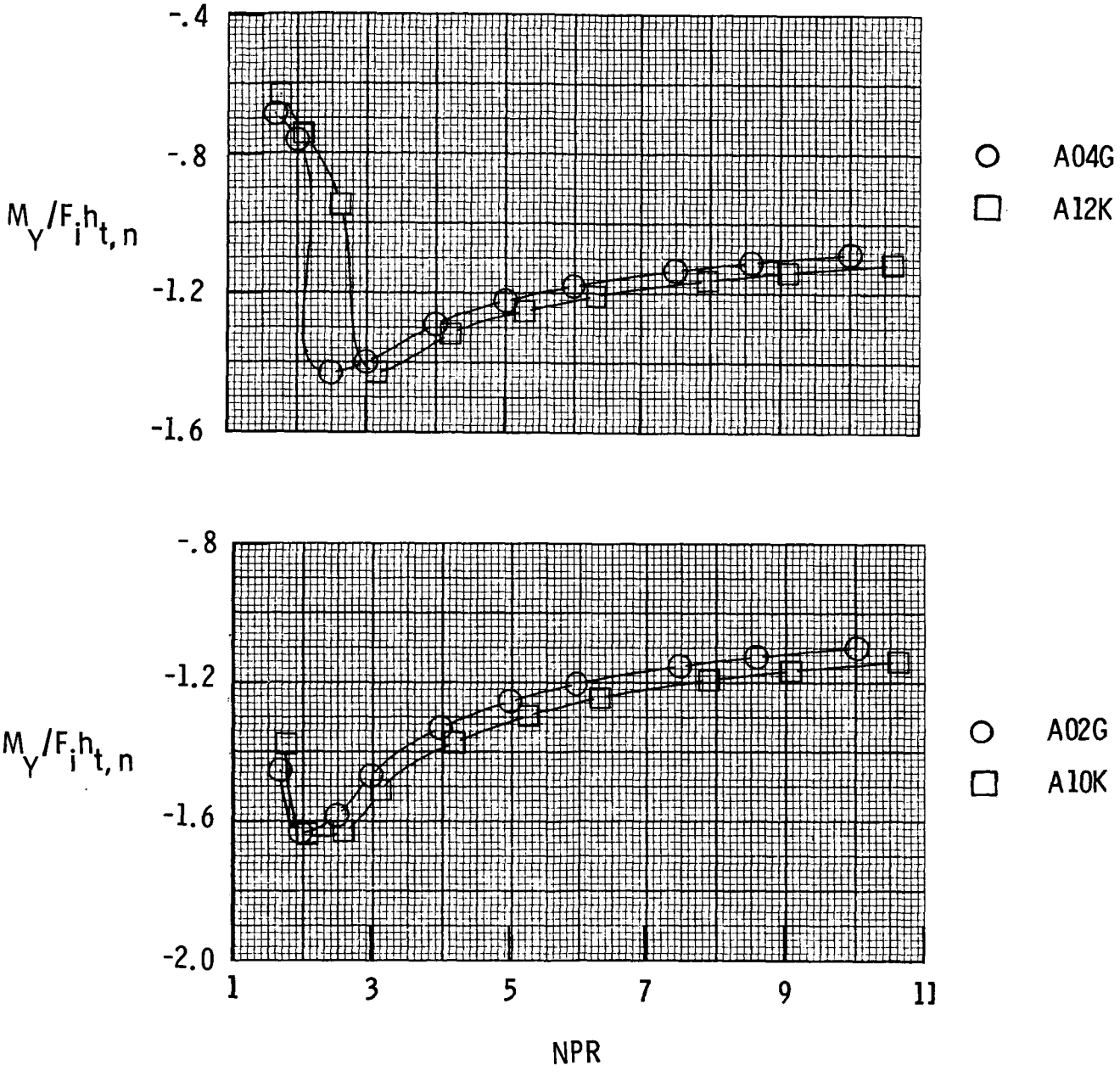

(c) Pitching moment.

Figure 13.- Concluded.

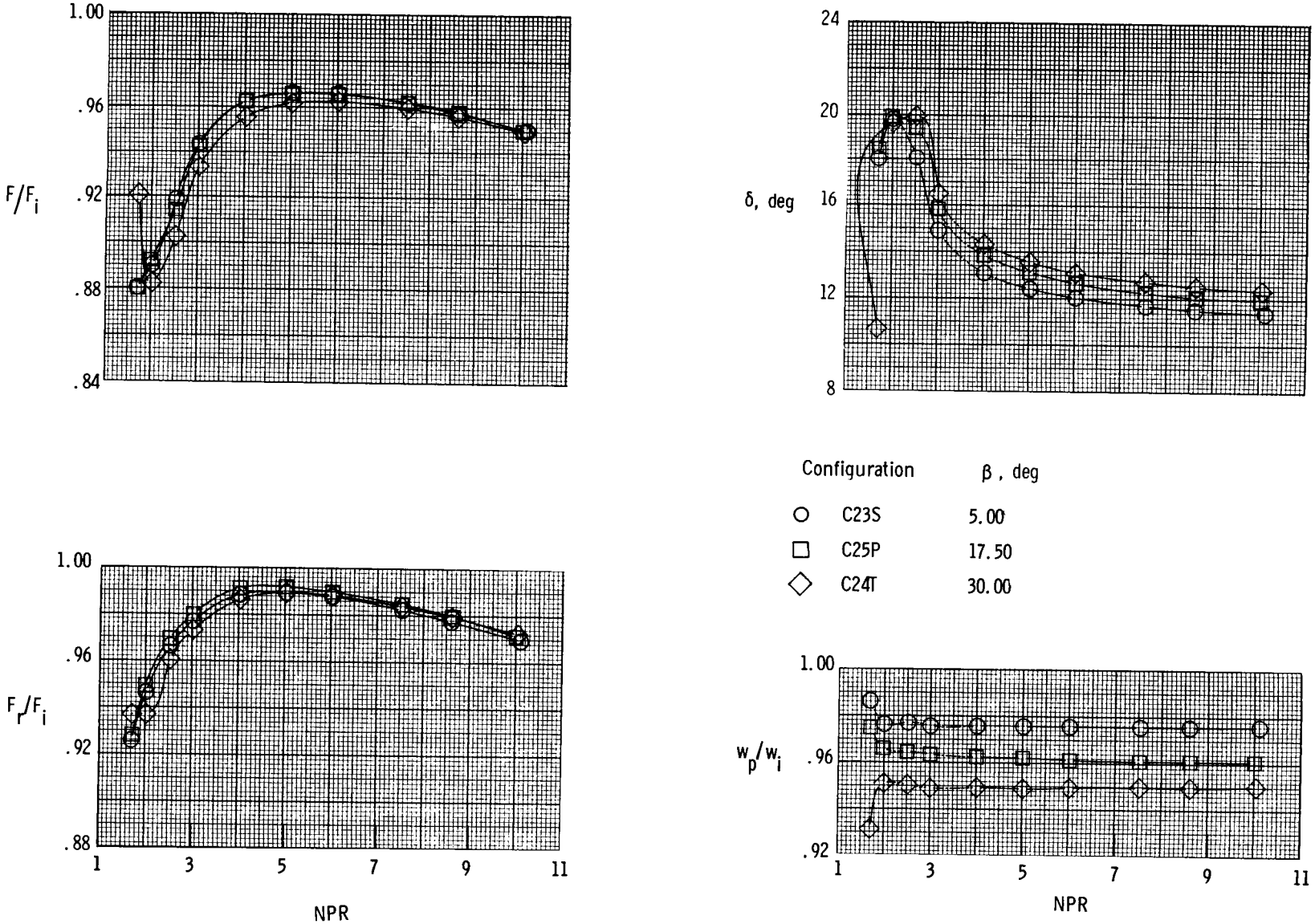

(a) Nozzle performance with $\delta_v = 13.50°$.

Figure 14.- Effect of throat approach angle on nozzle performance parameters and pitching moment with $\ell/h_{t,n} = 1.75$.

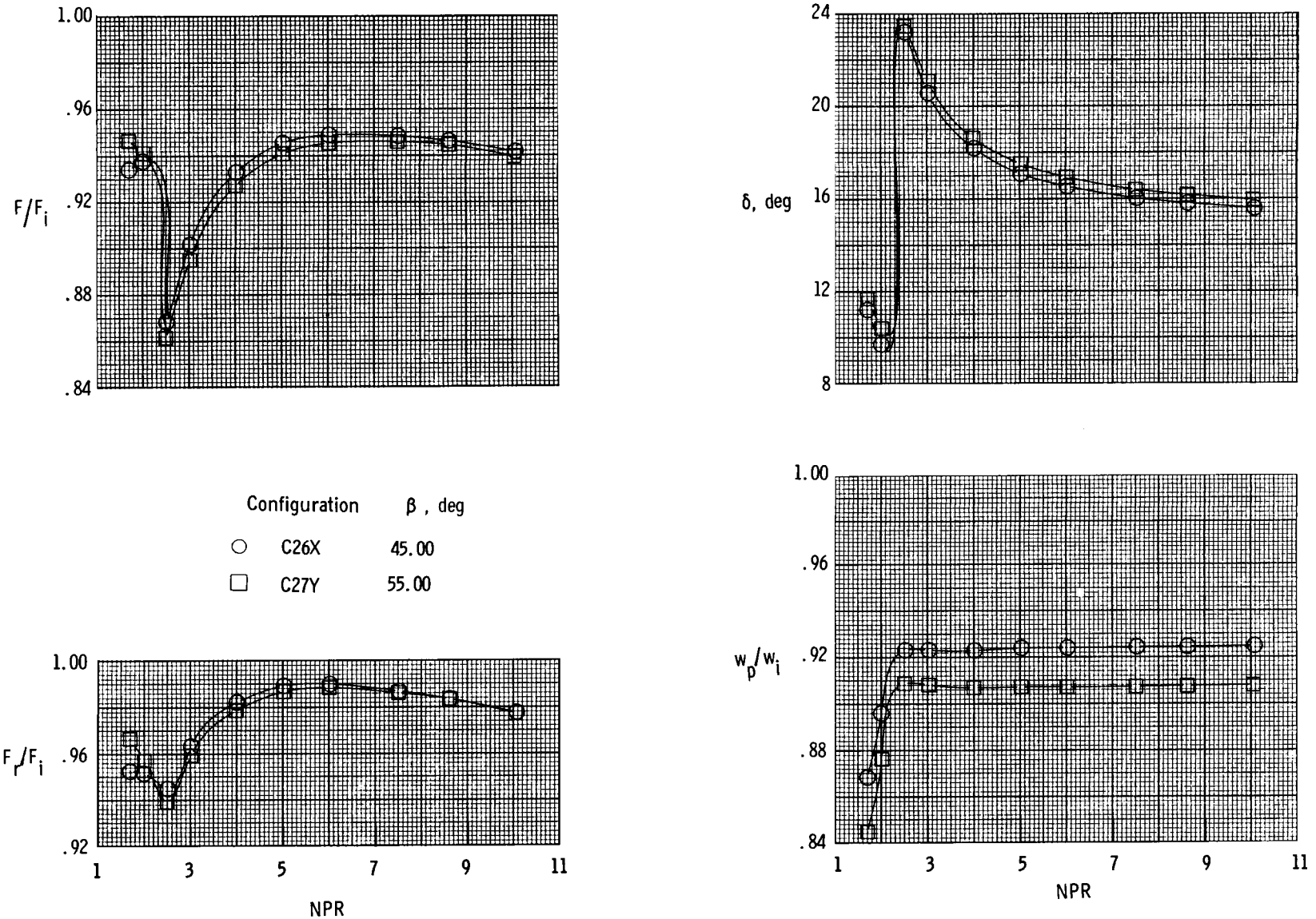

(b) Nozzle performance with δ_v = 15.00°.

Figure 14.- Continued.

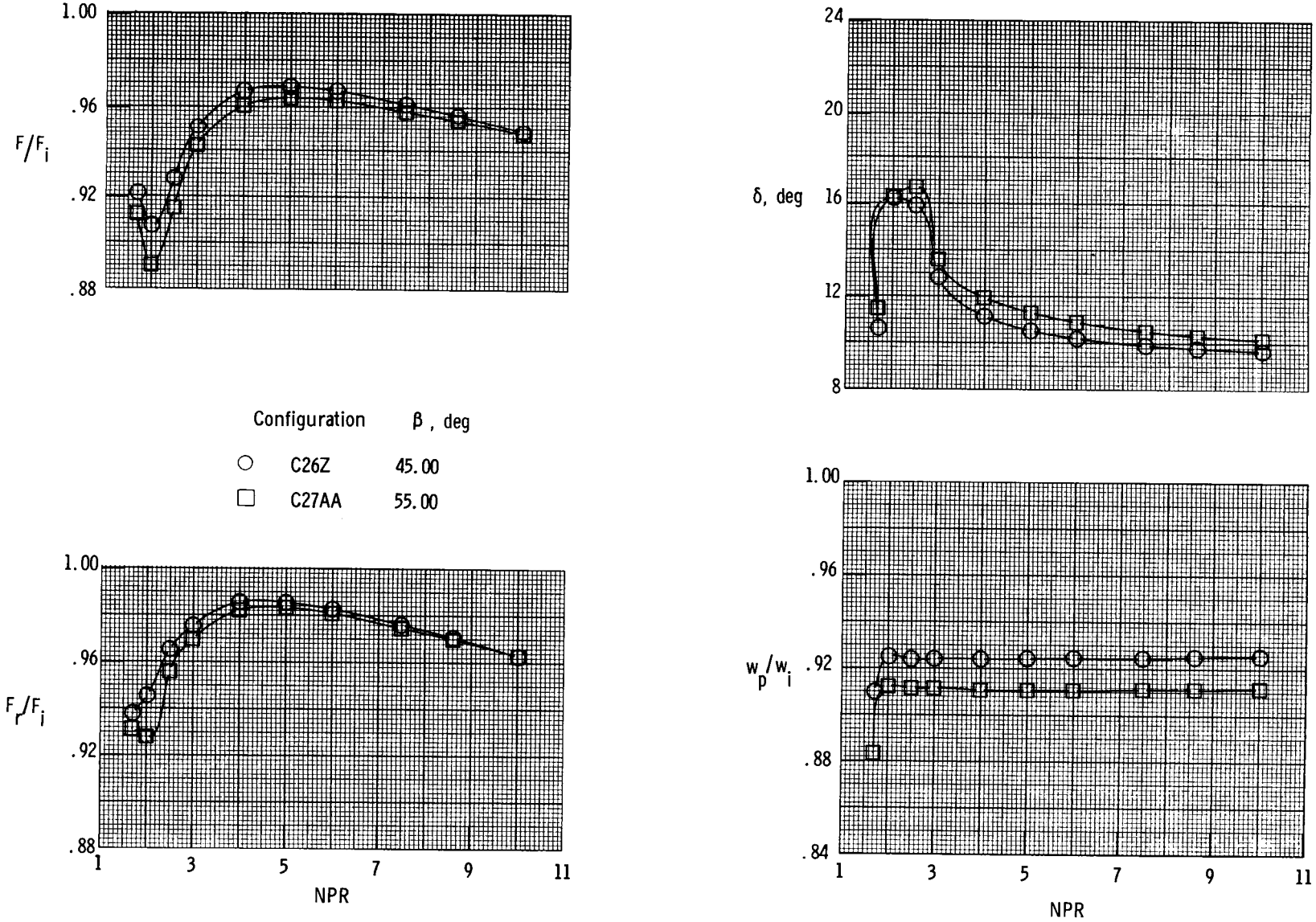

(c) Nozzle performance with $\delta_v = 12.50°$.

Figure 14.- Continued.

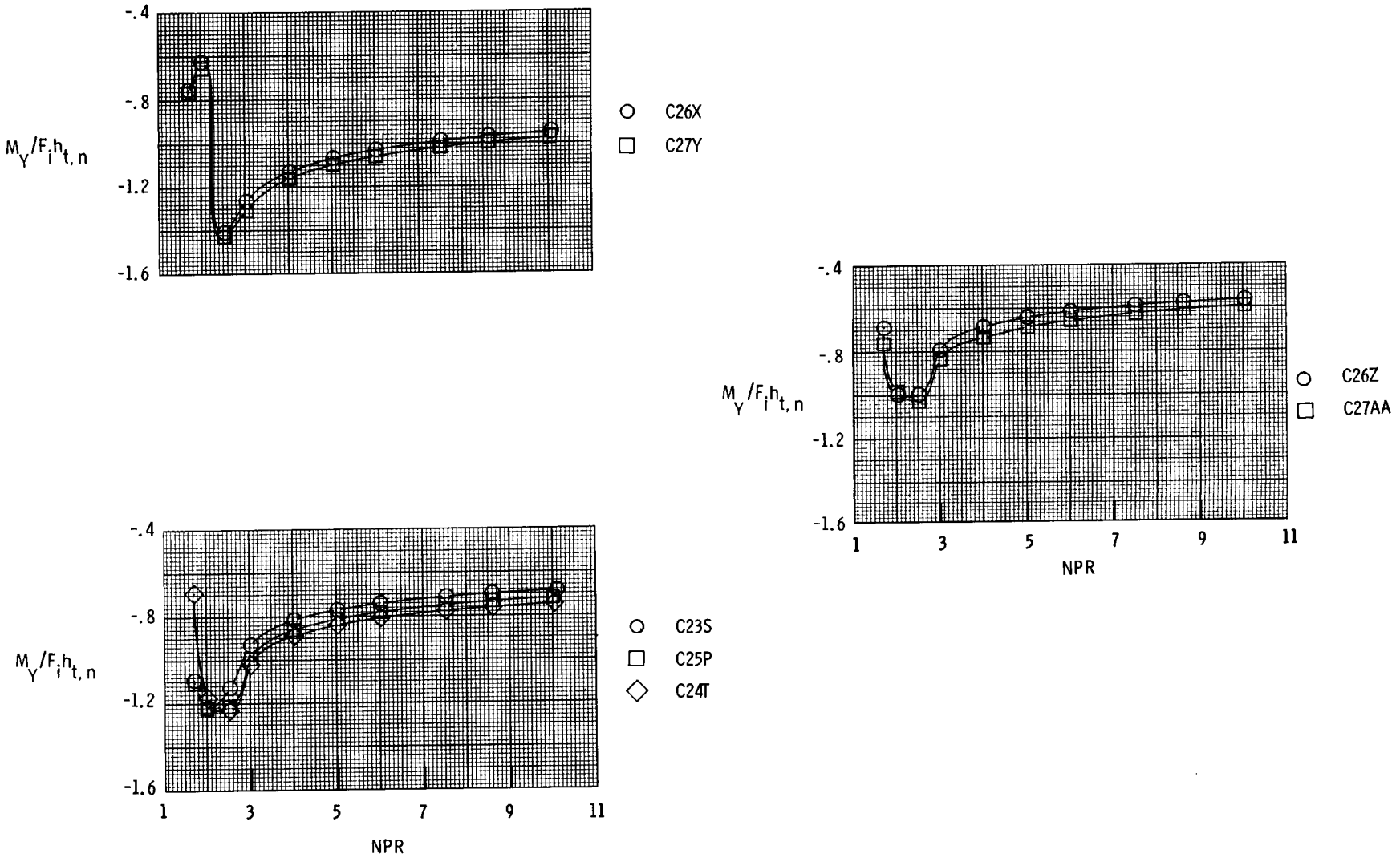

(d) Pitching moment.

Figure 14.- Concluded.

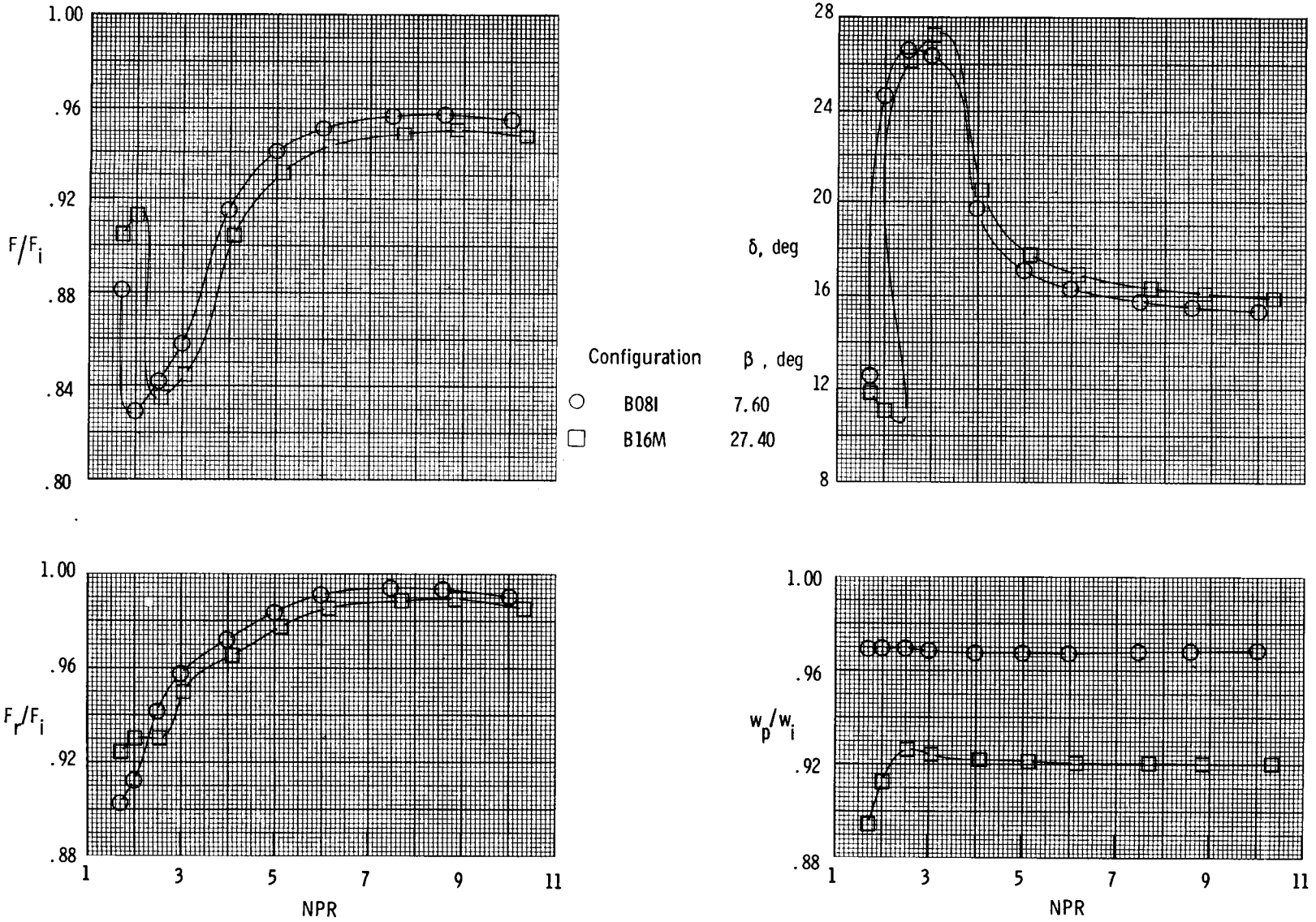

(a) Nozzle performance with $\delta_v = 16.90°$.

Figure 15.- Effect of throat approach angle on nozzle performance parameters and pitching moment with $l/h_{t,n} = 2.50$.

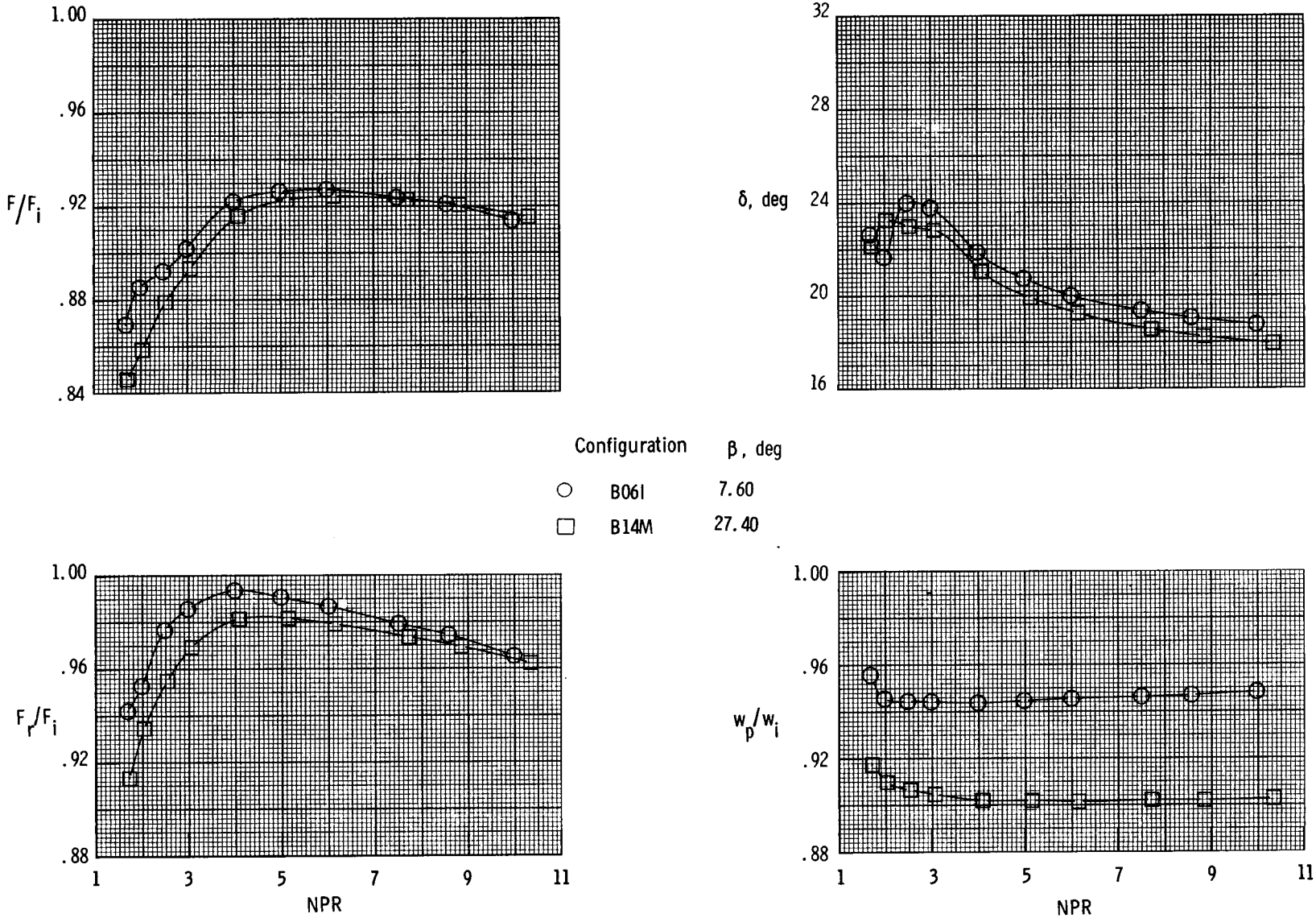

(b) Nozzle performance with δ_v = 21.90°.

Figure 15.- Continued.

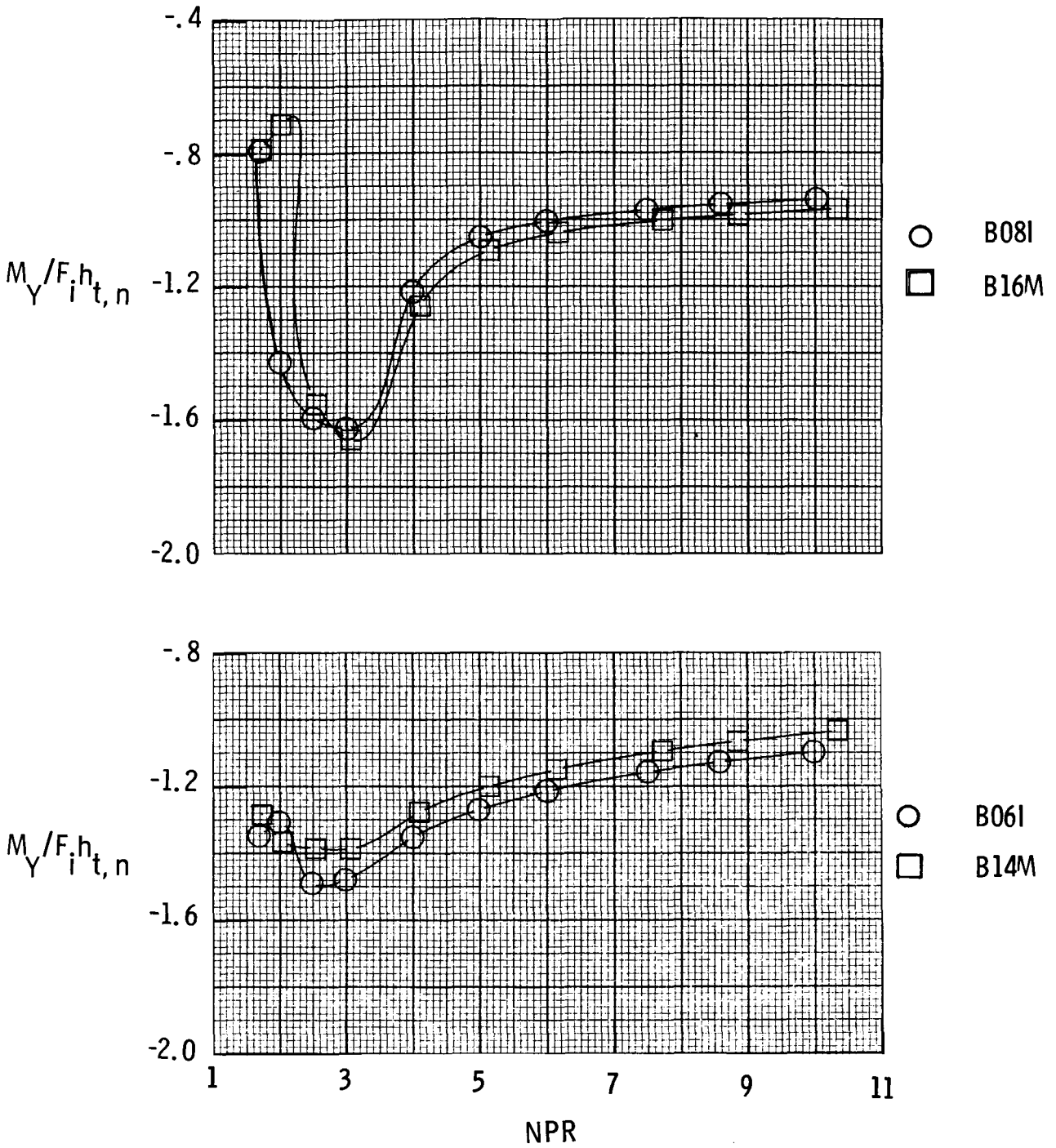

(c) Pitching moment.

Figure 15.- Concluded.

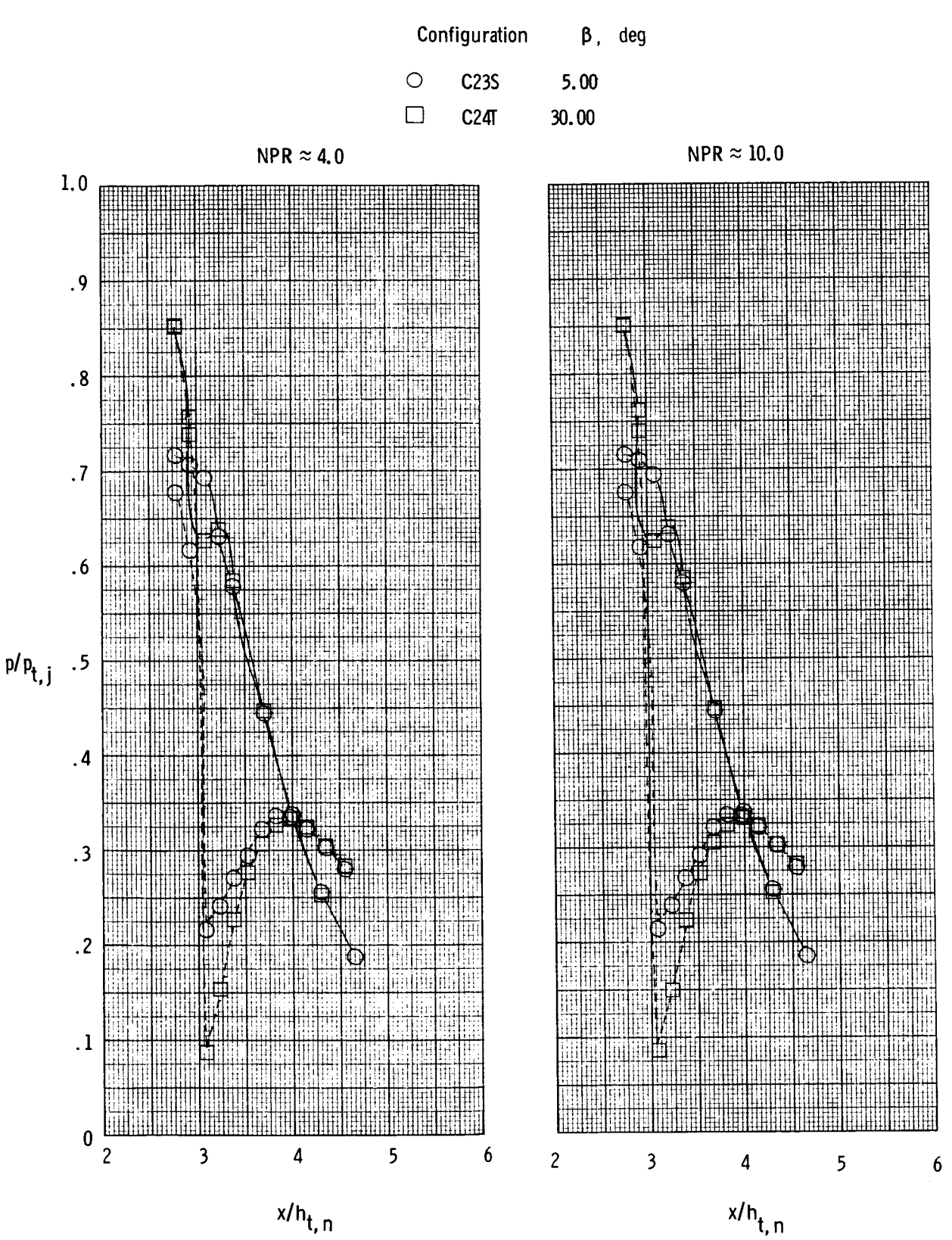

Figure 16.- Effect of throat approach angle on internal static pressure distributions for configurations C23S and C24T. Dashed lines indicate lower flap.

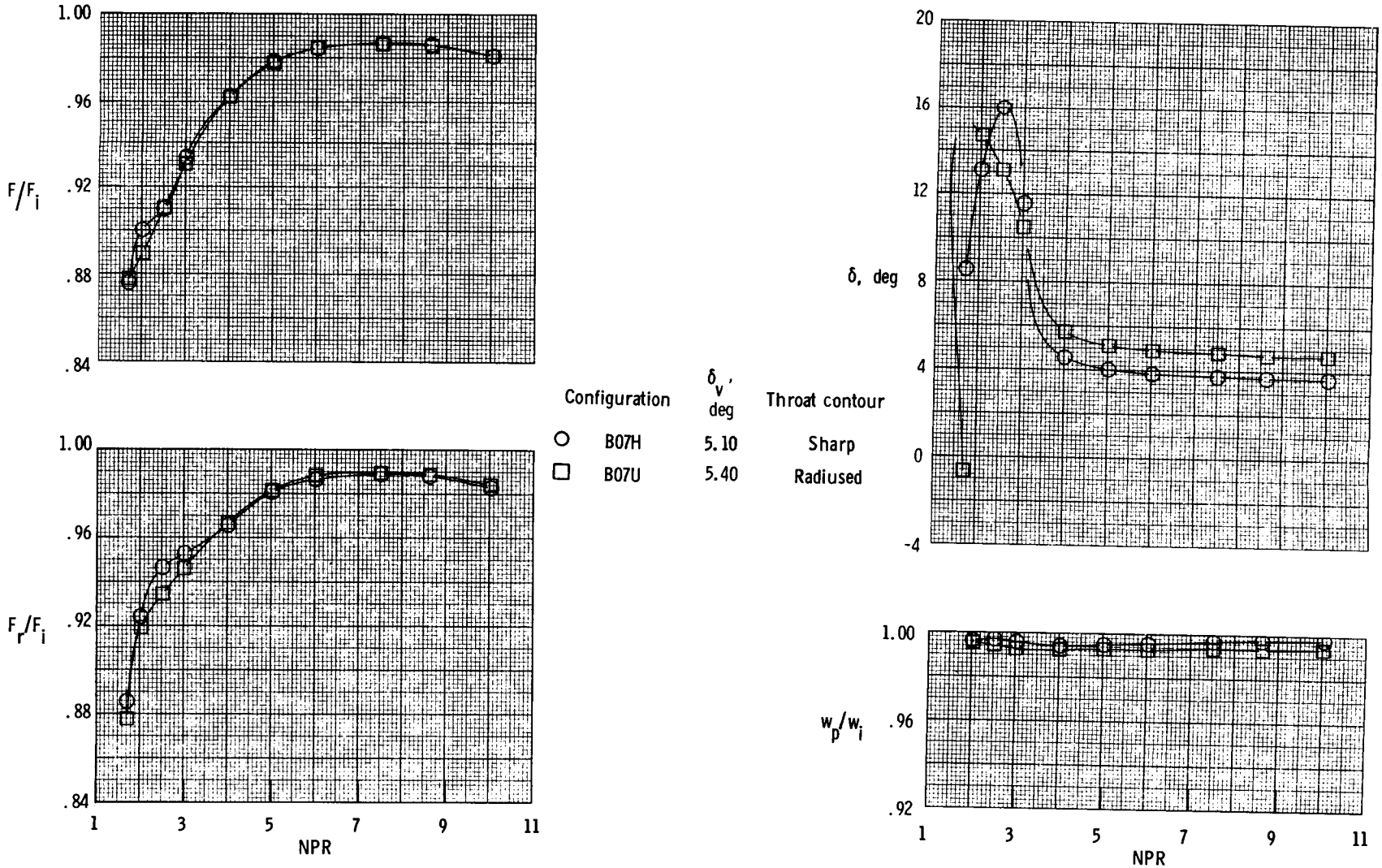

(a) $A_e/A_t = 1.56$.

Figure 17.- Effect of throat geometry on nozzle performance parameters and pitching moment.

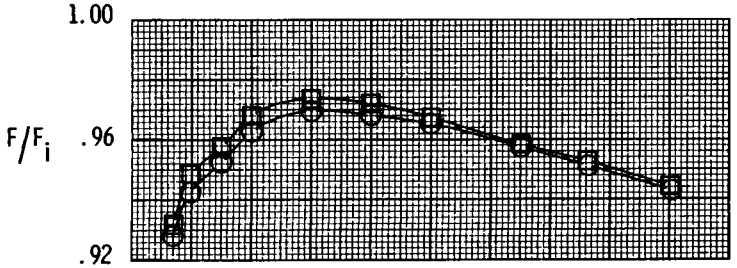

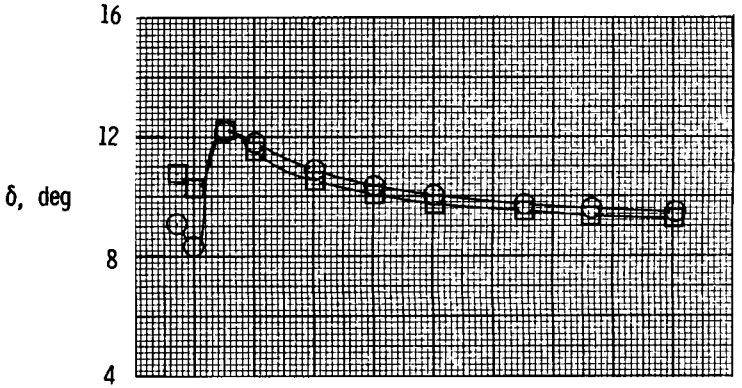

Configuration		δ_v, deg	Throat contour
○	B05H	10.10	Sharp
□	B05U	11.10	Radiused

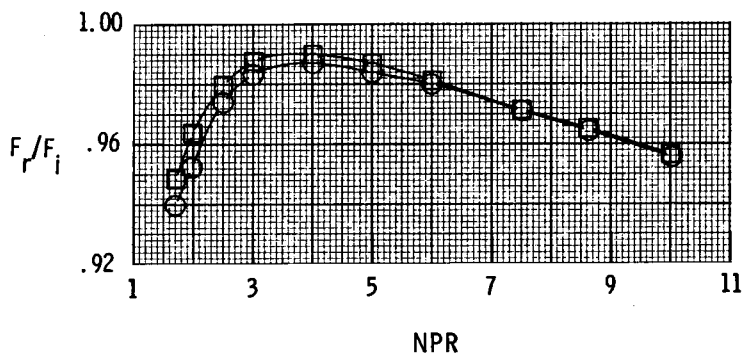

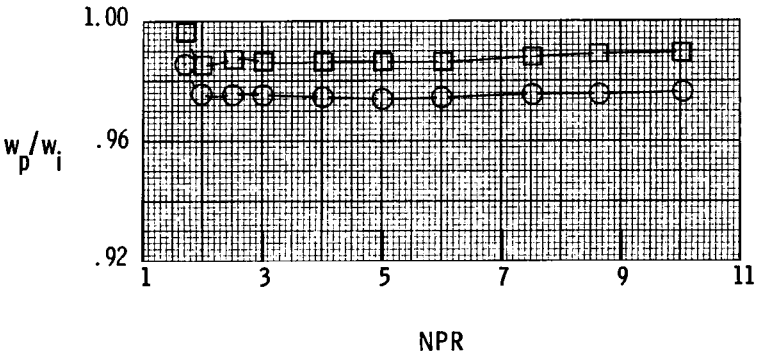

(b) $A_e/A_t = 1.13$.

Figure 17.- Continued.

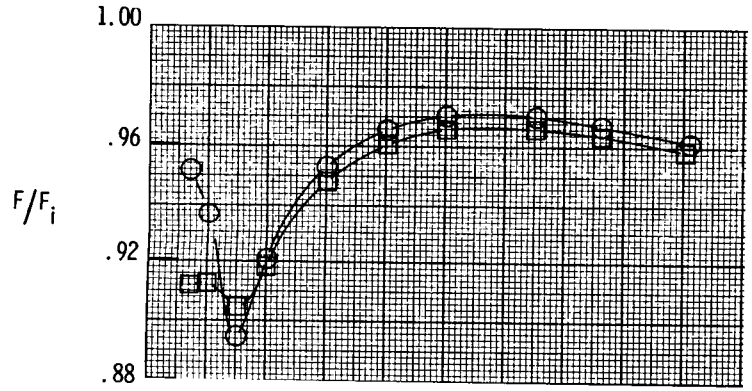

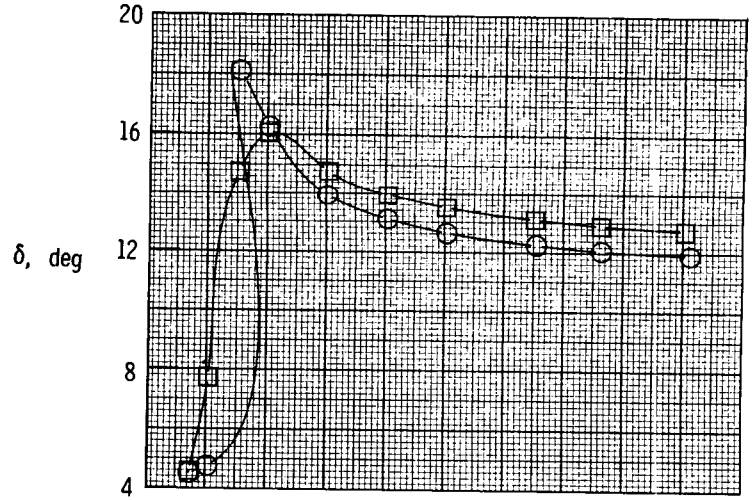

Configuration		δ_v, deg	Throat contour
○	C20P	10.35	Sharp
□	C20W	11.30	Radiused

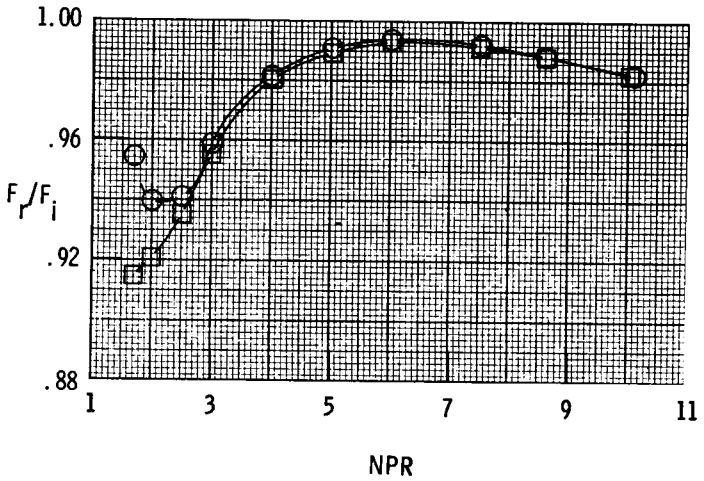

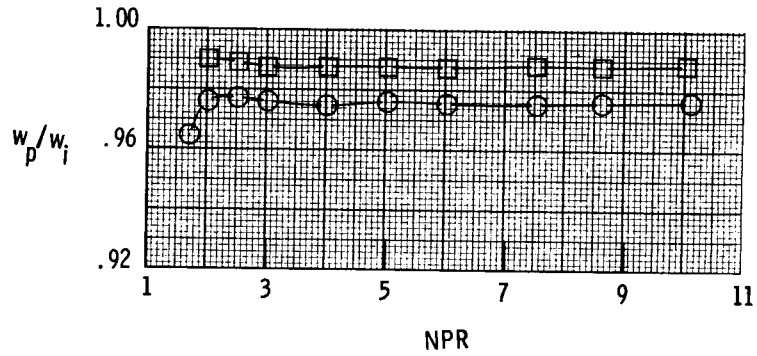

(c) $A_e/A_t = 1.43$.

Figure 17.- Continued.

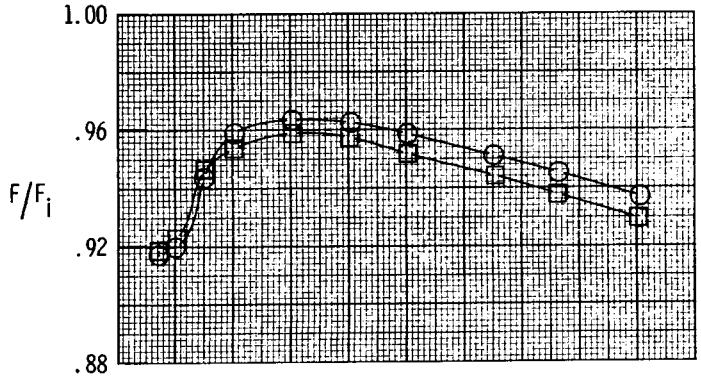

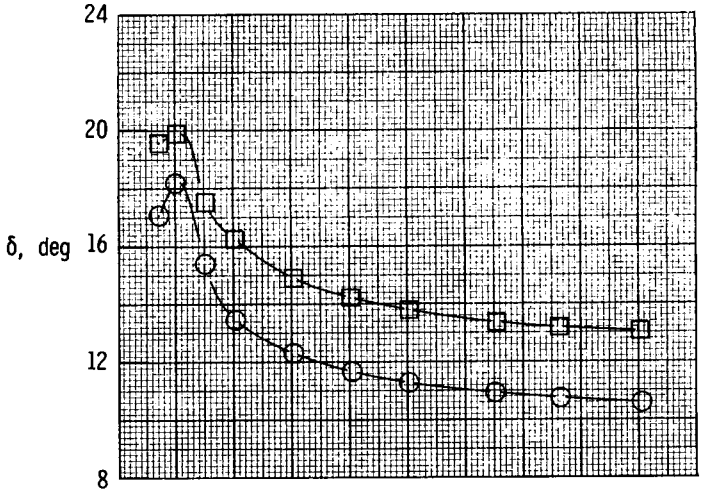

Configuration		δ_v, deg	Throat contour
○	C19P	16.65	Sharp
□	C19W	17.60	Radiused

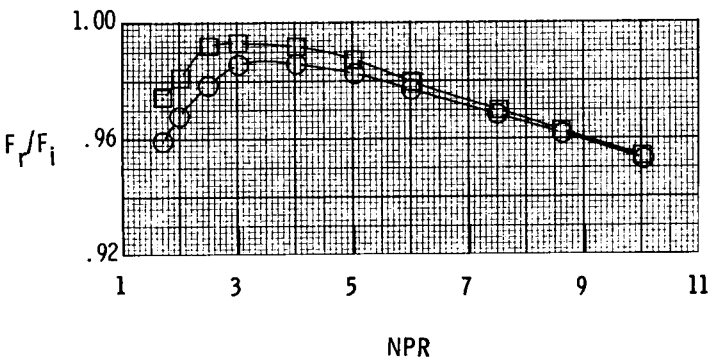

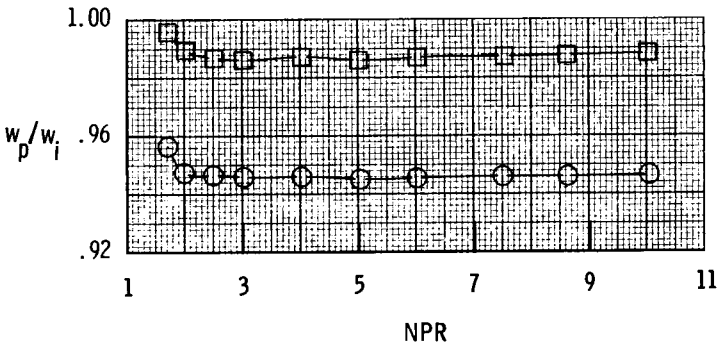

(d) $A_e/A_t = 1.05$.

Figure 17.- Continued.

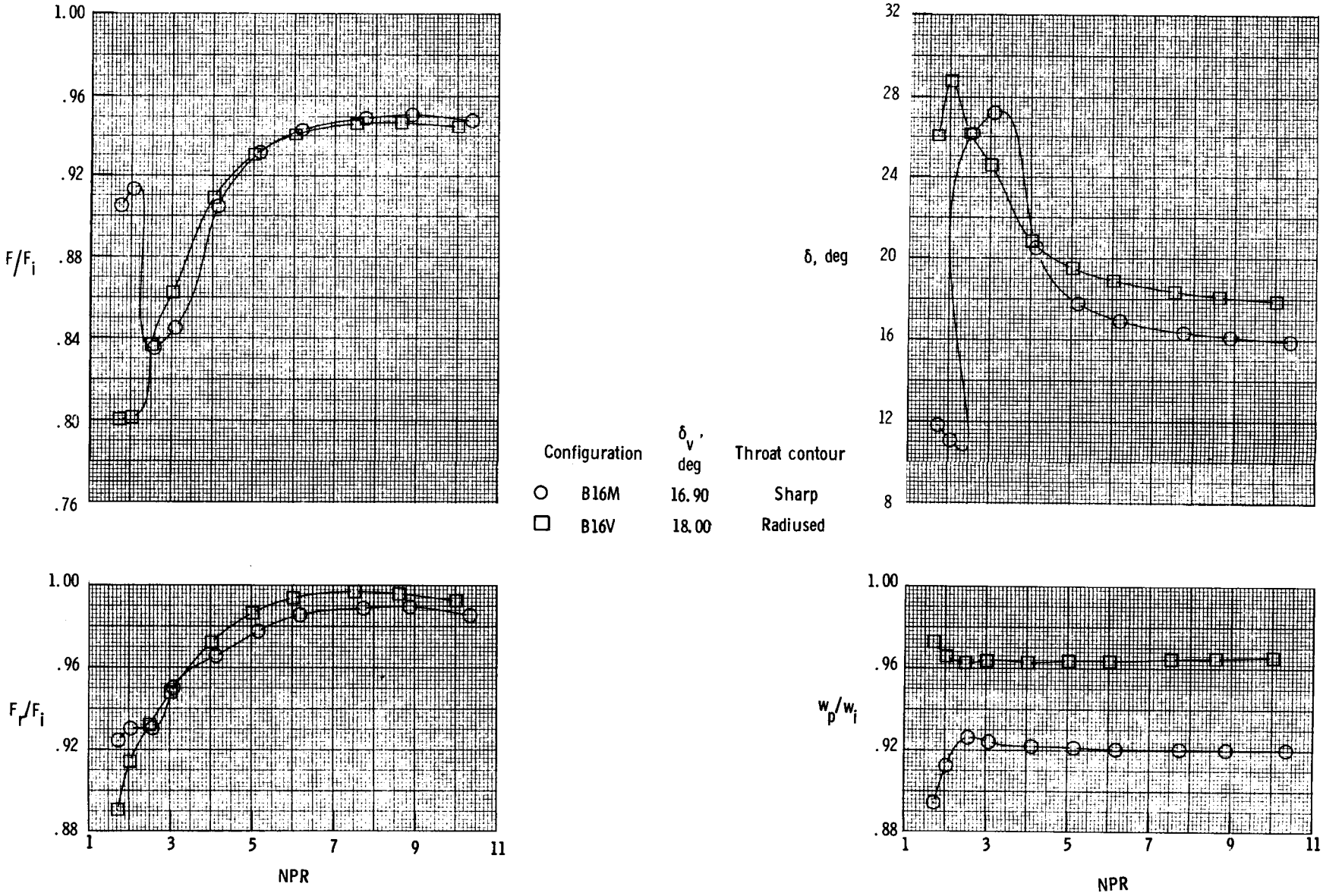

(e) $A_e/A_t = 1.55$.

Figure 17.- Continued.

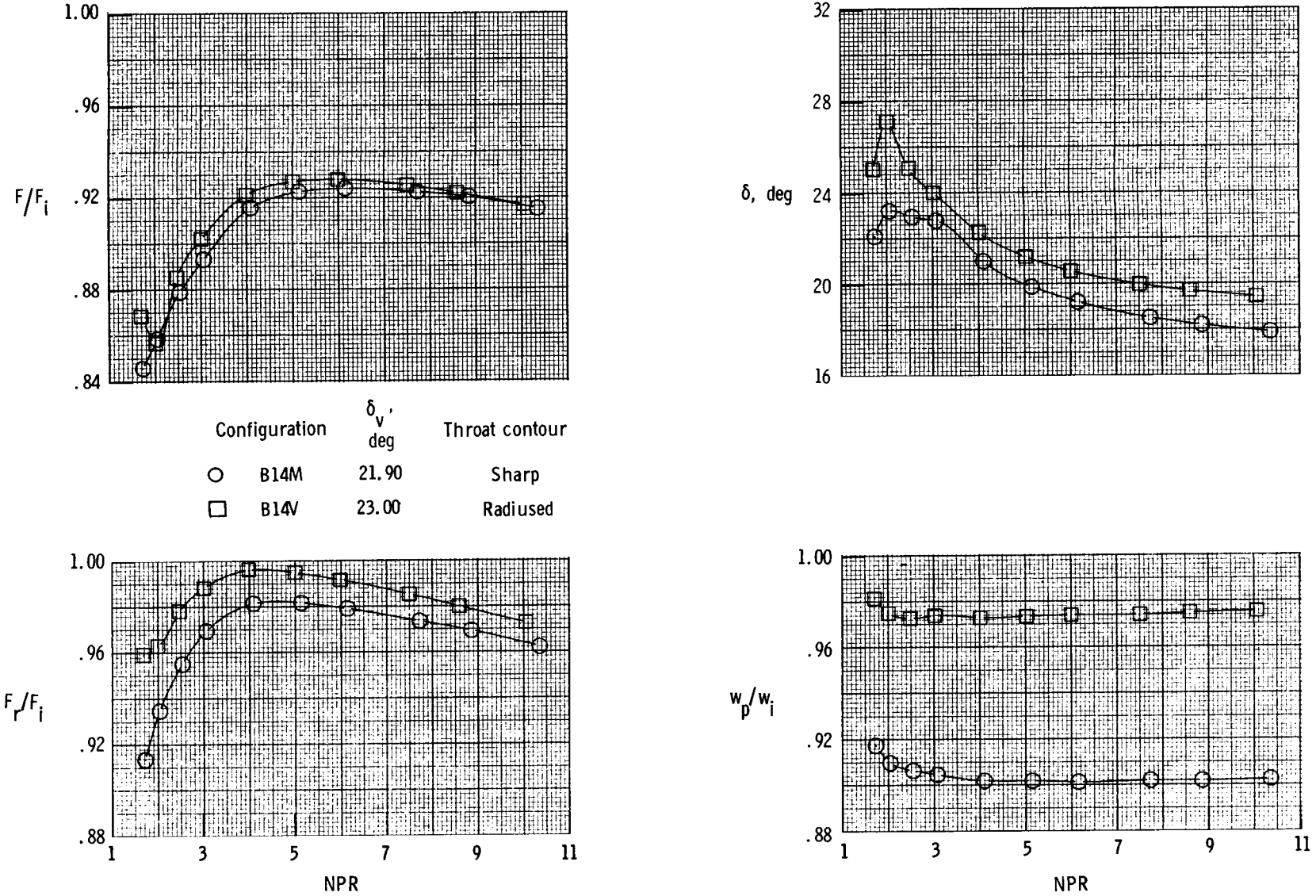

(f) $A_e/A_t = 1.12$.

Figure 17.- Continued.

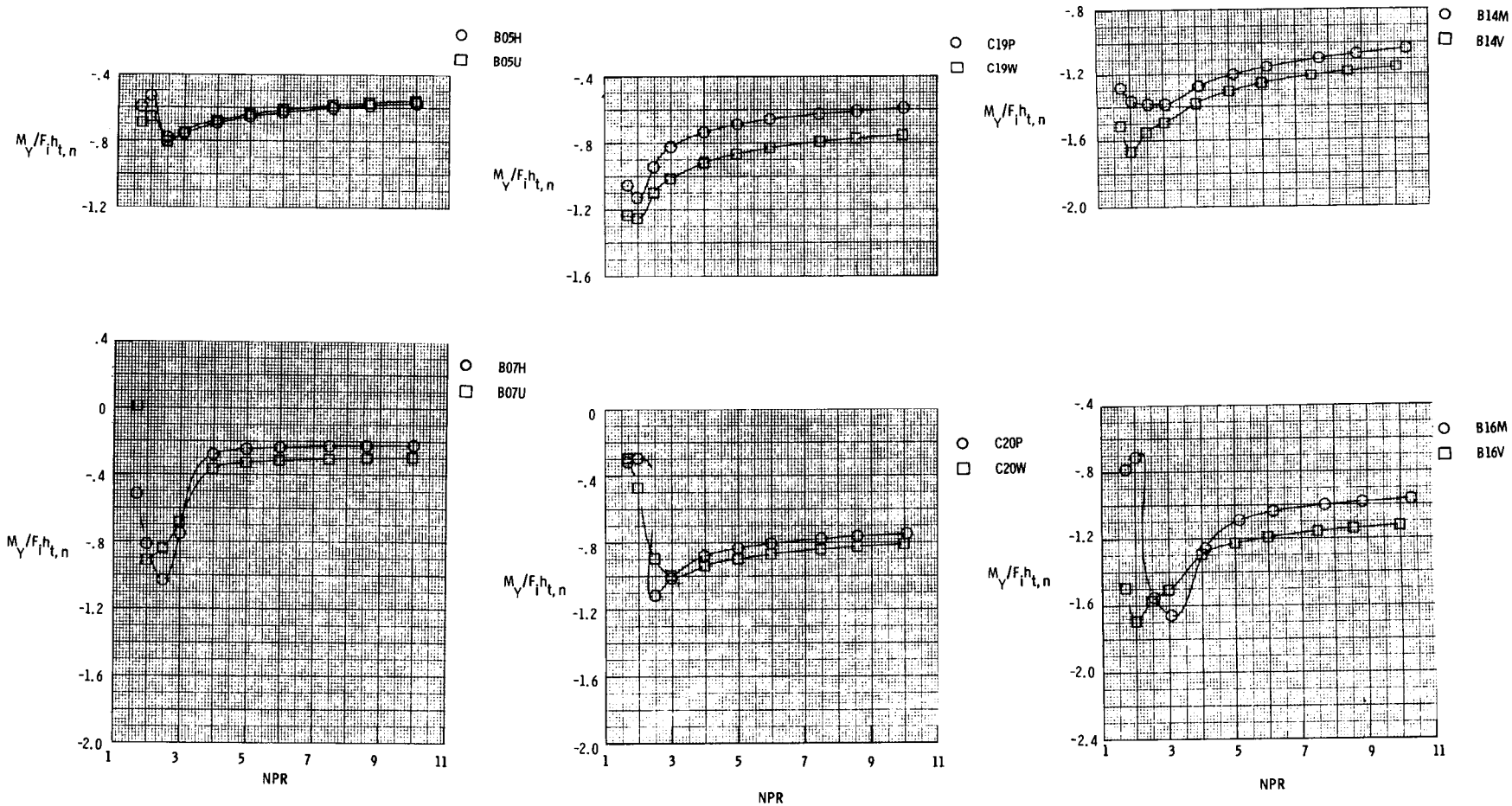

(g) Pitching moment.

Figure 17.- Concluded.

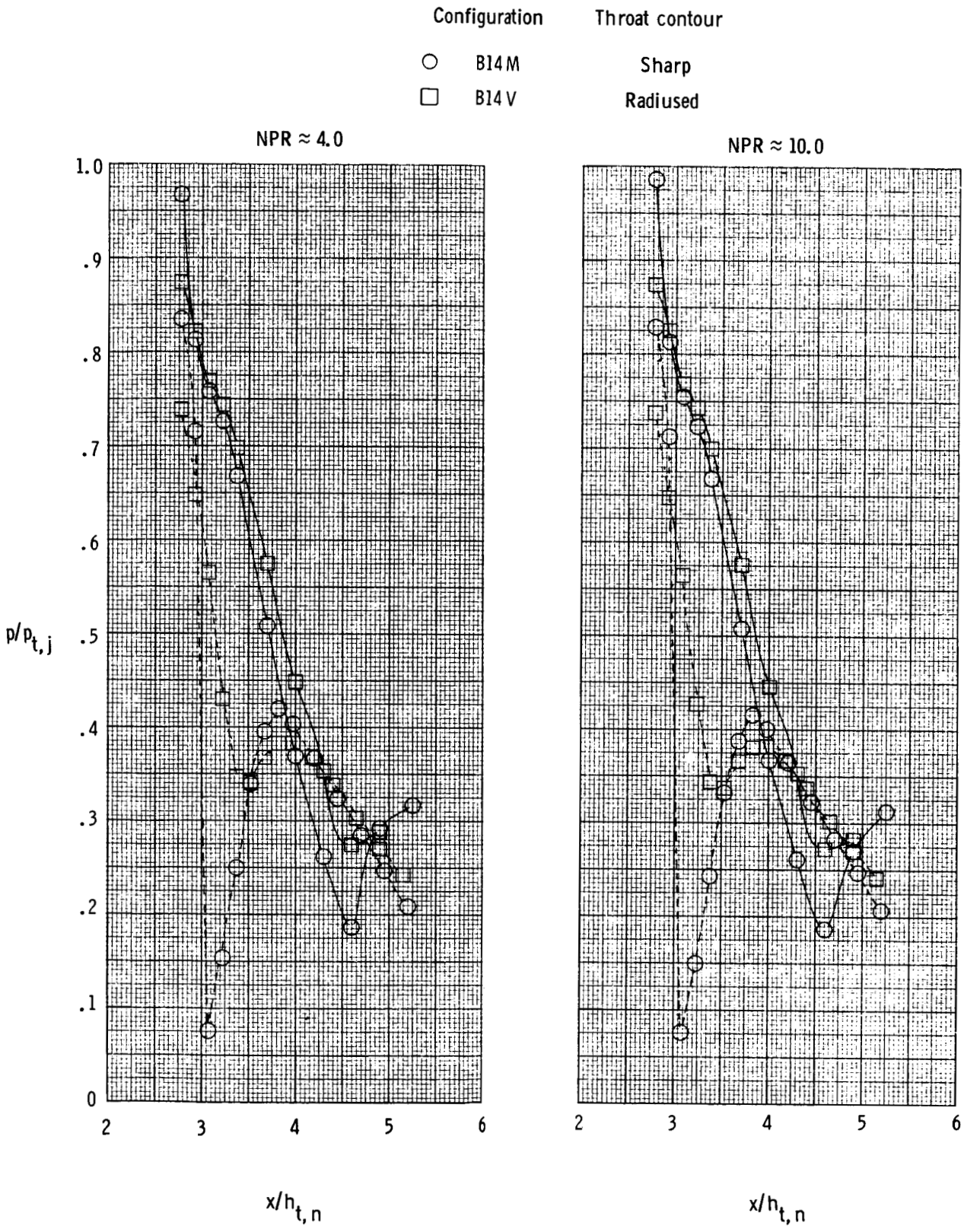

Figure 18.- Effect of throat geometry on internal static pressure distributions for configurations B14M and B14V. Dashed lines indicate lower flap.

APPENDIX A

INTERNAL GEOMETRY OF LOWER AND UPPER FLAPS

The internal geometry is presented in table AI for all lower flaps tested and in table AII for all upper flaps tested. Values of x and y are measured in inches.

TABLE AI.- INTERNAL GEOMETRY OF LOWER FLAPS

Lower Flap F	
x	y
0.0000	-1.3900
0.4574	-1.3900
0.8110	-1.2436
1.2125	-0.8421
1.5000	-0.7001
3.0000	-0.5000
3.9796	-0.7011

Lower Flap G	
x	y
0.0000	-1.3900
0.4574	-1.3900
0.8110	-1.2436
1.2125	-0.8421
1.5000	-0.7001
3.0000	-0.5000
3.9178	-0.8971

Lower Flap H	
x	y
0.0000	-1.3900
0.4574	-1.3900
0.8110	-1.2436
1.2125	-0.8421
1.5000	-0.7001
3.0000	-0.5000
5.4489	-1.0027

Lower Flap I	
x	y
0.0000	-1.3900
0.4574	-1.3900
0.8110	-1.2436
1.2125	-0.8421
1.5000	-0.7001
3.0000	-0.5000
5.2944	-1.4929

TABLE AI.- Continued

Lower Flap J	
x	y
0.0000	-1.3900
1.1611	-1.3900
1.3912	-1.3339
3.0000	-0.5000
3.9796	-0.7011

Lower Flap K	
x	y
0.0000	-1.3900
1.1611	-1.3900
1.3912	-1.3339
3.0000	-0.5000
3.9178	-0.8971

Lower Flap L	
x	y
0.0000	-1.3900
1.1611	-1.3900
1.3912	-1.3339
3.0000	-0.5000
5.4489	-1.0027

Lower Flap M	
x	y
0.0000	-1.3900
1.1611	-1.3900
1.3912	-1.3339
3.0000	-0.5000
5.2944	-1.4929

TABLE AI.- Continued

Lower Flap N	
x	y
0.0000	-1.3900
0.8058	-1.3900
1.1694	-1.2436
1.2968	-1.0962
1.5000	-0.9729
3.0000	-0.5000
4.7234	-0.8039

Lower Flap O	
x	y
0.0000	-1.3900
0.8058	-1.3900
1.1694	-1.2436
1.2968	-1.0962
1.5000	-0.9729
3.0000	-0.5000
4.5860	-1.2396

Lower Flap P	
x	y
0.0000	-1.3900
0.8058	-1.3900
1.1694	-1.2436
1.2968	-1.0962
1.5000	-0.9729
3.0000	-0.5000
4.6690	-1.0262

Lower Flap Q	
x	y
0.0000	-1.3900
0.8058	-1.3900
1.1694	-1.2436
1.2968	-1.0962
1.5000	-0.9729
3.0000	-0.5000
3.7630	-0.7406

TABLE AI.- Continued

Lower Flap R	
x	y
0.0000	-1.3900
0.8058	1.3900
1.1694	-1.2436
1.2968	-1.0962
1.5000	-0.9729
3.0000	-0.5000
5.5750	-1.3119

Lower Flap S	
x	y
0.0000	-1.3900
0.3685	-1.3900
0.7221	-1.2436
1.1900	-0.7757
1.5000	-0.6312
3.0000	-0.5000
4.6690	-1.0262

Lower Flap T	
x	y
0.0000	-1.3900
1.3245	-1.3900
1.5745	-1.3230
3.0000	-0.5000
4.6690	-1.0262

Lower Flap U	
x	y
0.0000	-1.3900
0.4486	-1.3900
0.8022	-1.2436
1.2125	-0.8333
1.5000	-0.6913
2.8677	-0.5088
3.0000	-0.5000
3.2096	-0.5222
5.4445	-1.0013

TABLE AI.- Continued

Lower Flap V	
x	y
0.0000	-1.3900
0.9174	-1.3900
1.1475	-1.3339
2.5398	-0.6122
3.0000	-0.5000
3.4321	-0.5982
5.2546	-1.4714

Lower Flap W	
x	y
0.0000	-1.3900
0.7473	-1.3900
1.1009	-1.2436
1.2968	-1.0477
1.5000	-0.9244
2.6933	-0.5463
3.0000	-0.5000
3.3305	-0.5562
4.6517	-1.0189

Lower Flap X	
x	y
0.0000	-1.3900
1.9028	-1.3900
2.2564	-1.2436
3.0000	-0.5000
4.6445	-1.0985

Lower Flap Y	
x	y
0.0000	-1.3900
2.1165	-1.3900
2.5261	-1.1768
3.0000	-0.5000
4.6445	-1.0985

TABLE AI.- Concluded

Lower Flap Z	
x	y
0.0000	-1.3900
1.9028	-1.3900
2.2564	-1.2436
3.0000	-0.5000
4.6904	-0.9529

Lower Flap AA	
x	y
0.0000	-1.3900
2.1165	-1.3900
2.5261	-1.1768
3.0000	-0.5000
4.6904	-0.9529

TABLE AII.- INTERNAL GEOMETRY OF UPPER FLAPS

Upper Flap 01	
x	y
0.0000	1.3900
0.4574	1.3900
0.8110	1.2436
1.2125	0.8421
1.5000	0.7001
3.0000	0.5000
3.9888	0.3505

Upper Flap 02	
x	y
0.0000	1.3900
0.4574	1.3900
0.8110	1.2436
1.2125	0.8421
1.5000	0.7001
3.0000	0.5000
3.9373	0.1514

Upper Flap 03	
x	y
0.0000	1.3900
0.4574	1.3900
0.8110	1.2436
1.2125	0.8421
1.5000	0.7001
3.0000	0.5000
3.9997	0.5244

Upper Flap 04	
x	y
0.0000	1.3900
0.4574	1.3900
0.8110	1.2436
1.2125	0.8421
1.5000	0.7001
3.0000	0.5000
3.9836	0.3195

TABLE AII.- Continued

Upper Flap 05	
x	y
0.0000	1.3900
0.4574	1.3900
0.8110	1.2436
1.2125	0.8421
1.5000	0.7001
3.0000	0.5000
5.4719	0.1262

Upper Flap 06	
x	y
0.0000	1.3900
0.4574	1.3900
0.8110	1.2436
1.2125	0.8421
1.5000	0.7001
3.0000	0.5000
5.3432	-0.3714

Upper Flap 07	
x	y
0.0000	1.3900
0.4574	1.3900
0.8110	1.2436
1.2125	0.8421
1.5000	0.7001
3.0000	0.5000
5.4993	0.5611

Upper Flap 08	
x	y
0.0000	1.3900
0.4574	1.3900
0.8110	1.2436
1.2125	0.8421
1.5000	0.7001
3.0000	0.5000
5.4589	0.0487

TABLE AII.- Continued

Upper Flap 09	
x	y
0.0000	1.3900
1.1611	1.3900
1.3912	1.3339
3.0000	0.5000
3.9888	0.3505

Upper Flap 10	
x	y
0.0000	1.3900
1.1611	1.3900
1.3912	1.3339
3.0000	0.5000
3.9373	0.1514

Upper Flap 11	
x	y
0.0000	1.3900
1.1611	1.3900
1.3912	1.3339
3.0000	0.5000
3.9997	0.5244

Upper Flap 12	
x	y
0.0000	1.3900
1.1611	1.3900
1.3912	1.3339
3.0000	0.5000
3.9836	0.3195

TABLE AII.- Continued

Upper Flap 13	
x	y
0.0000	1.3900
1.1611	1.3900
1.3912	1.3339
3.0000	0.5000
5.4719	0.1262

Upper Flap 14	
x	y
0.0000	1.3900
1.1611	1.3900
1.3912	1.3339
3.0000	0.5000
5.3432	-0.3714

Upper Flap 15	
x	y
0.0000	1.3900
1.1611	1.3900
1.3912	1.3339
3.0000	0.5000
5.4993	0.5611

Upper Flap 16	
x	y
0.0000	1.3900
1.1611	1.3900
1.3912	1.3339
3.0000	0.5000
5.4589	0.0487

TABLE AII.- Continued

Upper Flap 17	
x	y
0.0000	1.3900
0.8058	1.3900
1.1694	1.2436
1.2968	1.0962
1.5000	0.9729
3.0000	0.5000
4.7489	0.4389

Upper Flap 18	
x	y
0.0000	1.3900
0.8058	1.3900
1.1694	1.2436
1.2968	1.0962
1.5000	0.9729
3.0000	0.5000
4.6735	-0.0117

Upper Flap 19	
x	y
0.0000	1.3900
0.8058	1.3900
1.1694	1.2436
1.2968	1.0962
1.5000	0.9729
3.0000	0.5000
4.6839	0.0235

Upper Flap 20	
x	y
0.0000	1.3900
0.8058	1.3900
1.1694	1.2436
1.2968	1.0962
1.5000	0.9729
3.0000	0.5000
4.7473	0.4023

TABLE AII.- Continued

Upper Flap 21	
x	y
0.0000	1.3900
0.8058	1.3900
1.1694	1.2436
1.2968	1.0962
1.5000	0.9729
3.0000	0.5000
3.7890	0.3680

Upper Flap 22	
x	y
0.0000	1.3900
0.8058	1.3900
1.1694	1.2436
1.2968	1.0962
1.5000	0.9729
3.0000	0.5000
5.6630	0.0544

Upper Flap 23	
x	y
0.0000	1.3900
0.3685	1.3900
0.7221	1.2436
1.1900	0.7757
1.5000	0.6312
3.0000	0.5000
4.7260	0.2112

Upper Flap 24	
x	y
0.0000	1.3900
1.3245	1.3900
1.5745	1.3230
3.0000	0.5000
4.7260	0.2112

TABLE AII.- Concluded

Upper Flap 25	
x	y
0.0000	1.3900
0.8058	1.3900
1.1694	1.2436
1.2968	1.0962
1.5000	0.9729
3.0000	0.5000
4.7260	0.2112

Upper Flap 26	
x	y
0.0000	1.3900
1.9028	1.3900
2.2564	1.2436
3.0000	0.5000
4.7234	0.1961

Upper Flap 27	
x	y
0.0000	1.3900
2.1165	1.3900
2.5261	1.1768
3.0000	0.5000
4.7234	0.1961

APPENDIX B

INTERNAL STATIC PRESSURES FOR ALL CONFIGURATIONS TESTED

The internal static pressures are presented in table BI for configurations A01F to A05H and in table BII for configurations C05H to C27AA. The ratio of local static pressure to jet total pressure is presented as a function of nozzle pressure ratio and axial location.

TABLE BI.- RATIO OF INTERNAL UPPER AND LOWER FLAP STATIC PRESSURE TO JET TOTAL PRESSURE FOR CONFIGURATIONS A01F TO A05H

(a) Configuration A01F

upper flap pressures, $p/p_{t,j}$

NPR	$x/h_{t,n}$ 2.775	2.925	3.075	3.225	3.375	3.625	3.900
1.703	.736	.707	.674	.628	.575	.475	.515
2.011	.733	.705	.674	.627	.574	.473	.377
2.527	.733	.703	.673	.626	.572	.471	.376
2.532	.734	.703	.671	.625	.571	.470	.375
2.508	.733	.703	.673	.626	.572	.471	.375
2.996	.732	.702	.671	.625	.570	.469	.375
3.005	.732	.702	.672	.625	.571	.469	.375
3.997	.732	.701	.670	.624	.569	.467	.375
5.003	.732	.701	.670	.624	.569	.466	.375
5.994	.731	.701	.670	.624	.569	.465	.375
7.490	.732	.702	.670	.624	.569	.465	.375
8.597	.732	.702	.670	.625	.570	.466	.375
10.026	.733	.703	.671	.625	.570	.466	.375

lower flap pressures, $p/p_{t,j}$

NPR	$x/h_{t,n}$ 2.775	2.925	3.075	3.225	3.375	3.525	3.700	3.900
1.703	.717	.650	.265	.315	.354	.399	.527	.584
2.011	.714	.649	.264	.313	.353	.396	.433	.436
2.527	.713	.648	.263	.310	.352	.394	.432	.429
2.532	.713	.648	.263	.310	.352	.394	.431	.429
2.508	.713	.648	.263	.310	.352	.394	.432	.430
2.996	.713	.648	.262	.309	.351	.393	.431	.428
3.005	.713	.648	.262	.309	.352	.393	.431	.428
3.997	.714	.647	.261	.308	.351	.392	.429	.426
5.003	.714	.647	.260	.308	.351	.391	.428	.425
5.994	.714	.648	.260	.308	.351	.391	.428	.425
7.490	.714	.648	.261	.308	.350	.391	.427	.425
8.597	.714	.648	.261	.308	.350	.391	.427	.425
10.026	.715	.649	.261	.308	.350	.391	.427	.425

TABLE BI.- Continued

(b) Configuration A02G

upper flap pressures, $p/p_{t,j}$

NPR	$x/h_{t,n}$ 2.775	2.925	3.075	3.225	3.375	3.600	3.850
1.698	.817	.830	.822	.755	.691	.605	.502
1.992	.812	.823	.814	.743	.671	.567	.438
2.516	.811	.822	.814	.743	.670	.565	.434
3.009	.811	.822	.814	.742	.669	.564	.433
4.008	.811	.822	.814	.742	.668	.563	.432
5.010	.811	.823	.814	.742	.668	.563	.430
5.986	.811	.823	.814	.742	.668	.564	.430
7.501	.811	.825	.815	.743	.669	.565	.429
8.601	.812	.826	.815	.743	.669	.566	.429
9.987	.812	.827	.816	.744	.670	.567	.428
10.041	.812	.827	.816	.744	.670	.567	.427

lower flap pressures, $p/p_{t,j}$

NPR	$x/h_{t,n}$ 2.775	2.925	3.075	3.225	3.375	3.525	3.700	3.900
1.698	.765	.682	.394	.403	.429	.474	.525	.568
1.992	.760	.676	.161	.223	.295	.373	.489	.542
2.516	.758	.674	.160	.222	.293	.369	.421	.429
3.009	.759	.674	.160	.222	.292	.368	.420	.428
4.008	.758	.673	.159	.221	.291	.367	.418	.426
5.010	.759	.673	.159	.220	.291	.367	.417	.425
5.986	.760	.673	.157	.219	.291	.366	.416	.425
7.501	.759	.673	.158	.218	.290	.366	.416	.424
8.601	.759	.673	.158	.218	.290	.365	.416	.424
9.987	.759	.673	.157	.218	.289	.365	.416	.425
10.041	.759	.673	.157	.218	.289	.365	.416	.425

TABLE BI.- Continued

(c) Configuration A03F

upper flap pressures, $p/p_{t,j}$

NPR	$x/h_{t,n}$						
	2.775	2.925	3.075	3.225	3.375	3.625	3.900
1.694	.688	.609	.418	.464	.463	.455	.573
1.993	.686	.608	.416	.464	.461	.391	.423
2.502	.685	.607	.415	.465	.459	.388	.311
3.006	.684	.606	.414	.464	.458	.386	.311
4.025	.683	.606	.413	.463	.457	.384	.311
4.002	.683	.606	.413	.463	.456	.384	.310
5.013	.683	.606	.412	.463	.456	.383	.310
6.006	.682	.606	.412	.463	.456	.383	.310
7.512	.682	.607	.411	.462	.456	.382	.310
8.616	.683	.607	.411	.462	.456	.382	.310
10.031	.683	.608	.410	.462	.456	.383	.311

lower flap pressures, $p/p_{t,j}$

NPR	$x/h_{t,n}$							
	2.775	2.925	3.075	3.225	3.375	3.525	3.700	3.900
1.694	.695	.631	.409	.465	.492	.514	.535	.559
1.993	.695	.630	.249	.273	.284	.348	.446	.472
2.502	.696	.629	.248	.272	.282	.282	.266	.331
3.006	.694	.629	.247	.271	.281	.282	.265	.243
4.025	.696	.629	.246	.270	.281	.281	.265	.241
4.002	.695	.629	.246	.269	.281	.280	.265	.241
5.013	.695	.629	.245	.270	.281	.280	.264	.240
6.006	.694	.629	.245	.270	.281	.279	.264	.240
7.512	.695	.630	.246	.270	.280	.279	.264	.239
8.616	.694	.630	.246	.269	.280	.279	.264	.239
10.031	.694	.631	.245	.269	.280	.279	.264	.239

TABLE BI.- Continued

(d) Configuration A04G

upper flap pressures, $p/p_{t,j}$

NPR	$x/h_{t,n}$ 2.775	2.925	3.075	3.225	3.375	3.625	3.900
1.697	.776	.762	.736	.704	.667	.623	.572
2.009	.757	.740	.708	.668	.619	.553	.479
2.487	.747	.727	.691	.644	.582	.485	.373
2.501	.747	.727	.691	.644	.582	.485	.373
3.007	.747	.726	.690	.643	.581	.483	.372
4.007	.746	.725	.689	.642	.578	.481	.371
5.021	.746	.726	.689	.643	.578	.481	.371
6.000	.746	.726	.688	.643	.577	.480	.370
7.504	.746	.726	.688	.642	.577	.480	.370
8.592	.746	.727	.688	.643	.578	.481	.370
10.013	.747	.728	.688	.643	.578	.481	.370

lower flap pressures, $p/p_{t,j}$

NPR	$x/h_{t,n}$ 2.775	2.925	3.075	3.225	3.375	3.525	3.700	3.900
1.697	.752	.681	.563	.562	.560	.559	.563	.570
2.009	.734	.655	.472	.470	.469	.468	.470	.479
2.487	.728	.646	.143	.174	.201	.228	.246	.317
2.501	.726	.645	.143	.173	.200	.228	.246	.310
3.007	.727	.644	.142	.172	.199	.227	.245	.263
4.007	.725	.644	.142	.171	.198	.225	.245	.261
5.021	.725	.643	.141	.171	.197	.224	.244	.260
6.000	.725	.643	.141	.170	.197	.223	.244	.260
7.504	.724	.643	.139	.170	.196	.222	.243	.259
8.592	.723	.643	.139	.169	.195	.222	.242	.259
10.013	.723	.643	.139	.169	.195	.222	.242	.259

TABLE BI.- Continued

(e) Configuration B05H

upper flap pressures, $p/p_{t,j}$

NPR	$x/h_{t,n}$ 2.775	2.925	3.075	3.225	3.375	3.600	3.850	4.150	4.450	4.750	5.050	5.365
1.701	.726	.706	.675	.624	.566	.483	.388	.289	.293	.365	.516	.573
1.980	.732	.704	.675	.623	.565	.481	.387	.289	.293	.359	.367	.457
2.499	.745	.703	.673	.622	.564	.479	.387	.288	.293	.359	.366	.350
3.002	.726	.703	.673	.622	.563	.478	.387	.288	.293	.358	.365	.349
3.999	.731	.702	.672	.622	.562	.477	.386	.287	.292	.357	.363	.349
4.991	.731	.702	.672	.622	.562	.477	.386	.287	.289	.356	.362	.350
5.986	.726	.702	.672	.622	.562	.477	.386	.287	.284	.355	.362	.350
7.499	.733	.703	.672	.622	.562	.477	.386	.287	.276	.354	.360	.349
8.624	.732	.703	.672	.623	.563	.478	.386	.287	.270	.353	.359	.349
10.025	.727	.704	.672	.623	.563	.479	.386	.287	.263	.352	.358	.349

lower flap pressures, $p/p_{t,j}$

NPR	$x/h_{t,n}$ 2.775	2.925	3.075	3.225	3.375	3.525	3.675	3.825	3.975	4.150	4.350	4.600	4.850	5.100
1.701	.718	.643	.261	.312	.359	.400	.429	.436	.420	.394	.365	.337	.499	.534
1.980	.718	.642	.260	.310	.358	.399	.429	.434	.419	.393	.364	.330	.299	.458
2.499	.719	.641	.259	.309	.356	.397	.428	.431	.417	.392	.364	.328	.294	.262
3.002	.716	.641	.259	.308	.356	.396	.427	.430	.417	.391	.364	.327	.294	.261
3.999	.715	.640	.259	.308	.355	.396	.426	.428	.416	.390	.363	.327	.293	.261
4.991	.719	.640	.259	.308	.355	.395	.424	.427	.415	.390	.362	.326	.293	.260
5.986	.719	.641	.259	.308	.355	.395	.424	.426	.415	.390	.362	.326	.293	.259
7.499	.716	.641	.259	.307	.354	.394	.424	.426	.415	.389	.362	.326	.293	.259
8.624	.715	.641	.258	.307	.354	.393	.424	.426	.415	.389	.362	.326	.293	.259
10.025	.715	.642	.258	.307	.354	.393	.424	.426	.415	.389	.362	.326	.293	.259

TABLE BI.- Continued

(f) Configuration B06I

upper flap pressures, $p/p_{t,j}$

NPR	$x/h_{t,n}$									
	2.775	2.925	3.075	3.225	3.375	3.700	4.000	4.300	4.600	4.900
1.692	.823	.828	.822	.754	.685	.523	.375	.396	.451	.512
1.994	.806	.827	.821	.753	.683	.522	.374	.265	.197	.355
2.491	.817	.824	.818	.750	.679	.517	.373	.265	.197	.347
2.993	.809	.823	.817	.748	.678	.515	.372	.265	.196	.345
4.000	.812	.823	.817	.747	.676	.513	.371	.264	.196	.344
4.987	.805	.824	.816	.747	.676	.512	.371	.264	.196	.342
6.009	.802	.824	.816	.746	.676	.511	.371	.264	.196	.340
7.510	.805	.825	.816	.746	.676	.512	.372	.264	.196	.338
8.584	.804	.826	.817	.746	.677	.513	.372	.264	.196	.337
9.990	.806	.828	.817	.746	.677	.513	.373	.265	.196	.336

lower flap pressures, $p/p_{t,j}$

NPR	$x/h_{t,n}$												
	2.775	2.925	3.075	3.325	3.375	3.525	3.675	3.825	3.975	4.200	4.450	4.700	4.950	5.200
1.692	.764	.688	.162	.230	.303	.378	.424	.438	.456	.490	.530	.562	.584	.579
1.994	.763	.687	.161	.229	.303	.376	.423	.433	.415	.375	.332	.293	.451	.485
2.491	.761	.685	.160	.226	.301	.373	.421	.430	.413	.374	.331	.292	.254	.374
2.993	.760	.684	.160	.224	.299	.371	.420	.428	.412	.373	.331	.291	.254	.228
4.000	.759	.684	.159	.222	.297	.369	.418	.426	.411	.372	.331	.290	.253	.217
4.987	.760	.684	.159	.222	.296	.368	.417	.425	.410	.371	.330	.290	.252	.216
6.009	.759	.683	.157	.221	.295	.367	.416	.424	.410	.371	.329	.288	.252	.215
7.510	.759	.683	.157	.220	.295	.366	.416	.424	.410	.371	.329	.289	.252	.216
8.584	.759	.683	.156	.220	.294	.365	.415	.424	.409	.371	.329	.289	.253	.215
9.990	.758	.683	.156	.219	.294	.365	.414	.424	.409	.371	.329	.288	.253	.215

TABLE BI.- Continued

(g) Configuration B07H

upper flap pressures, $p/p_{t,j}$

NPR	$x/h_{t,n}$ 2.775	2.925	3.075	3.225	3.375	3.600	3.850	4.150	4.450	4.750	5.050	5.365
1.693	.721	.603	.429	.468	.459	.405	.427	.519	.523	.531	.542	.561
2.002	.706	.601	.427	.468	.458	.403	.328	.463	.475	.476	.477	.479
2.497	.706	.600	.426	.469	.456	.402	.328	.250	.368	.381	.382	.384
3.003	.700	.598	.425	.469	.455	.401	.328	.250	.192	.300	.309	.318
3.997	.684	.596	.424	.468	.452	.399	.327	.249	.192	.153	.127	.152
4.994	.694	.596	.424	.468	.452	.398	.327	.249	.192	.154	.127	.149
6.002	.691	.595	.424	.468	.451	.398	.327	.249	.192	.154	.127	.148
7.489	.691	.595	.424	.469	.451	.399	.328	.249	.192	.154	.127	.148
8.605	.685	.595	.423	.468	.451	.400	.328	.249	.192	.153	.127	.148
10.023	.684	.595	.423	.468	.451	.400	.328	.249	.192	.154	.126	.147

lower flap presssures, $p/p_{t,j}$

NPR	$x/h_{t,n}$ 2.775	2.925	3.075	3.225	3.375	3.525	3.675	3.825	3.975	4.150	4.350	4.600	4.850	5.100
1.693	.692	.625	.246	.273	.287	.285	.293	.418	.441	.465	.501	.549	.581	.593
2.002	.695	.624	.245	.272	.285	.284	.268	.255	.240	.356	.412	.450	.504	.532
2.497	.696	.623	.244	.271	.284	.283	.268	.252	.238	.250	.244	.228	.213	.349
3.003	.695	.623	.243	.270	.283	.282	.267	.251	.237	.249	.243	.227	.210	.196
3.997	.694	.622	.242	.268	.282	.279	.266	.249	.236	.247	.242	.226	.209	.195
4.994	.694	.622	.242	.268	.281	.279	.266	.248	.236	.246	.241	.226	.209	.194
6.002	.695	.622	.242	.268	.281	.279	.266	.248	.235	.245	.241	.225	.208	.194
7.489	.696	.623	.242	.268	.281	.278	.267	.247	.234	.245	.241	.225	.207	.192
8.605	.694	.623	.242	.268	.280	.278	.267	.247	.234	.244	.241	.225	.207	.191
10.023	.693	.623	.242	.267	.280	.278	.267	.247	.233	.244	.240	.225	.207	.191

TABLE BI.- Continued

(h) Configuration B08I

upper flap pressures, $p/p_{t,j}$

NPR	$x/h_{t,n}$										
	2.775	2.925	3.075	3.225	3.375	3.600	3.850	4.150	4.450	4.750	5.050
1.708	.724	.738	.716	.660	.624	.549	.510	.480	.510	.541	.558
2.005	.746	.727	.702	.638	.593	.490	.401	.301	.470	.476	.477
2.503	.741	.726	.700	.637	.591	.487	.401	.298	.233	.380	.383
3.004	.728	.725	.700	.636	.589	.485	.401	.298	.218	.276	.315
3.994	.731	.725	.699	.636	.588	.483	.401	.298	.217	.165	.132
5.004	.740	.725	.698	.635	.587	.482	.401	.298	.217	.165	.132
5.998	.735	.725	.698	.635	.588	.482	.401	.298	.217	.166	.132
7.484	.736	.726	.698	.635	.588	.482	.400	.298	.217	.165	.132
8.596	.739	.726	.698	.635	.588	.482	.400	.298	.217	.165	.132
10.020	.738	.727	.699	.635	.588	.483	.400	.299	.217	.165	.132

lower flap pressures, $p/p_{t,j}$

NPR	$x/h_{t,n}$													
	2.775	2.925	3.075	3.325	3.375	3.525	3.675	3.825	3.975	4.200	4.450	4.700	4.950	5.200
1.708	.732	.661	.467	.466	.467	.475	.484	.492	.498	.508	.520	.533	.548	.553
2.005	.725	.653	.141	.174	.203	.230	.246	.264	.349	.430	.474	.528	.543	.507
2.503	.726	.652	.141	.173	.202	.228	.246	.262	.267	.259	.240	.360	.411	.448
3.004	.724	.652	.140	.172	.201	.227	.245	.260	.266	.258	.239	.218	.194	.308
3.994	.724	.652	.140	.171	.199	.226	.244	.258	.265	.257	.238	.217	.193	.175
5.004	.723	.652	.140	.171	.198	.225	.244	.257	.264	.256	.238	.217	.193	.174
5.998	.724	.652	.140	.170	.198	.224	.243	.256	.264	.255	.237	.216	.192	.173
7.484	.725	.652	.140	.170	.197	.224	.243	.256	.263	.255	.237	.216	.192	.173
8.596	.724	.652	.140	.170	.196	.223	.242	.255	.263	.255	.237	.216	.192	.173
10.020	.724	.653	.140	.169	.196	.223	.242	.255	.263	.255	.237	.216	.192	.173

TABLE BI.- Continued

(i) Configuration A09J

upper flap pressures, $p/p_{t,j}$

NPR	$x/h_{t,n}$ 2.775	2.925	3.075	3.225	3.375	3.625	3.900
1.776	.846	.761	.633	.644	.609	.519	.454
2.100	.842	.755	.622	.630	.589	.482	.380
2.678	.841	.753	.620	.628	.587	.480	.377
2.611	.842	.753	.620	.628	.587	.480	.377
3.164	.842	.752	.618	.628	.587	.478	.378
4.215	.841	.751	.617	.628	.586	.476	.377
5.292	.840	.751	.617	.628	.586	.476	.377
6.328	.840	.751	.617	.629	.587	.476	.378
6.358	.840	.751	.617	.629	.587	.476	.378
7.942	.841	.752	.617	.629	.588	.477	.379
9.138	.841	.753	.617	.629	.588	.477	.379
9.110	.841	.752	.617	.629	.588	.477	.379
10.592	.842	.754	.617	.630	.589	.479	.380

lower flap pressures, $p/p_{t,j}$

NPR	$x/h_{t,n}$ 2.775	2.925	3.075	3.225	3.375	3.525	3.700	3.900
1.776	.850	.752	.356	.365	.401	.450	.507	.560
2.100	.851	.748	.132	.222	.320	.385	.425	.433
2.678	.846	.747	.130	.221	.318	.382	.424	.426
2.611	.853	.747	.130	.221	.319	.383	.424	.426
3.164	.848	.746	.130	.221	.317	.381	.423	.425
4.215	.847	.746	.129	.221	.314	.380	.421	.423
5.292	.847	.746	.129	.222	.312	.379	.420	.423
6.328	.848	.746	.130	.222	.310	.379	.420	.423
6.358	.848	.746	.130	.222	.310	.379	.420	.423
7.942	.848	.746	.130	.223	.308	.378	.419	.422
9.138	.846	.747	.130	.223	.307	.378	.419	.422
9.110	.846	.746	.130	.223	.307	.377	.419	.422
10.592	.846	.747	.130	.222	.305	.377	.419	.423

TABLE BI.- Continued

(j) Configuration A10K

upper flap pressures, $p/p_{t,j}$

NPR	$x/h_{t,n}$						
	2.775	2.925	3.075	3.225	3.375	3.600	3.850
1.787	.887	.853	.805	.778	.733	.651	.564
2.097	.879	.837	.783	.751	.696	.594	.485
2.646	.875	.833	.777	.743	.683	.571	.452
2.619	.875	.832	.777	.742	.683	.571	.451
3.153	.875	.832	.777	.742	.682	.570	.450
4.214	.874	.832	.776	.742	.681	.568	.448
5.304	.874	.832	.777	.742	.681	.568	.448
5.279	.874	.832	.777	.742	.681	.568	.448
6.349	.874	.833	.777	.742	.682	.569	.448
7.925	.874	.834	.777	.742	.682	.570	.448
9.099	.874	.835	.777	.742	.682	.570	.448
10.638	.876	.836	.778	.743	.683	.571	.448

lower flap pressures, $p/p_{t,j}$

NPR	$x/h_{t,n}$							
	2.775	2.925	3.075	3.225	3.375	3.525	3.700	3.900
1.787	.874	.776	.467	.460	.463	.481	.509	.546
2.097	.866	.759	.290	.287	.298	.340	.399	.459
2.646	.865	.755	.077	.155	.262	.352	.416	.430
2.619	.865	.755	.077	.155	.262	.351	.415	.429
3.153	.865	.754	.076	.155	.261	.350	.415	.428
4.214	.865	.753	.075	.154	.259	.348	.414	.426
5.304	.864	.753	.075	.154	.258	.347	.413	.426
5.279	.864	.753	.075	.154	.258	.347	.413	.426
6.349	.865	.753	.075	.153	.257	.346	.413	.426
7.925	.864	.753	.075	.152	.256	.345	.412	.426
9.099	.863	.753	.075	.152	.256	.345	.411	.425
10.638	.863	.754	.075	.151	.255	.344	.411	.426

TABLE BI.- Continued

(k) Configuration A11J

upper flap pressures, $p/p_{t,j}$

NPR	$x/h_{t,n}$						
	2.775	2.925	3.075	3.225	3.375	3.625	3.900
1.784	.830	.708	.253	.525	.589	.573	.580
2.103	.827	.704	.243	.384	.479	.428	.348
2.626	.826	.700	.242	.381	.471	.415	.317
3.158	.826	.699	.241	.382	.469	.414	.317
4.215	.824	.698	.239	.383	.468	.412	.317
5.278	.825	.698	.238	.382	.468	.412	.316
6.350	.824	.698	.238	.383	.468	.412	.316
7.926	.825	.698	.237	.383	.467	.412	.316
9.095	.825	.699	.237	.383	.466	.413	.317
10.614	.826	.700	.237	.383	.466	.413	.317

lower flap pressures, $p/p_{t,j}$

NPR	$x/h_{t,n}$							
	2.775	2.925	3.075	3.225	3.375	3.525	3.700	3.900
1.784	.848	.747	.428	.432	.453	.505	.555	.572
2.103	.844	.742	.205	.290	.357	.375	.447	.472
2.626	.844	.740	.125	.201	.258	.287	.268	.321
3.158	.842	.739	.124	.201	.255	.285	.267	.238
4.215	.841	.739	.124	.201	.253	.284	.267	.237
5.278	.839	.739	.124	.201	.251	.283	.266	.236
6.350	.840	.739	.124	.202	.250	.283	.266	.235
7.926	.841	.739	.125	.202	.249	.282	.266	.235
9.095	.839	.739	.126	.202	.249	.282	.266	.235
10.614	.841	.740	.126	.202	.249	.282	.266	.235

TABLE BI.- Continued

(1) Configuration A12K

upper flap pressures, $p/p_{t,j}$

NPR	$x/h_{t,n}$						
	2.775	2.925	3.075	3.225	3.375	3.625	3.900
1.768	.871	.801	.722	.724	.697	.643	.581
2.104	.856	.781	.687	.686	.650	.579	.506
2.638	.846	.768	.663	.661	.617	.530	.440
3.160	.846	.762	.651	.647	.596	.495	.384
4.228	.845	.761	.650	.647	.595	.494	.384
5.297	.845	.762	.649	.647	.595	.494	.383
6.354	.846	.762	.649	.648	.596	.495	.383
7.970	.846	.763	.649	.648	.596	.495	.383
9.091	.847	.764	.649	.649	.597	.496	.383
9.084	.847	.763	.649	.649	.597	.496	.383
9.119	.847	.763	.649	.648	.597	.496	.383
10.627	.847	.765	.649	.649	.598	.497	.383

lower flap pressures, $p/p_{t,j}$

NPR	$x/h_{t,n}$							
	2.775	2 925	3.075	3.225	3.375	3.525	3.700	3.900
1.768	.865	.772	.567	.566	.564	.562	.562	.562
2.104	.855	.750	.470	.468	.465	.462	.463	.466
2.638	.847	.738	.359	.355	.353	.350	.351	.365
3.160	.847	.734	.066	.115	.171	.212	.240	.259
4.228	.849	.733	.065	.113	.170	.211	.239	.258
5.297	.847	.733	.065	.113	.169	.210	.239	.257
6.354	.849	.733	.065	.113	.169	.209	.239	.256
7.970	.849	.733	.064	.112	.168	.209	.238	.256
9.091	.850	.734	.065	.112	.168	.209	.238	.256
9.084	.849	.733	.065	.112	.168	.209	.238	.256
9.119	.849	.733	.065	.112	.168	.209	.238	.256
10.627	.849	.734	.065	.112	.167	.208	.238	.256

TABLE BI.- Continued

(m) Configuration B13L

upper flap pressures, $p/p_{t,j}$

NPR	$x/h_{t,n}$ 2.775	2.925	3.075	3.225	3.375	3.600	3.850	4.150	4.450	4.750	5.050	5.365
1.721	.756	.717	.618	.617	.568	.478	.379	.291	.443	.466	.503	.557
2.001	.731	.712	.616	.614	.565	.478	.378	.288	.217	.343	.368	.451
2.024	.730	.712	.616	.613	.565	.477	.378	.289	.217	.343	.368	.444
2.580	.696	.707	.611	.611	.561	.472	.376	.287	.216	.339	.366	.340
2.574	.698	.707	.611	.611	.561	.473	.376	.287	.216	.340	.367	.338
2.552	.698	.707	.611	.611	.561	.473	.376	.287	.216	.340	.366	.338
3.066	.680	.705	.610	.611	.561	.473	.374	.286	.216	.336	.364	.332
4.107	.654	.702	.606	.610	.559	.470	.372	.286	.215	.332	.363	.333
5.137	.640	.700	.605	.609	.558	.469	.371	.285	.215	.328	.360	.331
6.161	.630	.700	.605	.609	.558	.469	.370	.285	.215	.325	.359	.330
7.737	.621	.700	.604	.610	.558	.470	.370	.285	.215	.320	.355	.332
8.878	.616	.700	.604	.610	.558	.471	.370	.285	.215	.317	.353	.352
10.316	.612	.700	.603	.610	.559	.471	.370	.286	.215	.313	.351	.351

lower flap pressures, $p/p_{t,j}$

NPR	$x/h_{t,n}$ 2.775	2.925	3.075	3.225	3.375	3.525	3.675	3.825	3.975	4.150	4.350	4.600	4.850	5.100	5.350
1.721	.821	.739	.133	.225	.315	.373	.408	.427	.417	.394	.381	.517	.545	.560	.565
2.001	.819	.735	.130	.221	.312	.370	.406	.424	.414	.391	.363	.331	.292	.451	.480
2.024	.817	.734	.130	.220	.312	.369	.405	.423	.414	.390	.363	.330	.290	.443	.474
2.580	.814	.731	.128	.217	.309	.365	.402	.420	.411	.388	.361	.328	.289	.256	.338
2.574	.816	.731	.128	.217	.309	.365	.402	.420	.411	.389	.361	.328	.289	.256	.340
2.552	.815	.731	.128	.217	.309	.365	.402	.420	.411	.388	.361	.328	.289	.256	.347
3.066	.817	.730	.128	.217	.309	.364	.402	.418	.410	.388	.360	.328	.290	.257	.219
4.107	.818	.728	.127	.217	.307	.362	.400	.415	.409	.387	.359	.326	.290	.256	.217
5.137	.819	.727	.127	.216	.306	.361	.398	.414	.408	.386	.358	.324	.289	.255	.216
6.161	.819	.727	.127	.216	.305	.360	.398	.413	.407	.386	.357	.324	.290	.255	.216
7.737	.819	.727	.127	.216	.304	.359	.397	.412	.407	.386	.357	.323	.290	.255	.216
8.878	.820	.727	.127	.216	.304	.359	.397	.412	.407	.386	.358	.323	.290	.256	.216
10.316	.820	.727	.127	.216	.303	.358	.396	.411	.406	.386	.357	.322	.290	.256	.216

TABLE BI.- Continued

(n) Configuration B14M

upper flap pressures, $p/p_{t,j}$

NPR	$x/h_{t,n}$ 2.775	2.925	3.075	3.225	3.375	3.700	4.000	4.300	4.600	4.900	5.250
1.729	.922	.826	.771	.738	.682	.531	.399	.393	.461	.503	.554
2.047	.935	.822	.767	.734	.676	.519	.374	.265	.400	.414	.461
2.528	.947	.818	.763	.731	.673	.515	.372	.264	.188	.301	.336
2.544	.947	.818	.764	.731	.673	.515	.373	.264	.188	.301	.334
3.073	.956	.815	.761	.728	.671	.512	.371	.263	.187	.297	.320
4.101	.968	.814	.759	.727	.669	.509	.369	.262	.186	.292	.317
5.148	.974	.813	.758	.726	.668	.508	.369	.261	.186	.287	.315
6.155	.979	.813	.757	.725	.668	.507	.368	.261	.186	.283	.314
7.729	.982	.813	.756	.724	.668	.507	.367	.261	.186	.278	.313
8.858	.985	.813	.756	.724	.668	.508	.367	.261	.186	.274	.312
10.350	.986	.814	.755	.724	.668	.508	.367	.261	.186	.270	.312

lower flap pressures, $p/p_{t,j}$

NPR	$x/h_{t,n}$ 2.775	2.925	3.075	3.325	3.375	3.525	3.675	3.825	3.975	4.200	4.450	4.700	4.950	5.200
1.729	.846	.728	.211	.222	.264	.329	.385	.428	.453	.485	.523	.556	.570	.574
2.047	.842	.724	.079	.158	.256	.348	.404	.429	.410	.372	.350	.477	.509	.487
2.528	.840	.721	.078	.157	.254	.345	.401	.426	.407	.370	.327	.287	.248	.366
2.544	.841	.721	.078	.157	.254	.345	.401	.426	.408	.370	.327	.287	.249	.362
3.073	.837	.719	.077	.156	.252	.342	.399	.423	.406	.368	.325	.286	.248	.216
4.101	.835	.716	.076	.154	.250	.339	.395	.420	.404	.367	.324	.284	.247	.209
5.148	.834	.715	.075	.152	.248	.338	.393	.418	.403	.366	.323	.284	.246	.208
6.155	.833	.714	.075	.152	.247	.336	.392	.417	.402	.365	.323	.283	.246	.207
7.729	.831	.713	.075	.150	.245	.334	.390	.416	.401	.365	.322	.282	.246	.207
8.858	.830	.713	.076	.150	.244	.333	.389	.416	.401	.365	.322	.282	.246	.207
10.350	.829	.713	.076	.149	.243	.332	.388	.415	.400	.365	.322	.282	.247	.206

TABLE BI.- Continued

(o) Configuration B15L

upper flap pressures, $p/p_{t,j}$

NPR	$x/h_{t,n}$ 2.775	2.925	3.075	3.225	3.375	3.600	3.850	4.150	4.450	4.750	5.050	5.365
1.724	.757	.715	.252	.443	.532	.520	.494	.514	.533	.543	.559	.569
2.034	.729	.708	.227	.365	.457	.420	.333	.445	.466	.467	.469	.475
2.548	.700	.703	.225	.363	.454	.415	.331	.246	.361	.375	.376	.377
3.085	.678	.701	.224	.362	.452	.412	.330	.246	.188	.298	.306	.312
4.104	.654	.698	.223	.362	.448	.408	.329	.245	.187	.141	.187	.231
5.125	.640	.696	.223	.360	.447	.406	.329	.245	.186	.140	.117	.166
6.174	.631	.695	.222	.360	.445	.405	.328	.244	.186	.140	.116	.091
7.732	.621	.695	.221	.359	.444	.404	.328	.244	.186	.140	.116	.089
8.845	.616	.695	.221	.358	.443	.404	.328	.244	.186	.140	.116	.089
10.319	.612	.696	.221	.357	.442	.404	.328	.244	.186	.140	.116	.089

lower flap pressures, $p/p_{t,j}$

NPR	$x/h_{t,n}$ 2.775	2.925	3.075	3.225	3.375	3.525	3.675	3.825	3.975	4.150	4.350	4.600	4.850	5.100	5.350
1.724	.837	.742	.445	.451	.455	.464	.473	.483	.491	.501	.509	.522	.534	.547	.552
2.034	.832	.732	.128	.206	.264	.282	.269	.250	.229	.366	.378	.404	.451	.497	.506
2.548	.829	.728	.126	.203	.262	.279	.266	.246	.220	.191	.161	.228	.310	.365	.408
3.085	.826	.727	.125	.202	.260	.278	.264	.244	.219	.190	.160	.226	.208	.194	.297
4.104	.823	.724	.123	.199	.259	.275	.263	.242	.217	.188	.159	.224	.207	.192	.174
5.125	.822	.723	.123	.198	.258	.274	.262	.241	.216	.187	.158	.223	.206	.191	.173
6.174	.821	.722	.122	.197	.257	.273	.262	.240	.215	.186	.157	.223	.206	.190	.172
7.732	.820	.722	.122	.197	.256	.273	.262	.240	.215	.186	.157	.222	.205	.190	.172
8.845	.819	.722	.122	.197	.256	.272	.261	.240	.215	.186	.157	.222	.205	.189	.172
10.319	.818	.722	.122	.197	.255	.272	.261	.240	.215	.186	.157	.221	.204	.189	.171

TABLE BI.- Continued

(p) Configuration B16M

upper flap pressures, $p/p_{t,j}$

NPR	$x/h_{t,n}$											
	2.775	2.925	3.075	3.225	3.375	3.600	3.850	4.150	4.450	4.750	5.050	5.365
1.727	.897	.774	.696	.699	.664	.613	.562	.530	.529	.543	.550	.569
2.011	.896	.754	.665	.666	.622	.556	.487	.424	.381	.388	.517	.498
2.028	.896	.753	.664	.664	.620	.553	.483	.419	.375	.376	.509	.502
2.558	.900	.737	.636	.633	.577	.490	.394	.291	.231	.372	.376	.370
3.070	.908	.735	.634	.631	.575	.487	.393	.291	.216	.269	.309	.309
4.134	.920	.732	.631	.629	.572	.485	.391	.290	.215	.163	.128	.229
4.110	.920	.732	.631	.630	.572	.485	.391	.290	.215	.163	.128	.231
5.142	.926	.731	.629	.629	.571	.484	.391	.289	.215	.162	.128	.159
6.166	.931	.730	.628	.628	.570	.483	.391	.289	.214	.162	.127	.101
7.724	.934	.730	.627	.628	.569	.483	.390	.289	.214	.162	.127	.101
8.863	.936	.730	.626	.628	.569	.483	.391	.289	.214	.162	.127	.100
10.336	.938	.730	.626	.627	.569	.484	.390	.289	.214	.162	.127	.100

lower flap pressures, $p/p_{t,j}$

NPR	$x/h_{t,n}$													
	2.775	2.925	3.075	3.325	3.375	3.525	3.675	3.825	3.975	4.200	4.450	4.700	4.950	5.200
1.727	.845	.734	.527	.522	.518	.515	.515	.516	.520	.525	.533	.541	.551	.547
2.011	.834	.714	.434	.429	.425	.421	.421	.425	.432	.441	.452	.460	.471	.467
2.028	.833	.713	.428	.424	.420	.416	.416	.420	.427	.436	.447	.456	.466	.463
2.558	.824	.699	.069	.116	.167	.209	.232	.256	.260	.254	.236	.371	.426	.453
3.070	.821	.698	.069	.116	.166	.207	.230	.254	.259	.253	.235	.215	.194	.299
4.134	.819	.695	.068	.115	.163	.205	.229	.251	.257	.251	.233	.214	.194	.170
4.110	.819	.695	.068	.115	.164	.205	.229	.251	.257	.251	.233	.214	.193	.170
5.142	.817	.694	.067	.114	.162	.204	.228	.250	.256	.250	.233	.213	.193	.168
6.166	.816	.693	.067	.113	.162	.203	.227	.249	.255	.249	.232	.213	.193	.168
7.724	.814	.692	.067	.112	.161	.202	.225	.248	.254	.248	.232	.212	.192	.167
8.863	.813	.692	.067	.111	.160	.201	.225	.247	.254	.248	.231	.212	.192	.166
10.336	.813	.692	.067	.111	.159	.200	.224	.247	.254	.248	.231	.212	.192	.166

TABLE BI.- Continued

(q) Configuration C17N

upper flap pressures, $p/p_{t,j}$

NPR	$x/h_{t,n}$								
	2.775	2.925	3.075	3.325	3.375	3.700	4.000	4.300	4.650
1.731	.510	.542	.559	.578	.578	.578	.773	.674	.383
1.697	.524	.550	.569	.589	.589	.589	.772	.674	.383
1.976	.308	.478	.491	.506	.506	.506	.772	.672	.380
2.008	.307	.470	.483	.498	.498	.498	.772	.672	.379
2.518	.306	.232	.384	.397	.397	.397	.772	.670	.376
3.006	.306	.231	.308	.333	.333	.333	.771	.668	.374
4.008	.306	.230	.169	.250	.249	.250	.771	.668	.374
5.005	.306	.230	.170	.200	.200	.200	.771	.667	.375
6.013	.306	.230	.170	.166	.166	.167	.771	.667	.375
7.503	.305	.229	.170	.133	.133	.134	.771	.668	.375
8.608	.306	.229	.170	.116	.116	.116	.771	.668	.375
10.039	.306	.229	.170	.100	.100	.100	.771	.669	.375

lower flap pressures, $p/p_{t,j}$

NPR	$x/h_{t,n}$											
	2.775	2.925	3.075	3.325	3.375	3.525	3.675	3.825	3.975	4.200	4.400	4.600
1.731	.783	.685	.214	.267	.301	.315	.324	.353	.485	.553	.589	.590
1.697	.785	.685	.213	.267	.302	.315	.324	.403	.500	.564	.599	.599
1.976	.782	.684	.213	.266	.300	.314	.323	.339	.338	.343	.493	.530
2.008	.782	.684	.213	.266	.300	.313	.323	.338	.338	.325	.470	.518
2.518	.781	.683	.213	.264	.299	.311	.322	.336	.336	.323	.306	.285
3.006	.782	.682	.212	.263	.298	.309	.321	.335	.335	.322	.305	.283
4.008	.782	.682	.212	.261	.297	.309	.320	.333	.334	.321	.304	.283
5.005	.782	.682	.212	.261	.297	.308	.319	.331	.333	.321	.304	.282
6.013	.782	.682	.213	.262	.296	.308	.319	.330	.332	.321	.303	.282
7.503	.781	.682	.213	.261	.296	.308	.318	.330	.332	.321	.303	.281
8.608	.780	.683	.213	.261	.295	.307	.318	.330	.332	.321	.304	.281
10.039	.780	.683	.213	.261	.295	.307	.318	.330	.332	.321	.304	.282

TABLE BI.- Continued

(r) Configuration C180

upper flap pressures, $p/p_{t,j}$

NPR	$x/h_{t,n}$ 2.775	2.925	3.075	3.225	3.375	3.650	3.950	4.250	4.570
1.695	.847	.819	.785	.748	.706	.610	.530	.505	.548
2.006	.832	.801	.762	.715	.660	.528	.397	.378	.483
2.502	.833	.799	.760	.714	.658	.525	.396	.287	.377
2.987	.834	.798	.759	.713	.658	.524	.396	.287	.259
4.001	.833	.799	.758	.714	.657	.523	.395	.287	.190
4.987	.834	.799	.758	.713	.657	.522	.395	.287	.189
6.010	.833	.799	.758	.713	.657	.523	.394	.287	.189
7.499	.833	.800	.758	.713	.658	.524	.394	.287	.188
8.598	.833	.801	.758	.714	.658	.525	.394	.287	.188
10.031	.833	.802	.758	.714	.659	.525	.394	.287	.188

lower flap pressures, $p/p_{t,j}$

NPR	$x/h_{t,n}$ 2.775	2.925	3.075	3.225	3.375	3.525	3.675	3.825	3.975	4.150	4.300	4.500
1.695	.822	.725	.481	.476	.473	.477	.487	.502	.518	.535	.550	.568
2.006	.811	.707	.096	.152	.213	.273	.312	.340	.401	.513	.547	.535
2.502	.811	.705	.096	.151	.212	.271	.310	.338	.337	.321	.304	.280
2.987	.811	.704	.095	.150	.211	.270	.310	.337	.336	.321	.303	.275
4.001	.811	.704	.095	.148	.210	.268	.309	.335	.334	.320	.303	.273
4.987	.811	.703	.095	.147	.209	.267	.308	.334	.333	.319	.302	.273
6.010	.811	.703	.095	.147	.208	.266	.307	.333	.333	.319	.302	.272
7.499	.810	.703	.095	.146	.207	.266	.307	.333	.333	.318	.301	.272
8.598	.810	.704	.095	.146	.207	.265	.307	.333	.333	.318	.301	.271
10.031	.810	.704	.095	.146	.207	.265	.306	.333	.334	.318	.301	.271

TABLE BI.- Continued

(s) Configuration C19P

upper flap pressures, $p/p_{t,j}$

NPR	$x/h_{t,n}$ 2.775	2.925	3.075	3.225	3.375	3.650	3.950	4.250	4.570
1.699	.835	.799	.756	.712	.652	.522	.371	.492	.557
1.984	.834	.796	.756	.709	.650	.518	.367	.296	.474
2.534	.829	.794	.753	.705	.647	.512	.364	.274	.323
2.486	.829	.792	.752	.703	.645	.511	.363	.274	.343
3.009	.825	.791	.750	.702	.645	.509	.362	.273	.217
4.006	.823	.791	.749	.700	.642	.505	.358	.272	.210
5.016	.822	.791	.749	.699	.642	.505	.363	.271	.209
5.997	.823	.792	.748	.699	.642	.504	.374	.271	.209
7.485	.822	.792	.748	.698	.643	.504	.373	.271	.209
8.613	.822	.793	.748	.698	.643	.504	.373	.271	.209
10.029	.823	.794	.748	.698	.644	.504	.372	.271	.209

lower flap pressures, $p/p_{t,j}$

NPR	$x/h_{t,n}$ 2.775	2.925	3.075	3.225	3.375	3.525	3.675	3.825	3.975	4.150	4.350	4.550
1.699	.820	.706	.184	.234	.318	.401	.467	.519	.544	.574	.590	.587
1.984	.817	.704	.177	.233	.316	.398	.454	.468	.449	.423	.486	.530
2.534	.811	.701	.167	.229	.314	.394	.451	.465	.447	.419	.384	.345
2.486	.813	.700	.167	.228	.313	.393	.450	.464	.447	.419	.385	.346
3.009	.811	.698	.162	.226	.311	.391	.449	.462	.445	.417	.384	.346
4.006	.806	.696	.154	.223	.309	.389	.446	.459	.444	.415	.382	.343
5.016	.805	.695	.151	.222	.309	.388	.445	.458	.444	.415	.382	.342
5.997	.805	.695	.148	.221	.308	.387	.445	.458	.444	.414	.381	.342
7.485	.803	.695	.143	.220	.307	.387	.444	.458	.444	.414	.381	.342
8.613	.802	.695	.142	.220	.306	.386	.444	.458	.444	.415	.382	.342
10.029	.802	.694	.141	.219	.306	.386	.444	.458	.444	.414	.381	.341

TABLE BI.- Continued

(t) Configuration C20P

upper flap pressures, $p/p_{t,j}$

NPR	$x/h_{t,n}$ 2.775	2.925	3.075	3.325	3.375	3.700	4.000	4.300	4.650
1.697	.796	.701	.604	.645	.615	.575	.561	.563	.538
2.003	.779	.682	.550	.598	.553	.463	.394	.400	.427
2.501	.773	.677	.526	.585	.531	.414	.312	.234	.385
3.037	.769	.674	.526	.582	.528	.409	.311	.233	.295
3.001	.769	.674	.526	.581	.528	.409	.311	.234	.304
3.989	.768	.672	.528	.580	.525	.406	.310	.234	.151
5.003	.767	.671	.526	.579	.523	.404	.310	.234	.150
5.997	.766	.672	.525	.578	.523	.404	.309	.234	.150
7.506	.766	.672	.522	.578	.522	.403	.309	.234	.150
8.601	.766	.672	.521	.578	.522	.403	.309	.233	.150
9.978	.767	.673	.520	.578	.522	.403	.309	.234	.150
10.090	.767	.673	.520	.578	.523	.403	.309	.233	.150

lower flap pressures, $p/p_{t,j}$

NPR	$x/h_{t,n}$ 2.775	2.925	3.075	3.225	3.375	3.525	3.675	3.825	3.975	4.150	4.350	4.550
1.697	.812	.703	.552	.554	.547	.545	.543	.547	.550	.558	.565	.563
2.003	.797	.680	.393	.397	.397	.399	.407	.428	.440	.453	.468	.473
2.501	.789	.674	.142	.178	.211	.234	.241	.251	.254	.252	.241	.372
3.037	.784	.672	.138	.175	.210	.231	.241	.248	.252	.249	.239	.227
3.001	.782	.672	.138	.174	.209	.231	.241	.248	.252	.249	.238	.227
3.989	.781	.670	.135	.172	.208	.229	.240	.246	.251	.247	.237	.225
5.003	.779	.669	.133	.170	.207	.228	.239	.244	.249	.246	.236	.223
5.997	.778	.669	.132	.170	.206	.227	.238	.244	.249	.246	.236	.223
7.506	.778	.668	.131	.169	.205	.226	.237	.243	.249	.245	.235	.222
8.601	.777	.668	.130	.169	.205	.226	.237	.243	.249	.245	.235	.222
9.978	.776	.668	.129	.168	.204	.226	.236	.242	.248	.245	.234	.221
10.090	.776	.668	.129	.168	.204	.226	.237	.242	.248	.245	.234	.221

TABLE BI.- Continued

(u) Configuration D21Q

upper flap pressures, $p/p_{t,j}$

NPR	$x/h_{t,n}$ 2.775	2.925	3.075	3.225	3.375	3.550	3.700
1.705	.819	.761	.704	.691	.662	.622	.582
1.996	.808	.743	.677	.659	.621	.566	.511
2.505	.801	.732	.659	.637	.588	.514	.451
3.000	.801	.731	.658	.635	.586	.513	.450
3.993	.801	.730	.657	.636	.585	.511	.450
5.006	.801	.730	.656	.636	.584	.511	.449
6.012	.801	.730	.656	.636	.585	.511	.449
7.500	.800	.731	.655	.636	.585	.511	.449
8.596	.800	.731	.655	.636	.585	.511	.448
10.032	.800	.732	.655	.636	.586	.512	.448

lower flap pressures, $p/p_{t,j}$

NPR	$x/h_{t,n}$ 2.775	2.925	3.075	3.225	3.375	3.525	3.675
1.705	.807	.720	.533	.530	.530	.540	.560
1.996	.797	.702	.444	.442	.443	.453	.474
2.505	.791	.694	.140	.196	.249	.291	.316
3.000	.791	.693	.140	.194	.249	.289	.315
3.993	.790	.692	.140	.193	.248	.288	.315
5.006	.790	.692	.139	.192	.247	.287	.314
6.012	.789	.692	.139	.191	.246	.287	.314
7.500	.789	.692	.138	.191	.246	.286	.314
8.596	.789	.692	.138	.191	.246	.286	.313
10.032	.789	.692	.137	.191	.245	.286	.313

TABLE BI.- Continued

(v) Configuration E22R

upper flap pressures, $p/p_{t,j}$

NPR	$x/h_{t,n}$ 2.775	2.925	3.075	3.225	3.375	3.700	4.000	4.300	4.600	4.900	5.200	5.550
1.709	.798	.737	.654	.643	.593	.458	.410	.470	.496	.512	.523	.551
1.989	.797	.735	.654	.642	.591	.456	.345	.424	.453	.456	.463	.479
2.509	.796	.734	.652	.640	.589	.454	.344	.255	.352	.367	.369	.379
3.017	.796	.733	.650	.639	.589	.453	.344	.255	.194	.254	.283	.308
4.008	.795	.732	.648	.640	.587	.451	.344	.254	.194	.145	.119	.223
5.012	.795	.733	.648	.640	.588	.451	.344	.254	.194	.144	.119	.222
6.018	.795	.733	.647	.641	.588	.451	.344	.254	.194	.144	.118	.222
7.520	.799	.734	.647	.641	.588	.452	.344	.254	.194	.144	.118	.221
8.599	.795	.734	.646	.641	.588	.452	.344	.254	.194	.144	.118	.220
10.019	.794	.735	.646	.641	.589	.453	.344	.254	.193	.144	.118	.220

lower flap pressures, $p/p_{t,j}$

NPR	$x/h_{t,n}$ 2.775	2.925	3.075	3.225	3.375	3.525	3.675	3.825	3.975	4.225	4.475	4.725	4.975	5.225	5.475
1.709	.790	.684	.150	.200	.251	.309	.381	.427	.457	.495	.529	.548	.567	.578	.581
1.989	.790	.682	.150	.199	.249	.291	.316	.337	.342	.412	.495	.531	.521	.506	.497
2.509	.790	.680	.150	.197	.247	.289	.314	.334	.337	.318	.293	.264	.280	.417	.410
3.017	.789	.679	.149	.196	.247	.287	.314	.333	.335	.317	.292	.263	.236	.214	.271
4.008	.790	.678	.149	.194	.246	.286	.313	.331	.334	.316	.291	.262	.236	.212	.193
5.012	.790	.678	.148	.193	.246	.286	.313	.330	.334	.316	.291	.262	.236	.211	.192
6.018	.790	.678	.148	.193	.245	.285	.313	.330	.333	.316	.290	.261	.235	.211	.191
7.520	.790	.678	.148	.192	.245	.285	.313	.330	.333	.315	.290	.261	.235	.210	.191
8.599	.790	.678	.148	.192	.245	.284	.313	.330	.333	.315	.290	.261	.235	.210	.191
10.019	.790	.678	.148	.192	.245	.284	.313	.330	.333	.315	.290	.261	.235	.209	.191

TABLE BI.- Continued

(w) Configuration C23S

upper flap pressures, $p/p_{t,j}$

NPR	$x/h_{t,n}$								
	2.775	2.925	3.075	3.325	3.375	3.700	4.000	4.300	4.650
1.688	.718	.711	.695	.635	.583	.452	.420	.548	.574
1.997	.717	.710	.695	.634	.582	.451	.338	.467	.486
2.514	.716	.709	.694	.633	.580	.448	.338	.256	.384
2.997	.717	.707	.693	.632	.579	.447	.338	.255	.287
4.003	.717	.707	.693	.631	.579	.445	.338	.256	.187
5.000	.717	.707	.693	.631	.579	.444	.338	.255	.185
5.996	.717	.707	.694	.631	.579	.444	.337	.255	.185
7.515	.716	.708	.694	.631	.579	.444	.338	.256	.185
8.583	.716	.709	.694	.631	.580	.444	.338	.256	.185
10.087	.716	.710	.695	.631	.580	.445	.338	.256	.185

lower flap pressures, $p/p_{t,j}$

NPR	$x/h_{t,n}$											
	2.775	2.925	3.075	3.225	3.375	3.525	3.675	3.825	3.975	4.150	4.350	4.550
1.688	.681	.619	.219	.246	.275	.300	.350	.478	.519	.567	.603	.602
1.997	.680	.618	.219	.245	.273	.299	.323	.341	.338	.357	.497	.528
2.514	.680	.617	.218	.243	.272	.297	.323	.339	.338	.324	.304	.284
2.997	.679	.617	.217	.242	.272	.296	.322	.338	.336	.323	.304	.281
4.003	.678	.617	.216	.241	.270	.294	.322	.336	.335	.322	.303	.280
5.000	.677	.617	.215	.240	.269	.294	.322	.335	.334	.322	.302	.279
5.996	.677	.617	.215	.240	.269	.293	.322	.334	.334	.321	.302	.280
7.515	.676	.617	.215	.240	.269	.293	.322	.334	.334	.321	.302	.279
8.583	.676	.618	.214	.240	.268	.292	.322	.334	.334	.321	.302	.279
10.087	.676	.618	.214	.239	.268	.292	.321	.335	.334	.321	.302	.279

TABLE BI.- Continued

(x) Configuration C24T

upper flap pressures, $p/p_{t,j}$

NPR	$x/h_{t,n}$ 2.775	2.925	3.075	3.325	3.375	3.700	4.000	4.300
1.702	.863	.762	.669	.681	.643	.548	.484	.517
2.006	.853	.743	.632	.641	.589	.453	.336	.465
2.511	.853	.741	.630	.639	.587	.451	.335	.253
2.998	.853	.740	.628	.639	.586	.449	.334	.252
4.010	.852	.739	.627	.639	.585	.447	.333	.252
5.003	.852	.738	.626	.639	.584	.446	.332	.252
6.002	.852	.739	.625	.639	.584	.446	.332	.252
7.506	.852	.740	.625	.639	.585	.447	.331	.252
8.601	.851	.740	.625	.639	.585	.447	.331	.252
10.054	.851	.741	.625	.639	.586	.447	.331	.252

lower flap pressures, $p/p_{t,j}$

NPR	$x/h_{t,n}$ 2.775	2.925	3.075	3.225	3.375	3.525	3.675	3.825	3.975	4.150	4.350	4.550
1.702	.865	.773	.474	.467	.464	.468	.479	.494	.509	.526	.545	.564
2.006	.854	.759	.088	.157	.230	.281	.310	.332	.337	.457	.529	.540
2.511	.855	.758	.088	.156	.228	.279	.309	.329	.336	.327	.306	.285
2.998	.855	.758	.088	.155	.228	.278	.308	.328	.335	.325	.305	.284
4.010	.853	.757	.087	.153	.227	.276	.307	.326	.333	.324	.304	.283
5.003	.854	.757	.087	.152	.226	.276	.306	.325	.332	.324	.304	.283
6.002	.853	.757	.087	.152	.225	.275	.306	.325	.332	.324	.304	.283
7.506	.853	.758	.086	.151	.225	.274	.306	.325	.332	.324	.303	.283
8.601	.853	.758	.086	.150	.224	.274	.306	.324	.332	.324	.303	.283
10.054	.852	.763	.086	.150	.224	.273	.305	.324	.332	.324	.303	.283

TABLE BI.- Continued

(y) Configuration C25P

upper flap pressures, $p/p_{t,j}$

NPR	$x/h_{t,n}$ 2.775	2.925	3.075	3.325	3.375	3.700	4.000	4.300
1.701	.805	.740	.669	.643	.594	.549	.404	.548
1.984	.805	.737	.668	.641	.592	.532	.342	.475
2.498	.802	.735	.667	.640	.590	.512	.340	.254
2.998	.801	.734	.666	.639	.589	.498	.339	.254
3.997	.799	.734	.665	.638	.588	.482	.338	.254
4.995	.799	.734	.665	.638	.588	.473	.338	.253
5.993	.798	.733	.664	.637	.587	.226	.337	.253
6.990	.798	.733	.664	.637	.587	.259	.337	.253
7.467	.798	.734	.664	.637	.587	.450	.336	.253
7.503	.798	.734	.664	.637	.588	.419	.336	.253
8.596	.798	.735	.664	.637	.588	.245	.336	.253
8.591	.797	.734	.664	.637	.587	.123	.336	.253
9.987	.798	.735	.664	.637	.588	.286	.336	.253

lower flap pressures, $p/p_{t,j}$

NPR	$x/h_{t,n}$ 2.775	2.925	3.075	3.225	3.375	3.525	3.675	3.825	3.975	4.150	4.350	4.550
1.701	.802	.684	.162	.198	.252	.297	.375	.484	.522	.573	.604	.597
1.984	.801	.682	.157	.196	.251	.295	.317	.339	.339	.442	.526	.539
2.498	.799	.680	.151	.194	.250	.292	.316	.336	.338	.327	.307	.262
2.998	.799	.679	.147	.193	.249	.291	.315	.335	.337	.326	.306	.281
3.997	.796	.678	.142	.191	.247	.290	.314	.333	.336	.325	.306	.280
4.995	.795	.677	.140	.190	.247	.289	.314	.332	.335	.325	.306	.280
5.993	.792	.677	.138	.190	.245	.288	.314	.331	.335	.324	.306	.280
6.990	.791	.677	.138	.190	.245	.288	.314	.331	.335	.325	.306	.280
7.467	.789	.677	.135	.189	.244	.288	.314	.331	.336	.324	.305	.279
7.503	.790	.677	.135	.189	.245	.288	.314	.331	.335	.324	.306	.279
8.596	.789	.677	.133	.189	.244	.287	.314	.331	.336	.324	.306	.280
8.591	.787	.677	.133	.189	.244	.287	.314	.331	.336	.324	.305	.280
9.987	.788	.678	.133	.188	.244	.287	.314	.331	.336	.324	.306	.279

TABLE BI.- Concluded

(z) Configuration A05H

upper flap pressures, $p/p_{t,j}$

NPR	$x/h_{t,n}$ 2.775	2.925	3.075	3.225	3.375	3.600	3.850	4.150	4.450	4.750	5.050	5.365
1.707	.748	.706	.675	.625	.566	.483	.388	.481	.558	.600	.600	.593
2.004	.724	.705	.674	.625	.566	.482	.388	.289	.372	.484	.528	.525
2.508	.739	.703	.673	.624	.564	.479	.387	.289	.285	.359	.376	.376
2.998	.724	.703	.673	.623	.563	.479	.388	.288	.285	.358	.369	.350
4.015	.733	.702	.672	.624	.563	.477	.387	.288	.284	.357	.367	.350
5.007	.728	.702	.672	.623	.563	.477	.387	.288	.282	.357	.366	.350
6.012	.726	.703	.672	.623	.563	.478	.387	.288	.278	.356	.366	.350
7.504	.731	.703	.672	.623	.563	.478	.387	.287	.271	.355	.365	.349
8.605	.728	.704	.672	.623	.563	.479	.387	.287	.267	.354	.364	.349
10.020	.733	.705	.672	.623	.564	.479	.387	.287	.260	.353	.363	.349

lower flap pressures, $p/p_{t,j}$

NPR	$x/h_{t,n}$ 2.775	2.925	3.075	3.225	3.375	3.525	3.675	3.825	3.975	4.150	4.350	4.600	4.850	5.100
1.707	.718	.643	.261	.312	.358	.399	.429	.440	.527	.582	.595	.596	.597	.593
2.004	.720	.643	.260	.311	.357	.398	.429	.434	.419	.394	.365	.454	.544	.546
2.508	.719	.642	.259	.309	.356	.396	.428	.432	.418	.392	.364	.329	.295	.264
2.998	.718	.642	.259	.308	.356	.395	.427	.430	.417	.391	.364	.328	.295	.263
4.015	.718	.641	.258	.308	.355	.395	.426	.428	.416	.391	.363	.328	.294	.262
5.007	.719	.641	.259	.308	.355	.395	.424	.427	.415	.390	.363	.327	.294	.261
6.012	.718	.641	.259	.308	.355	.395	.424	.427	.415	.390	.363	.327	.294	.261
7.504	.716	.641	.259	.307	.354	.394	.424	.427	.415	.390	.363	.327	.294	.261
8.605	.715	.642	.258	.307	.354	.393	.424	.426	.415	.390	.363	.327	.294	.261
10.020	.714	.642	.258	.306	.353	.393	.424	.426	.415	.390	.363	.327	.294	.261

TABLE BII.- RATIO OF INTERNAL UPPER AND LOWER FLAP STATIC PRESSURE TO JET TOTAL PRESSURE FOR CONFIGURATIONS C05H TO C27AA

(a) Configuration C05H

upper flap pressures, $p/p_{t,j}$

NPR	$x/h_{t,n}$											
	2.775	2.925	3.075	3.225	3.375	3.600	3.850	4.150	4.450	4.750	5.050	5.365
1.696	.744	.705	.673	.626	.565	.482	.389	.290	.445	.498	.542	.580
2.007	.728	.705	.673	.626	.565	.481	.389	.289	.262	.346	.362	.449
2.502	.733	.703	.672	.625	.564	.479	.388	.289	.262	.345	.362	.343
2.998	.722	.703	.671	.625	.563	.478	.389	.289	.261	.344	.362	.340
3.999	.735	.702	.671	.625	.563	.477	.387	.288	.261	.343	.361	.341
5.002	.730	.703	.671	.625	.563	.477	.387	.288	.259	.341	.361	.342
5.999	.725	.703	.671	.625	.563	.478	.388	.287	.258	.340	.361	.344
7.497	.728	.704	.671	.625	.563	.478	.388	.287	.253	.339	.360	.344
8.567	.733	.705	.671	.625	.564	.479	.388	.287	.251	.338	.360	.345
8.594	.733	.705	.671	.625	.564	.479	.388	.287	.250	.338	.359	.346
10.006	.727	.706	.672	.625	.564	.480	.387	.287	.245	.337	.359	.347

lower flap pressures, $p/p_{t,j}$

NPR	$x/h_{t,n}$												
	2.775	2.925	3.075	3.225	3.375	3.525	3.675	3.825	3.975	4.150	4.350	4.600	4.850	5.100
1.696	.711	.643	.261	.311	.355	.397	.427	.434	.420	.395	.370	.542	.578	.588
2.007	.711	.643	.260	.309	.354	.396	.427	.432	.419	.394	.365	.332	.296	.439
2.502	.713	.642	.259	.307	.353	.394	.426	.430	.418	.392	.364	.330	.295	.264
2.998	.713	.642	.259	.306	.354	.393	.425	.429	.417	.391	.363	.330	.295	.264
3.999	.715	.642	.258	.305	.354	.393	.424	.427	.416	.390	.363	.329	.294	.262
5.002	.715	.642	.258	.305	.353	.393	.423	.426	.415	.390	.362	.328	.294	.261
5.999	.718	.642	.258	.306	.354	.393	.423	.426	.415	.390	.362	.328	.294	.261
7.497	.717	.643	.257	.306	.353	.393	.423	.425	.415	.390	.362	.329	.294	.261
8.567	.717	.643	.257	.306	.353	.392	.423	.425	.415	.389	.362	.329	.294	.261
8.594	.719	.643	.257	.306	.353	.392	.423	.425	.415	.389	.362	.329	.294	.261
10.006	.720	.644	.258	.306	.353	.392	.423	.426	.415	.389	.362	.329	.295	.261

TABLE BII.- Continued

(b) Configuration A06I

upper flap pressures, $p/p_{t,j}$

NPR	$x/h_{t,n}$									
	2.775	2.925	3.075	3.225	3.375	3.700	4.000	4.300	4.600	4.900
1.706	.815	.829	.821	.754	.683	.524	.377	.543	.605	.604
2.002	.786	.827	.820	.752	.681	.522	.375	.268	.426	.464
2.491	.794	.824	.817	.749	.678	.517	.374	.266	.197	.362
2.989	.793	.824	.817	.749	.678	.516	.373	.265	.197	.349
3.997	.811	.824	.817	.748	.678	.514	.372	.265	.197	.344
4.996	.802	.824	.817	.747	.677	.513	.372	.265	.196	.342
5.993	.806	.825	.816	.747	.677	.513	.372	.264	.196	.343
7.497	.803	.826	.816	.747	.677	.512	.372	.264	.196	.341
8.628	.807	.827	.817	.747	.678	.513	.373	.264	.196	.340
8.609	.809	.827	.817	.746	.677	.513	.372	.264	.196	.339
10.010	.806	.828	.818	.746	.678	.513	.373	.265	.196	.338

lower flap pressures, $p/p_{t,j}$

NPR	$x/h_{t,n}$													
	2.775	2.925	3.075	3.325	3.375	3.525	3.675	3.825	3.975	4.200	4.450	4.700	4.950	5.200
1.706	.763	.689	.160	.232	.303	.432	.538	.582	.600	.604	.604	.598	.599	.582
2.002	.763	.686	.158	.229	.301	.376	.422	.434	.416	.377	.539	.529	.520	.495
2.491	.760	.685	.158	.228	.299	.373	.421	.431	.415	.374	.332	.292	.256	.379
2.989	.760	.685	.158	.226	.298	.371	.420	.429	.413	.374	.332	.291	.254	.229
3.997	.761	.685	.158	.225	.298	.370	.420	.428	.413	.373	.331	.291	.254	.220
4.996	.761	.685	.156	.225	.297	.369	.418	.426	.412	.372	.330	.289	.253	.219
5.993	.760	.684	.155	.224	.296	.368	.417	.426	.411	.372	.330	.290	.252	.217
7.497	.759	.684	.154	.223	.295	.367	.416	.425	.411	.372	.331	.290	.252	.217
8.628	.760	.685	.155	.222	.295	.367	.416	.425	.410	.372	.331	.290	.253	.217
8.609	.759	.684	.155	.222	.295	.366	.416	.425	.410	.371	.330	.290	.252	.217
10.010	.758	.685	.155	.221	.294	.365	.415	.425	.410	.371	.330	.290	.252	.217

TABLE BII.- Continued

(c) Configuration C06I

upper flap pressures, $p/p_{t,j}$

NPR	$x/h_{t,n}$ 2.775	2.925	3.075	3.225	3.375	3.700	4.000	4.300	4.600	4.900
1.692	.833	.828	.824	.749	.683	.524	.378	.408	.475	.518
1.995	.822	.828	.823	.748	.682	.522	.376	.267	.314	.404
2.495	.824	.825	.820	.745	.680	.518	.375	.266	.197	.353
2.992	.815	.824	.819	.745	.679	.516	.374	.266	.197	.351
3.999	.812	.824	.820	.744	.678	.514	.373	.265	.197	.348
5.000	.812	.825	.820	.744	.678	.514	.372	.265	.197	.346
5.984	.805	.826	.820	.744	.678	.514	.372	.264	.197	.344
7.485	.805	.827	.821	.743	.678	.514	.372	.264	.197	.342
8.614	.805	.828	.821	.743	.679	.514	.373	.265	.197	.341
10.019	.808	.829	.821	.742	.679	.514	.373	.265	.196	.339

lower flap pressures, $p/p_{t,j}$

NPR	$x/h_{t,n}$ 2.775	2.925	3.075	3.325	3.375	3.525	3.675	3.825	3.975	4.200	4.450	4.700	4.950	5.200
1.692	.761	.688	.160	.228	.300	.378	.423	.435	.418	.542	.565	.571	.585	.580
1.995	.763	.687	.159	.228	.301	.376	.422	.433	.416	.377	.334	.370	.493	.512
2.495	.761	.686	.158	.226	.299	.373	.421	.430	.414	.376	.334	.293	.254	.374
2.992	.759	.685	.158	.225	.299	.372	.420	.428	.413	.375	.334	.292	.253	.229
3.999	.759	.685	.157	.224	.297	.370	.418	.426	.412	.374	.333	.291	.252	.219
5.000	.761	.685	.157	.224	.296	.370	.418	.426	.411	.373	.333	.291	.252	.219
5.984	.761	.685	.157	.224	.296	.369	.417	.425	.411	.373	.332	.291	.253	.219
7.485	.761	.685	.157	.223	.295	.368	.417	.425	.411	.372	.332	.291	.252	.218
8.614	.760	.685	.157	.222	.295	.367	.417	.425	.411	.372	.332	.290	.253	.218
10.019	.759	.685	.156	.220	.294	.367	.416	.425	.410	.372	.332	.291	.252	.217

TABLE BII.- Continued

(d) Configuration A08I

upper flap pressures, $p/p_{t,j}$

NPR	$x/h_{t,n}$ 2.775	2.925	3.075	3.225	3.375	3.600	3.850	4.150	4.459	4.750	5.050
1.702	.743	.737	.712	.654	.610	.530	.485	.429	.550	.557	.569
2.009	.735	.731	.706	.645	.597	.495	.404	.298	.443	.446	.458
2.503	.748	.729	.704	.643	.595	.491	.402	.298	.224	.373	.379
2.999	.738	.728	.702	.641	.593	.488	.402	.298	.218	.270	.314
3.998	.740	.726	.700	.639	.590	.485	.401	.298	.218	.166	.132
4.997	.742	.726	.700	.637	.589	.483	.400	.298	.218	.165	.132
5.989	.738	.726	.699	.636	.589	.482	.400	.298	.218	.166	.132
7.494	.744	.727	.699	.636	.589	.482	.400	.298	.217	.166	.133
8.591	.744	.727	.699	.635	.589	.482	.400	.298	.217	.165	.132
10.064	.741	.728	.699	.635	.589	.482	.400	.299	.217	.165	.133

lower flap pressures, $p/p_{t,j}$

NPR	$x/h_{t,n}$ 2.775	2.925	3.075	3.325	3.375	3.525	3.675	3.825	3.975	4.200	4.450	4.700	4.950	5.200
1.702	.735	.659	.374	.389	.435	.455	.466	.483	.496	.515	.534	.551	.569	.583
2.009	.733	.657	.145	.180	.207	.233	.294	.396	.421	.453	.481	.500	.511	.508
2.503	.732	.656	.144	.179	.205	.231	.249	.265	.271	.263	.372	.419	.442	.434
2.999	.732	.655	.144	.178	.204	.230	.248	.264	.270	.263	.244	.222	.198	.312
3.998	.728	.654	.142	.175	.201	.227	.247	.260	.267	.260	.241	.219	.196	.178
4.997	.725	.653	.141	.173	.200	.226	.245	.259	.266	.257	.240	.218	.195	.176
5.989	.725	.653	.141	.172	.199	.225	.245	.258	.265	.257	.239	.218	.194	.175
7.494	.725	.653	.141	.172	.198	.224	.244	.257	.265	.256	.238	.217	.194	.175
8.591	.725	.653	.141	.171	.197	.224	.244	.257	.264	.256	.238	.217	.193	.174
10.064	.724	.653	.141	.170	.197	.223	.243	.257	.264	.256	.238	.216	.193	.174

TABLE BII.- Continued

(e) Configuration C08I

upper flap pressures, $p/p_{t,j}$

NPR	$x/h_{t,n}$										
	2.775	2.925	3.075	3.225	3.375	3.600	3.850	4.150	4.450	4.750	5.050
1.716	.733	.739	.714	.659	.614	.533	.487	.449	.523	.550	.564
2.003	.733	.731	.706	.647	.598	.498	.403	.298	.460	.466	.467
2.497	.739	.729	.703	.642	.594	.491	.401	.298	.231	.378	.382
2.993	.736	.727	.701	.640	.593	.488	.401	.297	.219	.272	.314
3.990	.746	.726	.700	.638	.589	.484	.401	.298	.218	.165	.132
5.003	.744	.725	.699	.636	.589	.482	.400	.298	.218	.165	.132
6.000	.734	.725	.699	.635	.588	.482	.400	.298	.218	.165	.132
7.462	.740	.726	.698	.635	.588	.482	.400	.298	.218	.166	.133
7.480	.743	.726	.698	.635	.588	.482	.400	.298	.218	.165	.133
8.585	.739	.727	.698	.635	.588	.482	.399	.298	.218	.165	.133
10.010	.743	.727	.698	.634	.588	.481	.399	.298	.218	.165	.133

lower flap pressures, $p/p_{t,j}$

NPR	$x/h_{t,n}$													
	2.775	2.925	3.075	3.325	3.375	3.525	3.675	3.825	3.975	4.200	4.450	4.700	4.950	5.200
1.716	.740	.662	.391	.399	.431	.450	.466	.485	.496	.513	.527	.539	.556	.569
2.003	.735	.658	.146	.181	.208	.233	.250	.302	.408	.442	.469	.499	.522	.514
2.497	.731	.656	.145	.177	.204	.230	.250	.265	.270	.262	.267	.399	.434	.437
2.993	.729	.655	.144	.176	.203	.228	.248	.262	.268	.261	.242	.220	.198	.315
3.990	.727	.653	.143	.173	.201	.226	.247	.260	.266	.258	.240	.219	.197	.178
5.003	.725	.653	.141	.172	.199	.225	.245	.258	.265	.257	.239	.218	.195	.176
6.000	.725	.652	.141	.171	.198	.224	.244	.257	.264	.256	.238	.218	.194	.176
7.462	.724	.652	.141	.170	.197	.223	.243	.256	.264	.256	.238	.217	.194	.175
7.480	.725	.652	.141	.171	.197	.223	.244	.257	.264	.256	.238	.217	.194	.175
8.585	.724	.653	.141	.170	.197	.223	.243	.256	.264	.256	.237	.217	.193	.175
10.010	.723	.652	.140	.169	.196	.222	.243	.256	.264	.255	.237	.216	.193	.174

TABLE BII.- Continued

(f) Configuration B05U

upper flap pressures, $p/p_{t,j}$

NPR	$x/h_{t,n}$ 2.775	2.925	3.075	3.225	3.375	3.600	3.850	4.150	4.450	4.750	5.050	5.365
1.711	.720	.704	.672	.629	.575	.500	.417	.329	.323	.355	.512	.560
1.997	.743	.701	.670	.627	.573	.498	.417	.328	.329	.348	.342	.460
2.505	.738	.701	.670	.627	.572	.497	.417	.327	.331	.346	.341	.342
3.006	.719	.700	.669	.626	.571	.495	.416	.327	.329	.345	.340	.342
4.001	.730	.699	.669	.625	.570	.494	.415	.326	.326	.344	.338	.342
4.994	.720	.700	.669	.625	.569	.493	.415	.326	.324	.343	.338	.342
6.001	.721	.700	.669	.625	.570	.494	.415	.325	.322	.342	.337	.344
7.499	.722	.701	.670	.626	.570	.494	.416	.325	.319	.342	.336	.345
8.609	.724	.701	.669	.626	.570	.495	.416	.325	.317	.341	.335	.344
10.001	.723	.702	.670	.626	.570	.495	.416	.325	.315	.340	.334	.344

lower flap pressures, $p/p_{t,j}$

NPR	$x/h_{t,n}$ 2.775	2.925	3.075	3.225	3.375	3.525	3.675	3.825	3.975	4.150	4.350	4.600	4.850	5.100	5.350
1.711	.691	.592	.429	.336	.374	.397	.414	.424	.410	.396	.367	.335	.478	.528	.569
1.997	.695	.590	.427	.335	.372	.396	.413	.421	.407	.394	.366	.334	.306	.443	.482
2.505	.697	.589	.426	.334	.372	.396	.411	.419	.405	.394	.365	.333	.305	.275	.303
3.006	.695	.589	.426	.333	.371	.394	.411	.418	.404	.393	.365	.332	.304	.275	.288
4.001	.695	.588	.425	.332	.370	.393	.409	.416	.403	.392	.364	.331	.304	.273	.283
4.994	.695	.589	.425	.331	.369	.392	.408	.415	.402	.392	.364	.331	.304	.272	.281
6.001	.695	.589	.424	.331	.369	.391	.408	.414	.402	.392	.364	.330	.305	.271	.278
7.499	.694	.589	.424	.330	.368	.391	.407	.413	.402	.392	.364	.330	.305	.271	.278
8.609	.692	.590	.424	.329	.368	.390	.407	.413	.401	.391	.364	.330	.304	.271	.276
10.001	.694	.590	.424	.329	.368	.389	.406	.412	.401	.391	.364	.329	.305	.271	.273

TABLE BII.- Continued

(g) Configuration B07U

upper flap pressures, $p/p_{t,j}$

NPR	$x/h_{t,n}$											
	2.775	2.925	3.074	3.225	3.375	3.600	3.850	4.150	4.450	4.750	5.050	5.365
1.696	.692	.593	.420	.450	.445	.403	.337	.383	.460	.516	.566	.587
2.011	.668	.592	.420	.451	.444	.402	.337	.429	.469	.472	.473	.477
2.474	.690	.587	.417	.450	.442	.399	.337	.268	.300	.377	.381	.386
2.497	.679	.590	.418	.451	.442	.399	.337	.268	.271	.372	.377	.383
2.989	.685	.588	.417	.450	.440	.398	.337	.268	.214	.181	.306	.318
3.989	.674	.586	.416	.449	.439	.396	.337	.267	.213	.176	.152	.149
4.994	.680	.588	.416	.449	.438	.396	.337	.267	.213	.175	.152	.147
5.994	.681	.588	.416	.449	.438	.396	.337	.267	.213	.176	.151	.147
7.480	.675	.588	.415	.449	.437	.396	.337	.267	.214	.176	.151	.146
7.488	.681	.588	.416	.449	.437	.396	.337	.267	.214	.176	.151	.146
8.618	.675	.588	.415	.449	.437	.396	.337	.267	.214	.176	.151	.146
9.974	.681	.588	.415	.449	.437	.397	.337	.267	.214	.176	.151	.146
9.996	.678	.588	.415	.448	.437	.397	.337	.267	.214	.176	.151	.146

lower flap pressures, $p/p_{t,j}$

NPR	$x/h_{t,n}$														
	2.775	2.925	3.075	3.225	3.375	3.525	3.675	3.825	3.975	4.150	4.350	4.600	4.850	5.100	5.350
1.696	.673	.569	.393	.285	.295	.292	.408	.442	.466	.491	.510	.527	.542	.556	.569
2.011	.671	.568	.393	.283	.293	.282	.264	.247	.227	.242	.379	.408	.451	.499	.514
2.474	.670	.567	.392	.281	.291	.280	.263	.245	.225	.238	.235	.220	.335	.361	.386
2.497	.671	.567	.392	.282	.292	.281	.263	.245	.225	.238	.235	.220	.333	.360	.382
2.989	.672	.567	.391	.281	.291	.280	.262	.243	.224	.237	.234	.218	.204	.190	.315
3.989	.669	.567	.391	.280	.289	.277	.261	.241	.223	.235	.233	.217	.203	.189	.178
4.994	.669	.567	.391	.279	.288	.277	.260	.240	.222	.235	.232	.217	.203	.188	.178
5.994	.668	.567	.391	.279	.288	.276	.260	.239	.222	.234	.232	.216	.203	.187	.177
7.480	.668	.567	.391	.278	.288	.276	.259	.238	.221	.234	.232	.215	.203	.188	.176
7.488	.668	.567	.391	.278	.288	.276	.259	.238	.221	.234	.231	.215	.203	.187	.176
8.618	.668	.568	.391	.277	.288	.275	.259	.238	.221	.234	.231	.215	.202	.187	.176
9.974	.669	.568	.391	.277	.288	.275	.259	.238	.220	.234	.231	.215	.202	.187	.175
9.996	.667	.568	.391	.277	.288	.275	.259	.238	.220	.233	.231	.215	.202	.187	.175

TABLE BII.- Continued

(h) Configuration B14V

upper flap pressures, $p/p_{t,j}$

NPR	$x/h_{t,n}$ 2.775	2.925	3.075	3.225	3.375	3.700	4.000	4.300	4.600	4.900
1.720	.910	.814	.762	.738	.693	.576	.448	.351	.486	.513
2.043	.921	.811	.760	.734	.690	.572	.445	.350	.271	.296
2.569	.936	.808	.757	.731	.687	.568	.443	.349	.271	.286
2.535	.936	.807	.756	.731	.687	.568	.443	.348	.270	.287
3.080	.946	.805	.754	.729	.684	.565	.441	.347	.269	.285
4.099	.956	.803	.752	.727	.682	.562	.439	.346	.268	.282
5.139	.963	.802	.751	.726	.681	.561	.437	.345	.267	.280
6.158	.968	.802	.749	.725	.681	.560	.436	.344	.266	.278
7.706	.973	.802	.749	.724	.681	.560	.435	.344	.266	.277
8.831	.974	.802	.749	.724	.681	.560	.434	.344	.265	.276
10.334	.976	.803	.748	.723	.681	.560	.433	.343	.265	.274

lower flap pressures, $p/p_{t,j}$

NPR	$x/h_{t,n}$ 2.775	2.925	3.075	3.325	3.375	3.525	3.675	3.825	3.975	4.175	4.400	4.650	4.900	5.150
1.720	.730	.644	.561	.430	.347	.342	.365	.384	.383	.368	.493	.569	.585	.585
2.043	.727	.641	.559	.427	.345	.340	.364	.381	.381	.366	.336	.302	.364	.464
2.569	.725	.639	.556	.425	.343	.337	.363	.379	.379	.364	.334	.300	.267	.307
2.535	.727	.638	.556	.425	.342	.337	.363	.379	.378	.363	.334	.300	.267	.326
3.080	.725	.636	.554	.423	.341	.335	.361	.376	.376	.362	.332	.298	.265	.239
4.099	.722	.634	.552	.420	.339	.333	.359	.374	.374	.360	.331	.296	.264	.237
5.139	.721	.633	.551	.419	.338	.331	.358	.372	.373	.359	.330	.295	.263	.236
6.158	.721	.632	.551	.418	.337	.330	.357	.372	.372	.358	.329	.294	.262	.235
7.706	.720	.631	.550	.417	.336	.329	.357	.371	.372	.357	.328	.294	.262	.234
8.831	.719	.631	.550	.416	.335	.329	.356	.371	.372	.357	.328	.293	.262	.234
10.334	.718	.630	.549	.415	.334	.328	.356	.370	.371	.356	.328	.293	.262	.234

TABLE BII.- Continued

(i) Configuration B16V

upper flap pressures, $p/p_{t,j}$

NPR	$x/h_{t,n}$											
	2.775	2.925	3.075	3.225	3.375	3.600	3.850	4.150	4.450	4.750	5.050	5.365
1.707	.822	.724	.609	.620	.579	.515	.440	.375	.542	.551	.556	.561
2.017	.821	.722	.608	.619	.578	.513	.438	.345	.417	.472	.476	.474
2.490	.820	.719	.606	.618	.576	.510	.438	.345	.272	.314	.380	.384
3.005	.820	.718	.604	.617	.575	.509	.437	.344	.272	.213	.264	.320
4.003	.820	.717	.603	.617	.573	.507	.437	.344	.271	.213	.170	.203
5.001	.819	.716	.602	.617	.573	.507	.436	.344	.271	.212	.170	.140
6.000	.818	.716	.602	.617	.572	.506	.436	.343	.270	.212	.170	.140
7.503	.818	.717	.601	.617	.572	.507	.437	.343	.270	.212	.169	.140
8.593	.818	.717	.600	.617	.572	.507	.437	.343	.270	.212	.169	.140
9.994	.817	.718	.599	.617	.572	.507	.436	.343	.270	.212	.169	.140

lower flap pressures, $p/p_{t,j}$

NPR	$x/h_{t,n}$													
	2.775	2.925	3.075	3.325	3.375	3.525	3.675	3.825	3.975	4.175	4.400	4.650	4.900	5.150
1.707	.686	.585	.472	.354	.255	.235	.237	.365	.401	.426	.486	.565	.600	.601
2.017	.685	.583	.471	.353	.253	.233	.234	.241	.238	.252	.386	.414	.461	.505
2.490	.687	.582	.470	.352	.252	.231	.233	.239	.237	.233	.226	.310	.361	.382
3.005	.685	.581	.469	.352	.251	.229	.233	.237	.236	.233	.225	.209	.192	.308
4.003	.685	.580	.469	.350	.249	.228	.231	.236	.235	.231	.224	.207	.191	.178
5.001	.685	.580	.469	.350	.249	.227	.231	.235	.234	.230	.223	.206	.190	.177
6.000	.684	.580	.469	.349	.248	.226	.230	.234	.234	.230	.223	.206	.190	.176
7.503	.684	.580	.469	.349	.248	.225	.230	.233	.233	.230	.222	.206	.190	.176
8.593	.684	.581	.469	.349	.247	.225	.229	.233	.233	.229	.222	.205	.189	.175
9.994	.683	.581	.469	.348	.247	.225	.229	.233	.233	.229	.222	.205	.189	.175

TABLE BII.- Continued

(j) Configuration C19W

upper flap pressures, $p/p_{t,j}$

NPR	$x/h_{t,n}$ 2.775	2.925	3.075	3.225	3.375	3.650	3.950	4.250	4.570
1.698	.823	.783	.742	.699	.653	.547	.445	.352	.559
2.004	.814	.784	.744	.701	.653	.546	.445	.341	.424
2.497	.817	.782	.743	.700	.653	.545	.444	.340	.323
2.999	.815	.780	.741	.699	.651	.543	.443	.339	.321
4.007	.814	.780	.741	.699	.651	.541	.442	.338	.319
4.993	.815	.781	.741	.699	.651	.540	.441	.338	.317
6.023	.815	.782	.741	.699	.651	.539	.441	.337	.315
6.001	.814	.782	.741	.698	.651	.539	.441	.337	.315
7.513	.815	.782	.742	.699	.651	.539	.440	.337	.313
8.632	.814	.783	.742	.698	.651	.539	.440	.337	.311
8.593	.815	.783	.742	.698	.651	.539	.440	.337	.311
10.000	.815	.784	.742	.699	.652	.540	.440	.337	.309

lower flap pressures, $p/p_{t,j}$

NPR	$x/h_{t,n}$ 2.775	2.925	3.075	3.225	3.375	3.525	3.675	3.825	3.975	4.150	4.350	4.550
1.698	.717	.602	.502	.386	.347	.379	.407	.421	.418	.471	.581	.585
2.004	.718	.603	.503	.388	.347	.379	.409	.421	.418	.399	.370	.378
2.497	.719	.602	.503	.388	.345	.378	.409	.418	.417	.399	.369	.340
2.999	.720	.601	.502	.387	.344	.377	.407	.416	.416	.398	.369	.341
4.007	.719	.601	.501	.385	.343	.375	.407	.415	.415	.397	.367	.339
4.993	.720	.601	.502	.386	.343	.375	.406	.414	.415	.397	.367	.339
6.023	.718	.601	.502	.385	.343	.374	.406	.414	.415	.397	.367	.339
6.001	.718	.600	.502	.385	.342	.374	.406	.414	.415	.397	.366	.338
7.513	.717	.601	.502	.385	.342	.374	.406	.413	.415	.397	.367	.338
8.632	.717	.601	.502	.385	.342	.373	.406	.413	.415	.397	.366	.338
8.593	.717	.601	.502	.385	.342	.373	.406	.413	.415	.397	.367	.338
10.000	.717	.601	.502	.385	.342	.373	.406	.413	.415	.397	.366	.337

TABLE BII.- Continued

(k) Configuration C20W

upper flap pressures, $p/p_{t,j}$

NPR	$x/h_{t,n}$								
	2.775	2.925	3.075	3.325	3.375	3.700	4.000	4.300	4.650
1.704	.760	.663	.383	.534	.523	.424	.383	.543	.566
2.002	.757	.660	.383	.537	.521	.422	.337	.426	.480
2.506	.752	.658	.380	.536	.518	.418	.336	.266	.378
3.036	.751	.656	.380	.535	.515	.416	.336	.266	.271
3.024	.751	.656	.380	.534	.515	.416	.335	.266	.274
2.991	.751	.655	.379	.533	.514	.415	.335	.266	.279
4.002	.749	.654	.378	.532	.511	.412	.335	.266	.176
5.006	.748	.654	.377	.530	.510	.411	.334	.266	.178
5.996	.748	.654	.376	.528	.509	.410	.334	.266	.180
7.491	.748	.654	.375	.527	.508	.409	.333	.265	.181
7.529	.748	.654	.375	.527	.508	.409	.333	.265	.181
8.594	.748	.654	.375	.526	.509	.409	.333	.265	.181
10.009	.749	.655	.375	.526	.509	.410	.333	.265	.182

lower flap pressures, $p/p_{t,j}$

NPR	$x/h_{t,n}$											
	2.775	2.925	3.075	3.225	3.375	3.525	3.675	3.825	3.975	4.150	4.350	4.550
1.704	.682	.538	.418	.315	.430	.450	.468	.490	.509	.530	.549	.564
2.002	.682	.537	.418	.300	.253	.378	.396	.412	.426	.443	.459	.471
2.506	.676	.536	.417	.297	.232	.222	.204	.225	.228	.237	.363	.382
3.036	.674	.535	.416	.296	.231	.220	.203	.223	.226	.225	.216	.230
3.024	.674	.535	.416	.296	.231	.220	.203	.223	.226	.225	.216	.234
2.991	.672	.534	.415	.295	.230	.219	.203	.222	.225	.224	.215	.246
4.002	.672	.534	.415	.294	.229	.218	.202	.221	.224	.223	.214	.206
5.006	.671	.534	.414	.293	.228	.217	.201	.219	.223	.221	.214	.206
5.996	.670	.533	.413	.292	.227	.216	.200	.218	.222	.220	.213	.205
7.491	.669	.532	.413	.291	.226	.215	.199	.217	.221	.219	.212	.204
7.529	.669	.532	.413	.291	.226	.215	.199	.217	.221	.219	.212	.204
8.594	.669	.532	.413	.291	.226	.215	.200	.216	.221	.220	.213	.204
10.009	.670	.532	.413	.292	.226	.215	.200	.216	.221	.220	.213	.204

TABLE BII.- Continued

(1) Configuration C26X

upper flap pressures, $p/p_{t,j}$

NPR	$x/h_{t,n}$							
	2.775	2.925	3.075	3.325	3.375	3.700	4.000	4.300
1.697	.928	.838	.606	.719	.697	.620	.572	.554
1.994	.922	.824	.540	.678	.651	.546	.465	.398
2.509	.916	.811	.480	.632	.606	.467	.349	.252
3.016	.916	.810	.476	.632	.606	.466	.350	.252
4.002	.915	.809	.471	.634	.605	.463	.350	.252
5.014	.915	.809	.471	.636	.605	.463	.350	.252
6.010	.915	.810	.471	.637	.604	.462	.349	.251
7.507	.914	.810	.475	.639	.602	.464	.349	.251
8.606	.914	.811	.479	.639	.602	.464	.349	.251
10.058	.914	.812	.481	.638	.601	.464	.349	.251

lower flap pressures, $p/p_{t,j}$

NPR	$x/h_{t,n}$										
	2.775	2.925	3.075	3.225	3.375	3.525	3.675	3.825	3.975	4.150	4.350
1.697	.932	.836	.544	.537	.532	.531	.533	.536	.544	.555	.556
1.994	.926	.820	.430	.421	.416	.419	.426	.436	.449	.465	.473
2.509	.918	.807	.039	.148	.231	.264	.283	.300	.296	.283	.292
3.016	.919	.807	.036	.148	.230	.262	.283	.299	.295	.283	.262
4.002	.919	.805	.033	.148	.229	.261	.282	.297	.293	.282	.262
5.014	.919	.805	.032	.148	.229	.261	.282	.296	.293	.282	.262
6.010	.919	.805	.031	.147	.229	.261	.282	.296	.292	.282	.261
7.507	.919	.806	.031	.147	.229	.261	.282	.295	.292	.281	.261
8.606	.919	.806	.030	.146	.229	.261	.282	.295	.292	.281	.261
10.058	.918	.807	.030	.146	.229	.261	.282	.295	.291	.281	.261

TABLE BII.- Continued

(m) Configuration C27Y

upper flap pressures $p/p_{t,j}$

NPR	$x/h_{t,n}$ 2.775	2.925	3.075	3.325	3.375	3.700	4.000	4.300	4.650
1.698	.962	.892	.568	.698	.715	.631	.581	.559	.558
2.007	.959	.880	.502	.640	.667	.552	.473	.412	.392
2.534	.955	.869	.435	.568	.616	.466	.350	.257	.376
2.496	.954	.869	.435	.567	.615	.465	.351	.256	.382
3.013	.954	.868	.434	.568	.615	.464	.350	.256	.284
3.989	.951	.867	.431	.573	.613	.461	.349	.256	.174
5.007	.947	.868	.429	.579	.612	.460	.349	.256	.174
5.996	.940	.868	.427	.583	.611	.458	.348	.256	.174
7.489	.934	.869	.427	.586	.610	.459	.348	.255	.173
8.598	.928	.870	.427	.586	.609	.458	.348	.255	.173
10.029	.923	.871	.427	.586	.609	.459	.348	.255	.173

lower flap pressures, $p/p_{t,j}$

NPR	$x/h_{t,n}$ 2.775	2.925	3.075	3.225	3.375	3.525	3.675	3.825	3.975	4.150	4.350	4.550
1.698	.961	.897	.551	.547	.544	.540	.538	.537	.538	.544	.555	.551
2.007	.955	.884	.436	.430	.425	.421	.421	.427	.434	.446	.461	.467
2.534	.955	.874	.031	.057	.170	.221	.245	.272	.292	.293	.279	.284
2.496	.953	.874	.031	.056	.170	.221	.245	.272	.292	.293	.280	.299
3.013	.953	.873	.028	.060	.169	.219	.244	.271	.291	.292	.279	.261
3.989	.953	.872	.024	.067	.168	.218	.244	.269	.291	.291	.278	.261
5.007	.952	.872	.024	.072	.168	.216	.245	.269	.288	.289	.277	.260
5.996	.952	.872	.060	.070	.133	.208	.245	.269	.287	.288	.276	.259
7.489	.953	.873	.060	.069	.131	.209	.246	.270	.287	.288	.276	.258
8.598	.951	.873	.059	.067	.130	.209	.246	.269	.287	.287	.275	.258
10.029	.951	.874	.057	.066	.130	.210	.246	.269	.287	.287	.275	.257

TABLE BII.- Continued

(n) Configuration C26Z

upper flap pressures, $p/p_{t,j}$

NPR	$x/h_{t,n}$ 2.775	2.925	3.075	3.325	3.375	3.700	4.000	4.300
1.711	.921	.824	.531	.673	.646	.539	.449	.411
2.019	.918	.813	.480	.632	.608	.472	.350	.424
2.501	.917	.810	.478	.631	.607	.470	.350	.253
2.999	.917	.809	.474	.632	.606	.469	.351	.253
4.001	.917	.808	.469	.634	.604	.467	.350	.253
5.003	.917	.808	.466	.637	.603	.467	.350	.252
6.006	.916	.809	.467	.638	.603	.466	.350	.252
7.495	.916	.810	.472	.637	.602	.466	.350	.252
7.520	.916	.809	.472	.637	.602	.466	.350	.252
8.614	.916	.810	.481	.634	.601	.466	.350	.252
10.022	.916	.811	.484	.635	.601	.467	.350	.252

lower flap pressures, $p/p_{t,j}$

NPR	$x/h_{t,n}$ 2.775	2.925	3.075	3.325	3.375	3.525	3.675	3.825	3.975	4.200	4.400
1.711	.922	.840	.407	.398	.411	.433	.458	.484	.518	.544	.567
2.019	.919	.831	.064	.218	.310	.349	.378	.384	.433	.543	.534
2.501	.919	.830	.059	.216	.308	.346	.376	.382	.365	.339	.316
2.999	.920	.830	.056	.216	.306	.344	.376	.381	.365	.339	.316
4.001	.919	.830	.052	.216	.305	.343	.374	.379	.364	.339	.316
5.003	.918	.830	.051	.216	.305	.343	.374	.378	.363	.338	.315
6.006	.918	.830	.050	.215	.305	.344	.374	.377	.363	.338	.315
7.495	.918	.830	.049	.215	.305	.344	.374	.377	.362	.338	.316
7.520	.917	.830	.049	.215	.305	.344	.374	.377	.362	.337	.316
8.614	.917	.831	.049	.214	.305	.344	.374	.377	.362	.337	.315
10.022	.918	.831	.048	.214	.305	.344	.374	.377	.362	.337	.316

TABLE BII.- Concluded

(o) Configuration C27AA

upper flap pressures, $p/p_{t,j}$

NPR	$x/h_{t,n}$ 2.775	2.925	3.075	3.325	3.375	3.700	4.000	4.300	4.650
1.698	.959	.882	.513	.649	.673	.565	.490	.506	.564
2.004	.956	.871	.438	.572	.616	.471	.351	.409	.481
2.522	.955	.869	.437	.571	.616	.468	.351	.257	.378
2.503	.955	.869	.437	.570	.616	.468	.351	.257	.382
2.993	.954	.868	.436	.570	.615	.465	.352	.257	.287
4.028	.952	.868	.433	.574	.615	.462	.353	.263	.184
3.995	.952	.868	.433	.574	.615	.463	.353	.263	.184
5.008	.935	.868	.432	.579	.615	.462	.352	.263	.183
6.000	.930	.869	.430	.582	.614	.461	.351	.262	.183
7.500	.935	.870	.429	.584	.613	.460	.350	.260	.181
8.615	.931	.870	.428	.588	.611	.460	.349	.260	.181
10.017	.928	.872	.428	.590	.611	.460	.349	.258	.180

lower flap pressures, $p/p_{t,j}$

NPR	$x/h_{t,n}$ 2.775	2.925	3.075	3.325	3.375	3.525	3.675	3.825	3.975	4.200	4.400	4.600
1.698	.958	.863	.455	.447	.443	.447	.852	.478	.496	.525	.547	.569
2.004	.953	.851	.045	.114	.236	.298	.575	.365	.382	.472	.545	.529
2.522	.953	.851	.040	.119	.234	.295	.552	.365	.383	.368	.341	.314
2.503	.952	.851	.041	.119	.234	.295	.554	.364	.383	.368	.340	.314
2.993	.951	.852	.037	.121	.233	.295	.514	.367	.382	.366	.339	.312
4.028	.949	.852	.101	.117	.192	.279	.460	.356	.370	.360	.337	.311
3.995	.950	.852	.101	.117	.192	.279	.461	.356	.370	.360	.337	.311
5.008	.950	.853	.100	.116	.189	.280	.428	.356	.371	.360	.337	.310
6.000	.949	.852	.098	.113	.188	.281	.416	.356	.371	.360	.335	.309
7.500	.948	.854	.093	.110	.189	.283	.398	.356	.370	.359	.335	.308
8.615	.947	.854	.090	.107	.190	.285	.382	.356	.370	.359	.335	.308
10.017	.947	.855	.085	.104	.194	.287	.378	.356	.371	.359	.335	.307

Standard Bibliographic Page

1. Report No.	2. Government Accession No.	3. Recipient's Catalog No.
NASA TP-2721		

4. Title and Subtitle	5. Report Date
Static Internal Performance of a Two-Dimensional Convergent-Divergent Nozzle With Thrust Vectoring	July 1987
	6. Performing Organization Code
7. Author(s)	8. Performing Organization Report No.
E. Ann Bare and David E. Reubush	L-16240
9. Performing Organization Name and Address	10. Work Unit No.
NASA Langley Research Center Hampton, VA 23665-5225	505-68-91-06
	11. Contract or Grant No.
12. Sponsoring Agency Name and Address	13. Type of Report and Period Covered
National Aeronautics and Space Administration Washington, DC 20546-0001	Technical Paper
	14. Sponsoring Agency Code

15. Supplementary Notes

16. Abstract

A parametric investigation of the static internal performance of multifunction two-dimensional convergent-divergent nozzles has been made in the static test facility of the Langley 16-Foot Transonic Tunnel. All nozzles had a constant throat area and aspect ratio. The effects of upper and lower flap angles, divergent flap length, throat approach angle, sidewall containment, and throat geometry were determined. All nozzles were tested at a thrust vector angle that varied from 5.60° to 23.00°. The nozzle pressure ratio was varied up to 10 for all configurations.

17. Key Words (Suggested by Authors(s))	18. Distribution Statement
Nonaxisymmetric nozzles Static internal performance Two-dimensional convergent-divergent nozzles Thrust vectoring	Unclassified - Unlimited Subject Category 02

19. Security Classif.(of this report)	20. Security Classif.(of this page)	21. No. of Pages	22. Price
Unclassified	Unclassified	114	A06

For sale by the National Technical Information Service, Springfield, Virginia 22161

NASA-Langley, 1987